USING NATURAL POPULATIONS OF THREESPINE STICKLEBACK TO IDENTIFY THE GENOMIC BASIS OF SKELETAL VARIATION

by
KRISTIN S. ALLIGOOD

A DISSERTATION

Presented to the Department of Biology
and the Graduate School of the University of Oregon
in partial fulfillment of the requirements
for the degree of
Doctor of Philosophy

March 2017

DISSERTATION APPROVAL PAGE

Student: Kristin S. Alligood

Title: Using Natural Populations of Threespine Stickleback to Identify the Genomic Basis of Skeletal Variation

This dissertation has been accepted and approved in partial fulfillment of the requirements for the Doctor of Philosophy degree in the Department of Biology by:

Matthew Streisfeld	Chairperson
William Cresko	Advisor
Patrick Phillips	Core Member
Judith Eisen	Core Member
Stephen Frost	Institutional Representative

and

Scott L. Pratt	Dean of the Graduate School

Original approval signatures are on file with the University of Oregon Graduate School.

Degree awarded March 2017

DISSERTATION ABSTRACT

Kristin S. Alligood

Doctor of Philosophy

Department of Biology

March 2017

Title: Using Natural Populations of Threespine Stickleback to Identify the Genomic Basis of Skeletal Variation

Across vertebrates, skeletal shapes are diverse, and much of this variation appears to be adaptive. In contrast, the early developmental programs of these structures are highly conserved across vertebrates. The question then becomes where in the conserved genetic programs of skeletal development does variation lie to direct diversity? In threespine stickleback, rapid changes in head and body shape have been documented during repeated and independent invasions of oceanic fish into freshwater habitats in regions deglaciated approximately 13,000 years ago. However, recent research indicates that similar phenotypic and genetic divergence can occur in decades. A remaining challenge is to link stickleback population genomic variation to causal genes that underlie such rapid phenotypic evolution.

Here I use genome wide association studies (GWAS) in natural populations of stickleback to uncover genomic regions that contribute to variation of two dermal bone derived traits, lateral plate number and opercle shape. The decrease of lateral plate body armor and change in opercle bone shape, important for feeding mechanics, are classically associated with freshwater divergence.

GWAS has recently begun to be used in natural populations but is still under scrutiny for performance among different populations. Using a population of phenotypically variable stickleback in Oregon, GWAS proved an effective method to uncover genomic regions and genetic variants known to contribute to lateral plate number and opercle shape, as well as new genomic regions and candidate genes not previously implicated in phenotypic variation. Although successful, using similar methods on decades old stickleback populations in Alaska revealed the challenges that accompany controlling population structure created by strong natural selection.

Together, I found that although lateral plate number and opercle shape rapidly evolve in a coordinated fashion during adaptation from marine to freshwater environments, phenotypic variation is largely driven by independent genetic architectures. However, in very rapidly evolving populations, despite this independence of genetic architecture, the genetic variants contributing to the traits co-localize to similar genomic regions. This finding could be either biological or methodological which highlights the promise and limitations of using GWAS to identify genetic variation that gives rise to phenotypic diversity.

This dissertation includes unpublished co-authored material.

CURRICULUM VITAE

NAME OF AUTHOR: Kristin S. Alligood

GRADUATE AND UNDERGRADUATE SCHOOLS ATTENDED:

University of Oregon, Eugene, Oregon
Smith College, Northampton, Massachusetts

DEGREES AWARDED:

Doctor of Philosophy, Biology, 2017, University of Oregon
Bachelor of Arts, Neuroscience, 2008, Smith College

AREAS OF SPECIAL INTEREST:

Evolutionary Genetics

PROFESSIONAL EXPERIENCE:

Graduate Teaching Fellow, Department of Biology, University of Oregon, Eugene
2010 — present

Laboratory Technician, Dr. Judith Eisen, University of Oregon, Eugene,
2008 — 2010

GRANTS, AWARDS, AND HONORS:

Wimber Fund Award Recipient, University of Oregon, Eugene, 2014

Doctoral Dissertation Improvement Grant, Dissecting the genetic basis of craniofacial variation in the threespine stickleback, National Science Foundation, 2013 — 2017

Genetics Training Grant Fellow, National Institutes of Health, 2011 — 2014

Highest Honors for Senior Honors Thesis in Neuroscience, Smith College, 2008

PUBLICATIONS:

Annah S. Rolig, Erika K. Mittge, Julia Ganz, Josh V. Troll, Ellie Melancon, Travis J. Wiles, **Kristin Alligood**, W. Zac Stephens, Judith S. Eisen, and Karen Guillemin. PLoS Biology. 2017. The Enteric Nervous System Promotes Intestinal Health by Constraining Microbiota Composition. (*in press*)

ACKNOWLEDGEMENTS

This research was only possible because of the tremendous efforts of many Cresko and von Hippel lab members who had previously collected stickleback and documented phenotypic and genetic variation. The work of Emily Lescak, Susan Bassham, Julian Catchen, Mary Sherbick, Ofer Gelmond, and Frank von Hippel provided me with the foundational dataset from which to develop my work about Middleton Island, as well as with valuable guidance and expertise. Chuck Kimmel gave much needed tutorials and an intellectual base for starting some of the major phenotypic analyses and interpretation. Sophie Sichel, my undergraduate mentee for several years, spent significant time helping to generate the phenotype data needed to complete my studies, and for this I am incredibly grateful. Further, only because of Mark Currey's detailed work examining stickleback populations on the McKenzie River were any of my data from Oregon interpretable. I have been a lucky benefactor of Mark's enthusiasm and knowledge of Oregon stickleback as well as his kindness and generosity in the lab. I would also like to thank our summer undergraduate Jamie Kim for her organized and diligent phenotyping effort of the opercle bone.

I am constantly humbled by the intellectualism and academic rigor of all members of the Cresko lab and throughout the Institute of Ecology and Evolution and Department of Biology which, through critique, discussions, and friendships, have helped make me a better and more critical scientist. I am also grateful to the members of my committee, Matt Streisfeld, Judith Eisen, Patrick Phillips, and Stephen Frost, for their help to guide and support my science as well as being advocates and supporters of my personal goals and success.

Finally, I would not have been able to be at all successful in this endeavor were it not for the enduring optimism, positivity, and vision of my advisor Bill Cresko. I am especially thankful for his kindness and compassion through the many unique challenges that accompanied my graduate education both in and outside of the lab.

Generous funding by the National Institutes of Health Genetics Training Grant (7T32GM007413), and Doctoral Dissertation Improvement Grant (209920) supported this work. Additional support came from National Institutes of Health grant awarded to W. A. Cresko (R24OD011199).

For my parents, who have always encouraged me to
find my own way

TABLE OF CONTENTS

Chapter Page

Chapter Page

LIST OF FIGURES

Figure Page

Figure Page

LIST OF TABLES

Table Page

CHAPTER I

INTRODUCTION

Discovering Genes behind the Evolution of Developmental Processes

A central goal for evolutionary developmental biology (evo-devo) is to understand how the genes of an organism are linked to its phenotype—its form and function—and how those relationships change over time (Müller 2007). Since the startling discovery of a developmental genetic toolkit conserved across taxa, one focus of evo-devo research has been geared towards understanding how changes in deeply conserved genes and pathways can lead to macroevolutionary changes (Carroll 2008). Modification to the homeobox (*hox*) gene cluster is now a classic example of how changes in regulation, organization, and presence/absence can affect broad morphology across species (Ronshaugen et al. 2002; Pearson et al. 2005; Hsia et al. 2010; Small et al. 2016). Additionally, in development, the same genes are found to be reused at different times and across processes (Carroll 2008). While extensive phenotypic variation is clearly evident among species, vast variation also exists within species, which ongoing research often attributes to modification of these deeply conserved elements (Albertson 2003; Albertson et al. 2009; Pottin et al. 2011).

Within species, connecting genotypes-to-phenotypes that matter for evolution has been a difficult task because often the map between these two levels is ambiguous: one genotype can affect multiple phenotypes through pleiotropy, and conversely one phenotype can be produced by multiple genotypes if constraint on the phenotype is imposed (Sansom and Brandon 2007). This link is also difficult to establish across evolution and between diverging species because the relative roles of pleiotropy, epistasis, and linked selection can be a challenge to unravel (Sinervo and Svensson 2002; Paaby and Rockman 2013). Evolutionary biologists once dreamed of having the resources to connect genotypes-to-phenotypes. Now we are just beginning to develop the tools to make these connections, and there is much to be learned.

Utilizing the genetic variation that occurs in natural populations provides a powerful system to parse out the genotype-to-phenotype link (Rockman 2008). Often,

forward mutagenesis screens are used to determine a gene's function and effect on phenotypes, and, because of the conserved genetic toolkit, many discoveries made in the laboratory are to some degree generalizable (Carroll 2008; Albertson et al. 2009). However, phenotypes must be visible to researchers, usually early in development, to warrant further study. This has led to a bias towards identifying large effect mutations which are usually not viable in nature. Unlike mutagenesis screens, genetic variation in natural populations has already been vetted by natural selection, allowed to integrate into developmental networks and persist in populations. Identifying genetic variants that contribute to phenotypic variation in these populations presents an opportunity to uncover novel factors contributing to phenotypic diversity.

Linking genetic and phenotypic variation in natural populations of organisms has long been a daunting task. Evolutionary geneticists have tried to adapt laboratory genetic mapping approaches from model organism research and apply them to naturally occurring genetic variation. Quantitative trait loci (QTL) mapping has proven a powerful technique to identify the genomic regions contributing to diverging traits. By crossing individuals from natural populations in the laboratory, environmental variance is limited and segregating genetic variation can be identified and mapped with relatively few genetic markers (Johanson et al. 2000; Hoekstra et al. 2006; Reed et al. 2011). Although challenging, this approach has led to success. In Florida, light colored beach mice diverged from their mainland ancestors likely within the last 6,000 years driven by selection for crypsis. In (2007), Steiner et al. traced color pattern divergence to two pigment genes melanocortin-1 receptor (*Mc1-r*) and *Agouti*. In another example, differences in Arabidopsis flowering time have also been shown to be due to a single locus of large effect, the FRIGIDA (*FRI*) locus (Burn et al. 1993; Johanson et al. 2000). In *Heliconius* butterflies, the genetic basis of red color pattern variation in wings has been identified as changes in *cis*-regulation of the single transcription factor optix, and similar regulatory changes have been demonstrated to be important in mimicry among distantly related species (Reed et al. 2011).

So far, in instances where clear links have been made between genotype and phenotype, the traits have been largely Mendelian or oligogenic, and can therefore be explained predominantly by a gene of large effect (Johanson et al. 2000; Colosimo et al.

2005; Hoekstra et al. 2006; Reed et al. 2011). While these investigations provide great insight into the traits studied, the generality of these results is unclear because quantitative traits are thought to dominate in the wild (Sansom and Brandom 2007). It is also possible, however, that traits previously identified as Mendelian are actually quantitative. Laboratory mapping crosses, by necessity, limit the phenotypic variation which can be examined to only variation from a very few parental organisms, which may result in a limited or skewed view of the underlying genetics (Korte and Farlow 2013; Savolainen et al. 2013; Remington 2015). An additional problem is that what can appear as a single locus of large effect segregating in the laboratory are actually several linked loci of small effect that act additively and segregate together (Mackay et al. 2009). Also possible is that methodological shortcomings may have allowed the discovery only of genes with large effects and that genes of smaller effect are still to be discovered (Slate 2013). Regardless, it is now clear that numerous single traits are controlled by many genes that coordinate in a complex genetic network and that also interact with the environment (Wagner and Altenberg 1996; Kimmel et al. 2005; Müller 2007). This coordinated and complex genetic network is clearly evident within vertebrate head, jaw, and skeletal structures.

The Vertebrate Head as a Model Complex Trait

The vertebrate skeleton comprises many interacting bone, cartilage and muscle structures which must develop in a coordinated manner to enable proper function (Olsen et al. 2000). One aspect of the vertebrate skeleton that has received much attention for the study of the genetic basis of variation is the vertebrate head (Albertson 2003; Schoenebeck et al. 2012). In spite of the immense variation that exists among species in heads and jaws, analysis of early development using zebrafish and other model organisms has revealed a conserved embryonic origin of major head structures in all lineages examined and relatively few highly conserved mechanisms that direct this development (Santagati and Rijli 2003; Eames and Helms 2004; Eames et al. 2012). For example, across all vertebrates, gill arches serve as a major organizing location for bones and cartilages, and distinct *hox* gene expression patterns direct migrating neural crest cells from the hindbrain rhombomeres to occupy specific arches where they will give rise to

stereotypical head structures (Santagati and Rijli 2003). Hedgehog (*Hh*) signaling is used multiple times in craniofacial development. Early, *Hh* functions to pattern and direct outgrowth of craniofacial skeletal precursors, but slightly later, *Hh* is critical for normal cartilage development especially in the anterior neurocranium (Eberhart 2006). Members of the endothelin (e*dn*) gene family (and the genes activated by Edn) are critical for growth, patterning, and establishing identity of individual bone structures (Olsen et al. 2000; Kimmel 2003). Much has been learned from these laboratory studies in terms of the developmental systems that are behind craniofacial morphogenesis.

Despite these advances, the question remains "Where does developmental genetic variation that contributes to evolution reside?" The genes and developmental pathways involved in bone shape evolution are just beginning to be discovered. For example, in cichlids, genes in the sonic hedgehog (*shh*) pathway appear to be involved. A derived allele of the *ptch1* receptor changes the shape and reduces mineralization of the lower jaw such that suction feeding is improved which likely contributes to the niche partitioning among the Lake Malawi cichlids (Roberts et al. 2011). Furthermore, in mice a recent manipulative study shows that changes in the dosage of key developmental genes such as *Bmp4* or *Noggin* somewhat recreate differences in mouse mandible shape found in natural populations (Boell et al. 2013). These studies provide some insight into the developmental genetic basis of craniofacial evolution, but by no means is our understanding complete. Only a few of the many instances of phenotypic evolution observed in natural populations have been attributed to specific genes, and even fewer have identified the specific changes within these genes that allow for phenotypic evolution (Barrett and Hoekstra 2011). This is likely because of previous methodological limitations now dissipating due to new genomic approaches, and because few good model systems exist in which examination of both developmental and evolutionary processes can be assessed. By using natural populations, our field is moving towards gaining a better understanding of the loci that are utilized by evolution. However, a remaining question in this work is whether or not the same genes identified in developmental laboratory mutagenesis studies are also targeted by evolution (Mackay et al. 2009).

In the last decade, genome wide association studies (GWAS) have become a widely used approach, not just in humans, but also in natural populations to identify the genes that contribute to adaptive and complex quantitative traits (Visscher et al. 2012; Lee et al. 2014). By being able to survey many more species, capture a broader amount of phenotypic variation, and fine map loci more easily, GWAS has the potential to link the genotype-to-phenotype map in natural populations in the context of the environment and help determine if evolution targets the same loci as are found to contribute to phenotypes though mutagenesis studies in the laboratory. In addition, GWAS may prove useful to address fundamental questions in evolutionary biology that are different from identifying the genes responsible for phenotypic variation. For example, GWAS might make it possible to identify the range of effect sizes and physical location of loci that contribute to the genetic and genomic architectures of traits, a long standing goal (Pasaniuc and Price 2016). However, identifying populations in nature that are amenable to GWAS is still a challenge (Smith and O'Brien 2005; Korte and Farlow 2013). In this Dissertation, I use the threespine stickleback as a model system to begin to address some of these fundamental evolutionary questions using a GWAS approach.

The Threespine Stickleback as an Ideal Evolutionary Genomic Model

The threespine stickleback, *Gasterosteus aculeatus,* is a small fish that is broadly distributed both geographically and ecologically within coastal marine, coastal freshwater, and brackish water habitats of the northern hemisphere. Stickleback have long received attention for the study of behavioral ecology and evolution, speciation, population and quantitative genetics (Bell and Foster 1994; Cresko et al. 2007). Because of advances in genomic and developmental techniques in stickleback, it is now an ideal system in which to investigate the genetic basis of adaptive phenotypic evolution (Kingsley et al. 2004; Baird et al. 2008; Hohenlohe et al. 2010). Across the stickleback's geographical distribution thousands of freshwater populations have been independently derived from marine populations. Despite the independence of their evolutionary origins, the morphological and behavioral characteristics of freshwater stickleback are repeatable and predictable based on the particular ecology of the habitat even across great geographic distances (Bell and Foster 1994; Schluter 1995; Rundle et al. 2000; von

Hippel 2010). While many traits evolve as populations colonize and adapt to their freshwater environments, morphological differences, such as those in skeletal armor traits, are some of the most immediately apparent (Bell 2001; Cresko et al. 2004; Shapiro et al. 2004).

Brief Outline of the Dissertation

The work in this dissertation focuses on two skeletal structures which evolve stereotypically as marine stickleback adapt to freshwater environments and uses GWAS as a method to identify genomic regions contributing to phenotypic variation. The first structure is the opercle bone which is a superficial craniofacial bone important in feeding and respiration. The evolution of the shape of this bone is a trait thought to have a complex genetic architecture (Kimmel et al. 2005). The second structure is among the most prominent and well-studied changes accompanying the marine-freshwater transition, lateral plate loss (Bell 2001). The loss of bony lateral armor is thought to be a trait regulated by a relatively simple genetic architecture.

Identifying a population appropriate for GWAS requires investigation into the nature of phenotypic variation and population structure. In Chapter II, I explore the phenotypic variation in opercle shape and lateral plate count and population structure among sampling collections along the McKenzie River in Oregon. Much of this work was spurred by previous studies done by Mark Currey who identified the likely presence of a phenotypic and genetic cline along the river and observations made by Susan Bassham, Paul Hohenlohe, and Taylor Wilson that extensive variation existed within at least one of the collection sites, Riverbend. Here, I examine lateral plate count and opercle shape and find that phenotypic variation is largely governed by independent genetic architectures. My analysis of population structure reveals divergence due to spatial differentiation, but that little population structure exists within collection sites showing that Riverbend is an ideal population to implement GWAS. In this site, phenotypic variation is extensive but population structure is low which allowed us to identify genomic regions contributing to opercle shape as well as a novel genomic region that may contribute to the transmission genetics of lateral plate variability. These results demonstrate the utility of using GWAS to aid in a better understanding of the genes that

contribute to adaptive evolution as well as to other fundamental questions in evolutionary biology.

A hallmark of the stickleback system is the rapid pace at which phenotypes are modified in a freshwater environment from the marine invaders. In Chapter III, I take the GWAS approach to a system of recently formed freshwater ponds on Middleton Island in Alaska to try to identify the genetic architectures of opercle shape and lateral plate count within the context of very rapid evolution. This study builds upon efforts to capture the phenotypic and genomic evolution of rapidly evolving populations done in collaboration with William A. Cresko, Frank von Hippel, Emily Lescak, Susan Bassham, and Julian Catchen. We found that the genomic regions contributing to phenotypic variation of each trait co-localize to similar genomic regions and may suggest that genomic covariation of loci contributes to rapidly diverging traits through linked selection. Evaluating these results is challenging because although the populations are very young, extensive populations structure has developed and we find ourselves at the limits of current GWAS methods.

Finally, in Chapter IV I summarize the findings of Chapters II and III and put the results into a broader context of how to continue to connect the genotype-to-phenotype map in systems with differing evolutionary histories.

CHAPTER II

UNCOVERING NEW GENOMIC REGIONS THAT CONTRIBUTE TO CLASSIC SKELETAL TRAITS WITH GWAS IN A PHENOTYPICALLY VARIABLE POPULATION OF OREGON STICKLEBACK

Stickleback collections used in this study were made by M.C. Currey. I and M.C. Currey prepared individuals to be phenotyped and sequenced, and subsequently phenotyped and processed sequencing reads. S. L. Bassham and J. Catchen were important in initial characterization of some of the populations used in this study. I performed all the data analysis and writing. W. A. Cresko was the principal investigator for this study.

INTRODUCTION

The evolution of cartilage and mineralized skeletons are major innovations hypothesized to be key in the diversification of vertebrates (Shimeld 2000; Hirasawa and Kuratani 2015). Vertebrate morphological variation involves adaptations to better locomote, forage, capture prey, compete, and defend territory and oneself. These traits in turn have enabled resource utilization in an array of new ecological niches. Biologists have long studied vertebrate body shape and skeletal systems to learn about their phenotypic evolution, and more recently have begun unraveling their genetic and developmental basis (Shubin et al. 1997; Ackermann and Cheverud 2002; Pavlicev et al. 2011; Schoenebeck et al. 2012; Franchini et al. 2013). As genomic technologies have improved, many research programs now focus on finding the genes and developmental pathways underlying evolutionary change. Numerous questions are only now being addressed, such as what the genes are and how they function, whether lineages that show similar phenotypic changes utilize the same genes and pathways (Arendt and Reznick 2008), and if so whether those mutations are novel or part of standing genetic variation that exists in natural populations (Barrett and Schluter 2008).

A fundamental question that is a logical extension of this area of inquiry is whether phenotypic evolution in natural populations is largely driven by changes in genes

and pathways that have already been identified by induced mutagenesis studies in the laboratory, or whether evolution finds novel solutions. Until the 1990s skeletal system research utilized a handful of vertebrate models - primarily mice, chicken and zebrafish - and the inferences were mainly limited to the particular model organism of interest. However, the discovery of deep homology shared among even distantly related taxa, and the presence of a conserved genetic toolkit, made researchers look for common genetic pathways across vertebrates (Shubin et al. 1997; Prud'homme et al. 2007; Shubin et al. 2009). Coupled with the ease of mutagenesis techniques, skeletal biology research was spurred to focus on the early developmental genetics of bone and cartilage morphologies in model systems (Satokata and Maas 1994; Olsen et al. 2000; Huycke et al. 2012). Developmental skeletal biologists have now deciphered fundamental and intricate developmental genetic networks that consist of a handful of players, for example Wnt, BMPs, Hedgehog, and FGF, all of which are critical in the establishment of a functioning skeletal system (Olsen et al. 2000; Ornitz and Marie 2002; Westendorf et al. 2004; Merrill et al. 2008). While there is much to be discovered, the core genetic networks for the early development of cartilage and bone have been outlined.

Despite the advances in model organism research in the laboratory, it remains unclear if evolution utilizes these developmental pathways and their constituent genes as the major players in phenotypic adaptation in natural populations. Mutagenesis screens in the laboratory and natural selection in the wild share some similarities, but significant differences between them exist that may lead to different genetic outcomes in each. Natural selection works on multiple phenotypes throughout ontogeny to maximize lifetime fitness (Orr 2009; Anderson et al. 2014). Many mutations uncovered in the laboratory would be highly deleterious either directly, or through negative pleiotropic effects, were they to occur in the wild. With the advance of genomic technologies, the study of the developmental genetic basis of phenotypic adaptation in the wild provides an excellent opportunity in a variety of different organisms beyond the classic laboratory models.

Most recently, quantitative trait locus (QTL) studies, which involve modifications of methods for mapping induced mutations in the laboratory but instead using natural genetic variants, have often been used with marked success (Slate 2005; Edwards and

Weinig 2010; Laporte et al. 2015). Across organismal systems, these approaches have enabled the discovery of chromosomal regions, and in some cases the causal genes, that affect interesting and important phenotypes. Examples include coat color of beach mice (Hoekstra et al. 2006), Arabidopsis flowering time (Clarke and Dean 1994), color pattern variation in Heliconius butterfly wings (Reed et al. 2011), floral color contributing to reproductive isolation in Mimulus spp. (Yuan et al. 2013), and lateral plate and pelvic structure morphology in stickleback fish (Colosimo et al. 2004; Cresko et al. 2004; Shapiro et al. 2004; Colosimo et al. 2005), among others. The loci discovered through QTL mapping often have modest to large effects on the phenotype but generally do not explain all of the observed genetic variance (Slate 2005; Scoville et al. 2011). In addition, the mapping resolution for QTLs often leads to identifying regions that capture many hundreds of genes, and subsequent identification of causative changes can be difficult (Colosimo et al. 2004). Finally, because QTL crosses comprise a small number (often two) of genetically divergent parents for families raised in a common environment, the QTL may be specific to those parents, or caused by unnatural genetic combinations from the laboratory environment itself (Remington 2015).

A powerful complement to QTL approaches in the laboratory are studies of the genotype-to-phenotype map in natural populations. As the cost of generating thousands of markers throughout the genome declines, natural populations are more accessible than ever to address questions about the genetic variation that gives rise to expression of phenotypes and ultimately to an organism's performance and fitness within the context of selective forces and the environment. Broadly, genome wide association studies (GWAS) can be used to identify genetic variants that contribute to phenotypic variation in the wild. GWAS can exploit historic recombination performed by nature to increase mapping precision, and it provides a path to investigate species and traits impractical for laboratory mutagenesis studies (Winkler et al. 2010; Korte and Farlow 2013). For example, in a recent study, Delmore et. al. (2016) used a hybrid population of Swainson's thrushes (*Catharus ustulatus*) and geolocators to track migration routes of the birds over an entire year. They combined the tracking data with genomic data and identified specific genomic regions to support the idea that different migratory routes in these birds have a significant

genetic component. This trait in Swainson's thrushes is more challenging to map genetically using laboratory approaches.

While there are clear benefits to the use of GWAS for traits that are difficult to study except in natural populations (Wood et al. 2014), there are requirements for the efficient use of this method. GWAS relies on identifying the appropriate populations that are segregating the phenotypes and genetic variants of interest, and requires controlling for or eliminating population structure, expressed as systematic differences in allele frequencies, to remove spurious associations (Astle and Balding 2009; Winkler et al. 2010; Flint and Eskin 2012). In addition, although the increased number of recombinations typical in GWAS creates an advantage for providing an opportunity for finely mapping loci that contribute to a trait, the potentially more significant effects of environmental variation on individuals grown and reared in the wild requires many more individuals and markers than in laboratory crosses (Remington 2015). GWAS will therefore be most successful when using deep genomic and biological sampling in populations that have phenotypic variability but low population structure. These criteria are most often met in hybrid or admixed populations (Pallares et al. 2014).

The threespine stickleback (*Gasterosteus aculeatus*) is an ideal system to study the genotype-to-phenotype-to-fitness map in both the laboratory and natural environments. These small fish are found nearly ubiquitously in the Holarctic and have a long history as a model system for ecological and behavioral research reaching as far back as the early 1800's (Bell and Foster 1994; Colosimo et al. 2004). The power of the stickleback model system arises because these small fish occupy a range of ecological habitats from freshwater, brackish, to marine environments and display extraordinary morphological and behavioral diversity, all of which can be easily captured, maintained, and propagated in the laboratory under constant conditions. The diversity of the species complex is driven by a dynamic process where anadromous fish repeatedly and independently invade, and subsequently adapt to, isolated or semi-isolated freshwater environments. Over the millions of years that the threespine stickleback has been a species, the freshwater environments have experienced more or less connectivity to the sea that results in persistent gene flow between the isolated, phenotypically diverse

freshwater stickleback and their panmictic marine counterparts (Bell and Foster 1994; Bell et al. 2009).

A striking aspect of the stickleback system is the morphological and genetic parallelism that underscores the repeated and independent invasions of anadromous stickleback into freshwater environments. Although stickleback are phenotypically diverse among freshwater populations, the marine to freshwater transition is notably stereotypical for several genomic and phenotypic attributes. Many of the same genomic regions appear responsible for divergence across marine and freshwater populations globally (Chan et al. 2010; Hohenlohe et al. 2010; Jones et al. 2012), and numerous behavioral, life history and morphological traits shift as oceanic stickleback adapt to freshwater (Bell and Foster 1994).

Loss of bony armor and change in body and craniofacial shape are some of the most apparent and well-studied phenotypes in stickleback. These traits were also some of the first to be targeted for more detailed developmental genetic QTL analyses (Shapiro et al. 2004; Colosimo et al. 2005; Kimmel et al. 2005). The transmission genetics of lateral plate loss was extensively investigated in the 20th century and explained through models of inheritance all of which proposed a largely simple genetic basis (Hagen 1973; Hagen and Gilbertson 1973; Banbura 1994; Banbura and Bakker 1995; Bell 2001). These models were supported by the identification of a locus of major effect (ectodysplasin *eda*, linkage group IV) as well as several loci of smaller effect in a large QTL mapping cross between a marine female from Hokkaido Island, Japan and a freshwater benthic male from Paxton Lake, British Columbia (Colosimo et al. 2004). Since the initial studies in 2004, QTL studies between individuals from different populations implicate the reuse of the major effect locus *eda* in lateral plate loss around the world (DeFaveri et al. 2011; Jones et al. 2012).

Parallel changes in stickleback craniofacial shape have been investigated in a variety of head and jaw features (Arnegard et al. 2014; Miller et al. 2014; Conte et al. 2015). One well-studied craniofacial bone in the transition from marine environments to freshwater is the opercle, which is an important trophic trait, acts as a protective gill cover, and aids in respiration (Kimmel et al. 2005; Kimmel et al. 2008). The opercle bone is also a subject of developmental studies because its early appearance and superficial

location enables ease of visualization (Kimmel et al. 2010). Unlike lateral plate loss, the genetic basis of opercle shape is thought to be complex (Schluter et al. 2004; Kimmel et al. 2005). Unfortunately, though the opercle has been the subject of one QTL study and one of many traits examined in other QTL studies, no candidate genes have been identified.

As technologies have become available that enable dense sets of genome-wide markers to be identified, we have the opportunity to explore the genetic basis of traits important for adaptive phenotypic and parallel evolution in nature. As a field, we have perhaps put an unbalanced emphasis on divergent populations particularly since the discovery that *eda* was responsible for lateral plate loss in laboratory crosses (Colosimo et al. 2004; Colosimo et al. 2005; DeFaveri et al. 2011). Although many successful QTL studies have subsequently been performed using divergent stickleback populations to identify linkage groups that contribute to a huge number of traits that evolve in parallel, identifying candidate loci still remains a tremendous effort because of the relatively small family sizes in laboratory and the complex nature of the traits. Stickleback populations which are phenotypically and genetically variable provide an excellent system to use GWAS to link the genotype-phenotype map, an enduring goal in evolutionary biology. We have the opportunity to do this in a population of stickleback from Oregon.

The focus of the current study is to confirm the utility of a natural population in Oregon for current GWAS methods, and to use these approaches to examine the genetic sources of opercle bone shape and lateral plate number variation. Although these traits have been studied using QTL mapping methods in other populations, we chose to focus on lateral plate count and opercle shape because previous studies provide an expectation about the genomic regions that contribute to these phenotypes. Stickleback sampled from the Riverbend site of the McKenzie River in the Oregon, Willamette Basin are phenotypically variable for many skeletal phenotypes some of which span the morphological space between stereotypical marine and freshwater phenotypes (Fig. 2.1). We do not yet fully understand why phenotypic variation is maintained in this freshwater population. However, population genomic evidence (Currey 2014) argues that recent human introductions of anadromous stickleback upstream of Riverbend at the Leaburg fish hatchery created this diversity. As gene flow occurred downstream from the

hatchery, anadromous alleles were likely introduced into the presumably monomorphic freshwater Riverbend population and created the phenotypically variable population we utilize in our study. Because we found that the Riverbend population has little population structure, we have an opportunity to ask if the same genomic regions contribute to phenotypic changes across large geographic areas and if we can learn something new about the genetic variation contributing to phenotypes using GWAS.

METHODS

Field Collections

We collected threespine stickleback from locations along the McKenzie River in Oregon in the fall of 2010 (Riverbend), 2012 (Leaburg Fish Trap and Waterville), and 2013 (Riverbend) (Fig. 2.1A). The stickleback were collected from minnow traps (0.32- and 0.64-cm mesh) which were placed near the riverbank and retrieved the following day, sacrificed with an overdose of MS-222 anesthetic, and preserved in 95% ethanol.

Sample Preparation

We assigned each individual a unique identifier so that an individual's genotype and phenotype could be associated in future analyses. We extracted genomic DNA using the Qiagen DNeasy kit from clipped caudal and pectoral fins and fixed the somas in ~4% formaldehyde solution (Macron Fine Chemicals) in water for at least 8 hrs to overnight. After the fixative was removed, we rinsed the bodies in 1% KOH (in water) for one or more hours, then bleached the bodies in a room temperature solution of 30% hydrogen peroxide, 1% KOH until skin pigment was gone. We rinsed the fish in 1% KOH for several hours, stained the fish in a 0.25% Alizarin red S, 1% KOH solution for two hours, destained in 1% KOH, and stored the fish in 50% isopropanol longterm.

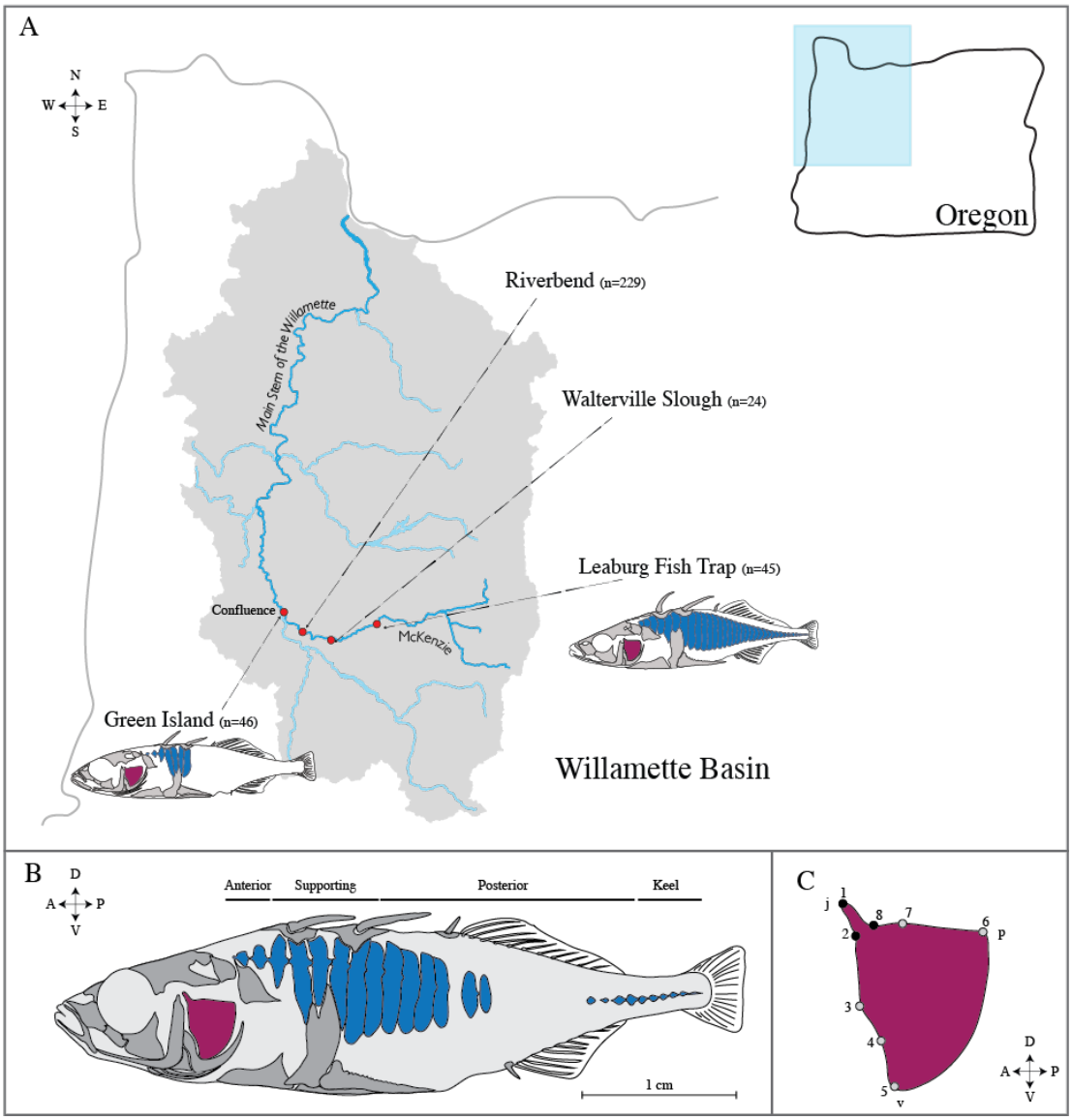

Figure 2.1 Oregon collection sites and phenotypes measured. A) Map of the Willamette Basin in Northwest Oregon; major rivers are indicated as blue lines. Stickleback were collected from three sites along the McKenzie River and one site at the confluence of the McKenzie and Willamette Rivers (red circles). Sample size for each collection site is indicated. Many completely plated fish are found at Leaburg fish trap (line drawing; lateral plates, blue) and only low plated fish are found at Green Island (line drawing; lateral plates, blue). Walterville Slough and Riverbend show intermediate lateral plate morphologies. B) Line drawing of threespine stickleback collected at the Riverbend site highlight a representative partially plated individual with phenotypes measured— lateral plate number (blue), opercle shape (violet). Lateral plates are divided into four subtypes: anterior, supporting, posterior, and keel. C) Opercle shape was measured with geometric morphometrics using previously established landmarks (Kimmel et. al. 2012). Gray dots indicate sliding semi-landmarks, black dots are fixed landmarks. 'j', 'v', 'p' indicated at the three opercle edges indicate the joint, the ventral edge, and the posterior edge respectively.

Phenotypic Analysis

We photographed the left side of alizarin-stained fish with a tripod-mounted Canon DSLR camera and Canon EOS ViewerUility software. We used these images to count lateral plate number and, in conjunction with ImageJ software, measure standard length (SL) which we defined as the most anterior tip of the upper jaw to the most posterior end of the hypural plate.

For a more detailed view, we imaged the left side of the head with an Olympus SZX16 dissecting microscope equipped with an Olympus DP71 microscope digital camera and processed the image with Olympus DP Controller version 3.3.1.292. We used geometric morphometrics to assess opercle shape and digitized the positions of eight reproducible landmarks (Fig. 2.1C) with the 'tps' software package from the State University of New York at Stony Brook [tpsDig2 version 2.10; (Rohlf 2006)]. We used the `geomorph` R package (Adams and Otárola-Castillo 2013) to treat landmarks as either sliding semi-landmarks (landmarks 3-7) or as fixed landmarks (landmarks 1, 2, and 8) (Fig. 2.1C) (Bookstein 1997a). The fixed landmarks capture the region where the opercle connects to the hyomandibula at the opercle joint. Sliding semi-landmarks 3-5 show the curvature of the anterior edge of the bone which reflects the curvature of the adjacent subopercle bone. Semi-landmarks 5 and 6 denote the points at the far ventral and posterior edges, between which is the opercle fan (dotted line). Semi-landmarks 6 and 7 show the dorsal edge of the bone, also the edge to which the elevator opercular muscle attaches to rotate the opercle, an important function in the opening of the jaw (Hulsey et al. 2005; Kimmel et al. 2008; Anker 2010). To eliminate variation imposed due to size, location, or orientation, we performed a Generalized Procrustes Analysis, with the `geomorph` R package (Klingenberg 2010; Adams and Otárola-Castillo 2013) and treated landmarks 3, 4, 5, 6, and 7 as sliding based on minimum bending energy.

We also used `geomorph` (Adams and Otárola-Castillo 2013) to capture the major axes of opercle shape variation with principle component analysis (PCA) on the Procrustes Coordinates derived from the GPA. Importantly, in our analyses, we included opercle shapes of laboratory reared stickleback individuals derived from wild caught, Alaskan anadromous and freshwater populations isolated from each other for thousands of years. We included these individuals because previous research has shown that

principle component 1 (PC1) for opercle shape captures the marine to freshwater transition, and the shape change in similar around the globe (Kimmel et al. 2012a). The Alaskan individuals were, therefore, used to set the boundaries of the morphospace and as a reference to visualize where along that space the individuals from McKenzie River fell.

Genotyping

For each individual from the four populations along the McKenzie River, we digested genomic DNA with SbfI-HF (NEB) restriction enzyme and prepared RAD-seq libraries as previously reported (Baird et al. 2008; Hohenlohe et al. 2012b). We ran approximately 96 uniquely barcoded individuals in a single lane on the Illumina HiSeq 2500 platform and used a total of 39 lanes. On average, each lane of sequencing generated ~23 million single end reads, and, post quality filter, we retained ~19 million reads (82%). The sequence output was 101 nucleotides (nt) long and included a 6-nt in-line barcode which we used to identify individual fish. After we demultiplexed by barcode and quality filtered the raw sequence data with the `process_radtag` program in *Stacks* software suite (Catchen et al. 2011), we aligned the reads against the stickleback reference genome (version BROADSs1, Ensemble release 64) with GSnap (Wu and Watanabe 2005). For our alignment to the reference, we allowed up to five mismatches and gaps of length 2. We also disabled terminal alignments and required unique alignments in GSnap (Wu and Watanabe 2005) and then used the *Stacks* programs `pstacks`, `cstacks`, and `sstacks` to process and call genotypes at each locus for all individuals. We used the *Stacks* `populations` program (Catchen et al. 2011; Catchen et al. 2013) to identify loci that would be included in further analyses by requiring that loci must be present in all populations, genotyped successfully in at least 75% of the individuals within each population, and have minor allele frequencies greater than 10%.

Association Mapping

To utilize SNP data for genome wide association studies, we used the `populations` program in the *Stacks* suite (Catchen et al. 2011; Catchen et al. 2013) to

output filtered SNP data (see above) in PLINK (Purcell et al. 2007) format from the 21 linkage groups. We used PLINK v1.07 (Purcell et al. 2007) to make these files compatible with the genome-wide efficient mixed-model association (GEMMA v.0.94.1) software package (Zhou and Stephens 2012). We performed all genotype-phenotype associations with the univariate linear mixed model (LMM) implemented in GEMMA which allowed us to control for relatedness and population structure within the mapping population and thus reduce spurious associations (Zhou and Stephens 2012, 2014). Because SNPs were quality filtered through *Stacks*, we modified GEMMA's default parameters to ensure that all SNPs were included in the association analysis. We report *p*-values calculated from the Wald test and likelihood-ratio test (LRT) in GEMMA and the likelihood of odds (LOD) scores which we back calculated from the LRT *p*-values (Zhou and Stephens 2012).

We used GEMMA to control for population structure and relatedness by creating a mean-centered relatedness matrix (Zhou and Stephens 2012). Unfortunately, a problem can arise when the relatedness matrix is created from all SNPs across the genome because the causative SNP is fitted to the LMM twice, once in the relatedness matrix and once in the association. This phenomenon is called 'proximal contamination' and it reduces the power to identify the causative SNP (Lippert et al. 2011; Listgarten et al. 2012). To account for 'proximal contamination' we employed a 'leave one chromosome out' method whereby we created relatedness matrices for all linkage groups (LG) except for the LG used in the association (Pallares et al. 2014). We then performed associations on each LG individually with the appropriate relatedness matrix.

We accounted for multiple testing with permutation to identify the genome-wide significance threshold. We performed association mapping on 1000 permuted datasets. The phenotype values were randomized for each dataset but the genotypes were kept intact. We recorded the minimum *p*-value for each statistical test (Wald, LRT, score) and used the 95% quantile from the *p*-value distribution as the genome-wide significance threshold (Pallares et al. 2014).

Identifying a Credible Interval around Association

To identify the credible genomic interval around the most associated SNP from our GWAS, we found the most downstream and upstream SNPs which were correlated with the top SNP at a minimum of $r^2 \geq 0.8$ (Pallares et al. 2014). We used PLINK 1.07 (Purcell et al. 2007) to calculate r^2 values. There were several instances in which no SNPs were correlated with the top SNP at r^2 values of 0.8 or above. In these cases, we used $r^2 \geq 0.4$ as our minimum criteria which we expect is a conservative estimate.

We also estimated linkage distances by calculating LOD (logarithm of the odds) scores from *p*-values output from the LRT in GEMMA. Because GEMMA does not output the LRT test statistics directly, we used the LRT *p*-values to back calculate the test statistics. In R, LRT=qchisq(1-p, df=1)/2 where p is the *p*-value. Using the LRT we were able to calculate the LOD score with LRT=2ln(LR), where LR is the likelihood ratio. We then identified the 2-LOD support interval and found that for associations hovering around the genome-wide significance threshold, the support interval often spanned the entire linkage group.

Examining Effect of Genotype on Phenotype

The effect of the genotypes of most highly associated SNPs on the phenotypes was tested with analysis of variance (ANOVA). If genotype had a significant effect on phenotype, we used Tukey's HSD (honest significant differences) to identify pairwise differences between genotypes. All analyses were performed with the R `stat` package (R core team 2015).

Analysis of Genomic Correlation Patterns Using Linkage Disequilibrium

We tested all pairwise combinations of SNPs for genotypic linkage disequilibrium (LD) by calculating the squared correlation coefficient (r^2) in PLINK v1.07 (Purcell et al. 2007). We used *Stacks* (Catchen et al. 2011) to output a reduced dataset for LD analysis with only one SNP per RAD locus. This reduced the number of pairwise comparisons and the number of SNPs with r^2 values of 1 due to tight physical linkage within a RAD site.

RESULTS

McKenzie River Stickleback Phenotypic Variation Encompasses the Marine-Freshwater Phenotypic Range Seen in Divergent Stickleback Populations

Skeletal phenotypes of stickleback sampled along the McKenzie River vary dramatically. We pooled individuals from three populations sampled from the McKenzie River (Leaburg Fish Trap, Walterville Slough, Riverbend), and one population sampled from the confluence of the McKenzie and main stem of the Willamette River (Green Island) (Fig. 2.1A). Although the stickleback we sampled are resident in freshwater environments, we found that lateral plate number covered the range of phenotypes across the typical marine (high plate number)-freshwater (low plate number) morphospace and that the distribution is relatively trimodal (Fig. 2.2B, n=344). For ease, we include Green Island as a McKenzie population. Individuals with very low plate counts (~4 plates) only had supporting and a subset of anterior plates while those individuals with a very high plate count (~34 plates) had a full complement of anterior, supporting, posterior, and keel plates (Fig. 2.1A, Fig. 2.2B). The high plated phenotype is most commonly associated with marine or anadromous stickleback populations. Typically, individuals with an intermediate plate count were missing plates along the posterior region (Fig. 2.1B, Fig. 2.2B). We never saw intermediate individuals which had posterior or keel plates but were missing anterior or supporting plates. This is consistent with lateral plate patterns observed in other phenotypically variable, freshwater populations (Bell 2001).

When we examined each site separately, we observed differences in the distribution of lateral plate number variability. The site located farthest upstream, Leaburg Fish Trap, is bimodal in lateral plate number containing high and low plated fish with no evidence of fish with intermediate plate counts. Moving downstream, the Walterville Slough and Riverbend sites contain fish with all three phenotypes, high, low, and intermediate lateral plate number. The site located furthest downstream, Green Island, only contains fish with low lateral plate numbers (Fig. 2.3A) and is the only site with significantly different lateral plate counts from the other sites (Tukey HSD; $p<0.05$). Although the McKenzie River individuals span the marine-freshwater morphospace when pooled together (Fig. 2.2B), only two sites show all three general plate morphologies.

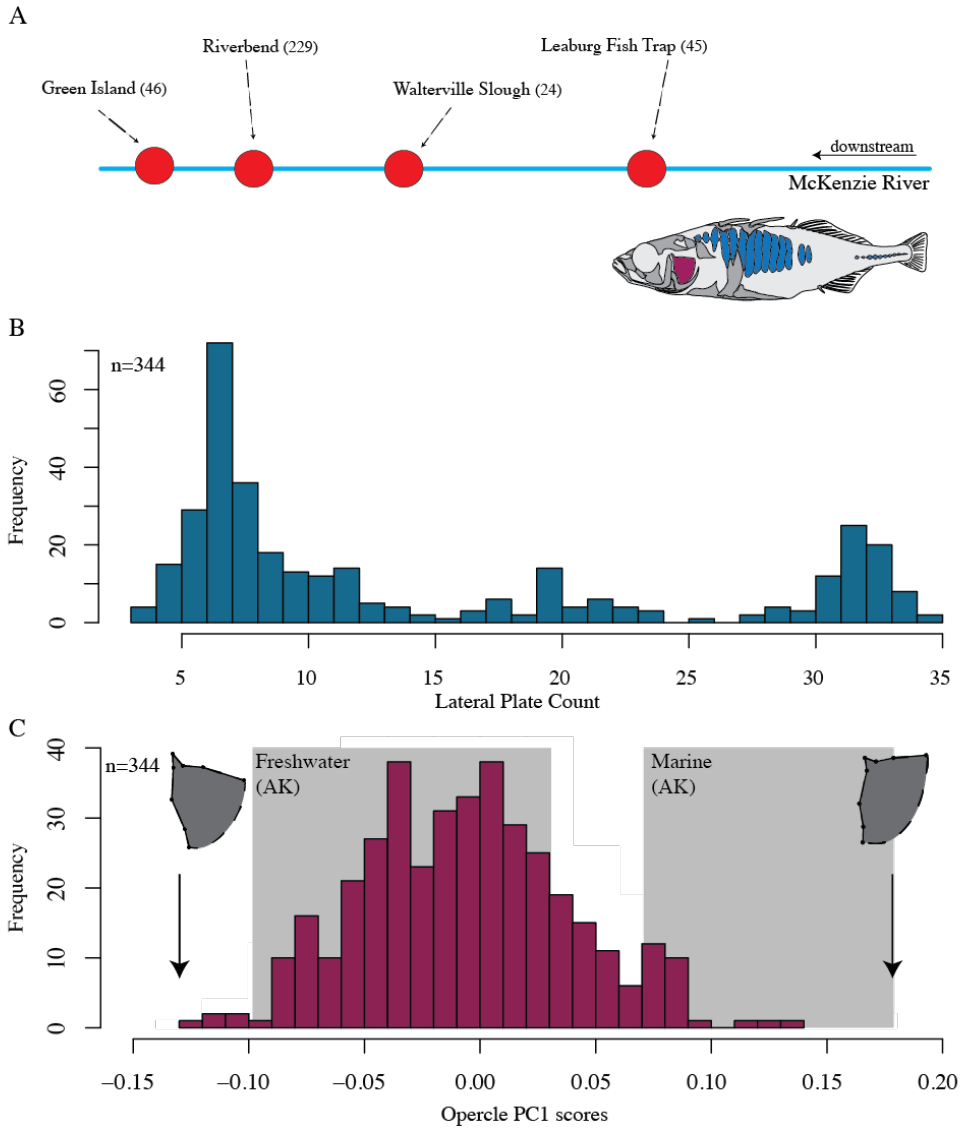

Figure 2.2 Discordant phenotype distributions between lateral plate number and operate shape of pooled individuals across the four McKenzie River sampling locations. A) McKenzie River sampling locations from which individuals were pooled, reflect relative geographic locations along the river. Sample sizes are indicated at each site, and lateral plates (blue) and opercle shape (purple) are indicated on line drawing. B) Frequency distribution lateral plate count. C) Frequency distribution of opercle PC1 scores. Gray boxes indicate morphospace occupancy of post-glacial, divergent marine and freshwater Alaskan stickleback which were included in PCA to help anchor the morphospace. Opercle shapes at the extremes of PC1 are shown.

Unlike lateral plate count, opercle bone shape did not fill the entire morphospace typical between marine and freshwater stickleback. Instead, opercle shape primarily reflects freshwater variation (Fig. 2.2C). Previously, using PCA, (Kimmel et al. 2012a) showed that the majority of opercle shape variation segregates between marine and freshwater populations and that the shape change along the major axis of variation is similar among independently derived populations around the northern hemisphere. We therefore used PCA to identify where opercle shapes of McKenzie River stickleback populations fell along PC1 morphospace. To anchor the shape space (Fig. 2.2C, gray boxes) we included one monomorphic marine and one monomorphic freshwater population from South Central Alaska which enabled us to assess marine and freshwater characteristics of opercle shape. We found that opercle PC1 scores were normally distributed and the majority of McKenzie River individuals had PC1 opercle shapes that fell within the phenotypic region defined by the Alaskan freshwater population. Only a few McKenzie River individuals had PC1 opercle shapes that fell within the phenotypic region defined by the Alaskan marine population. PC1 explained ~42% of opercle shape variation in the combined McKenzie and Alaskan dataset (Fig. 2.2C, Fig. 2.4).

Following a second PCA with Alaskan populations removed, we found that opercle variation of only McKenzie River individuals along PC1 looks similar to the shape changes with the Alaskan populations included except that the opercles are not as narrow along dorsal edge, characteristic of marine populations. PC1 explains ~37% of shape variation without Alaskan populations included. This underscores the idea that opercle PC1 shape changes are shared among populations globally.

To determine if opercle PC1 scores displayed population specific distributions, we separated the PC1 scores for each population. We observed that opercle PC1 scores in populations along the McKenzie did not follow the distributions observed for lateral plates, rather, the PC1 scores were normally distributed across populations (Fig. 2.3B). Riverbend had the majority of observations and was the only site to differ significantly towards a more freshwater shape than the other McKenzie River populations (Tukey HSD; $p<0.05$).

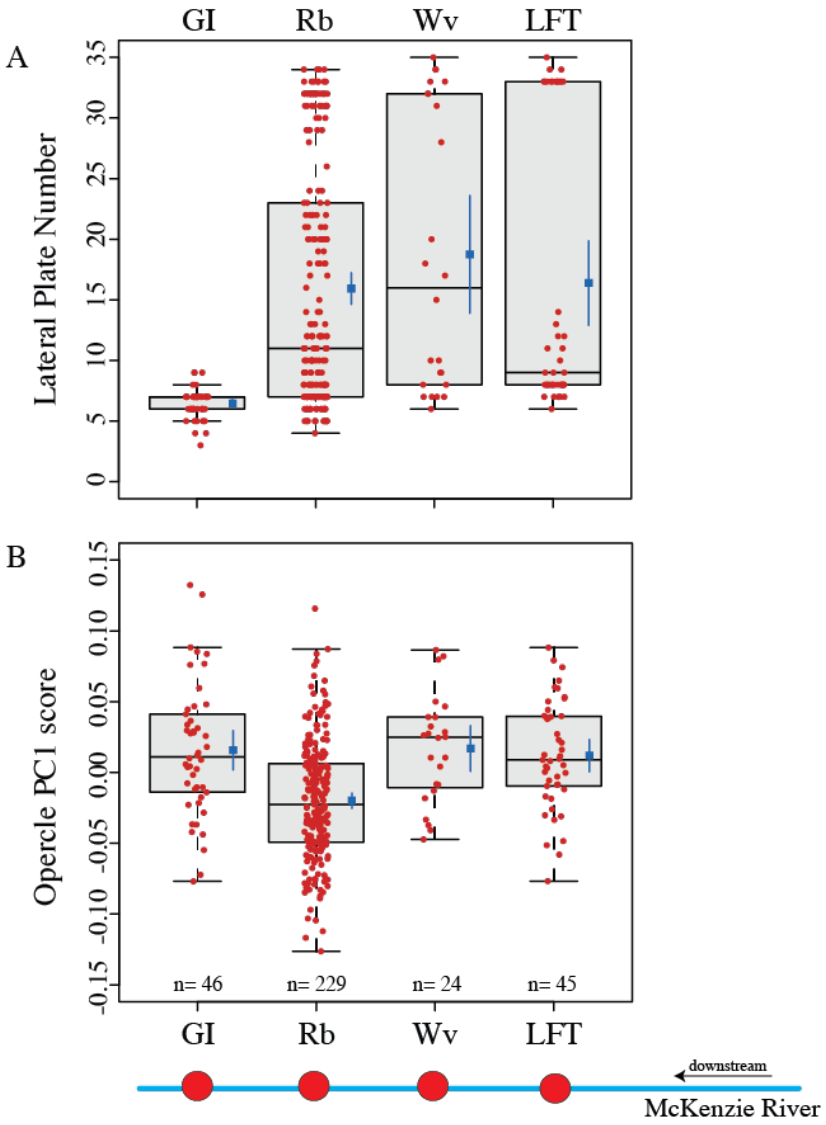

Figure 2.3. Phenotypic distributions of lateral plate number (A) and opercle PC1 scores (B) for individuals collected along the McKenzie River at each collection site. Boxplots are overlaid with individual values (jittered red dots). The mean (blue square) and 95% confidence interval around the mean are offset. Sites are organized according to their position along the McKenzie with direction of flow labeled. GI, Green Island; Rb, Riverbend; Wv, Walterville Slough; LFT, Leaburg Fish Trap.

.

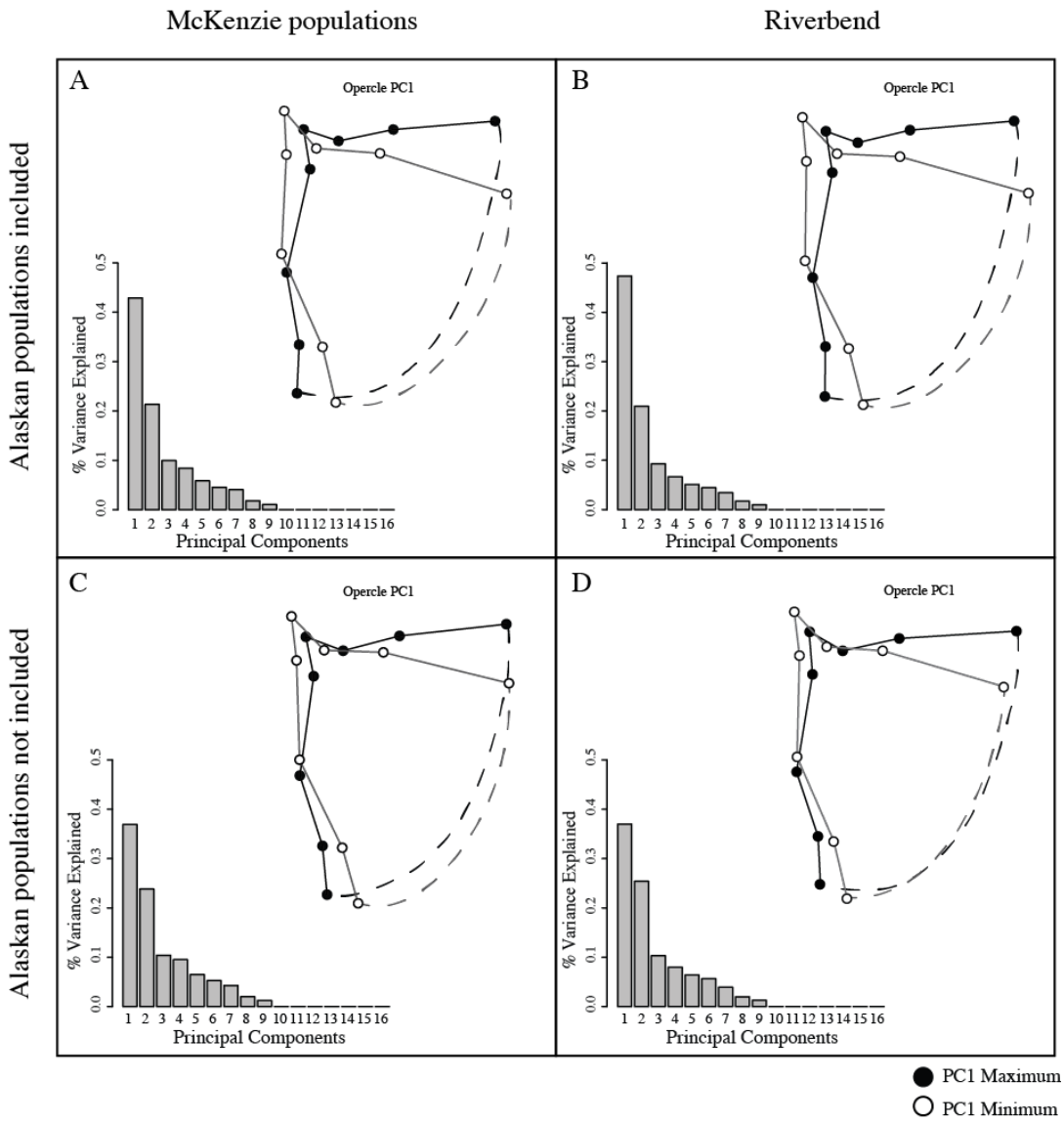

Figure 2.4 Opercle shape variation among populations along the McKenzie, within Riverbend, and with and without divergent, post-glacial Alaskan populations to anchor morphospace. Wireframe opercle shapes depict rendered shapes at the extremes of PC1. Black circles are PC1 maximum, open circles are PC1 minimum, dotted lines depict the opercle fan. Percent variance explained by each PC is shown.

The presence of phenotypic variation among McKenzie River stickleback suggest that this population may be well suited to identify the genomic regions and potentially genes that contribute to skeletal variation using a GWAS approach. Furthermore, the differences in distribution and range of the phenotypic space covered by lateral plate count and opercle shape in the McKenzie river also suggests that the genomic sources that contribute to phenotypic variation may be independent.

Absence of Phenotypic Correlations between the Opercle and Lateral Plate Phenotypes Indicates Independent Genetic Architectures

Pleiotropy has been hypothesized to contribute to the correlated evolution of phenotypes, often through constraint caused by different opposing directions of selection on each trait (Lande 1980; Pavlicev et al. 2006; Pavlicev et al. 2008). We decided to first examine this hypothesis by assessing if phenotypic variation is correlated between traits both within and among populations (Berg 1960; Armbruster et al. 2014). If correlations exist among evolving phenotypes, pleiotropic effects cannot be ruled out. However, if correlations are absent, pleiotropic effects are likely not major contributors to present phenotypic variation. Based on the differences in the distributions of lateral plate number and opercle PC1 shape variation described above (Fig. 2.3B,C), we do not expect that pleiotropy contributes to patterns of lateral plate number and opercle PC1 shape variation.

To explicitly test this hypothesis, we calculated the correlations between opercle PC1 shape and lateral plate count, among and within populations, using bivariate linear regression. We found no evidence for phenotypic correlation among or within populations (all populations, r^2= -0.003, p=0.8; GI, r^2= 0.036, p=0.1; Rb, r^2= -0.002, p=0.5; Wv, r^2= -0.043, p=0.8; LFT, r^2= -0.007, p=0.4). This suggests that, for these phenotypes, pleiotropy does not contribute significantly to phenotypic variation present in stickleback from the McKenzie River, and that the genetic architectures of lateral plate number and opercle PC1 shape variation are distinct (Fig. 2.5).

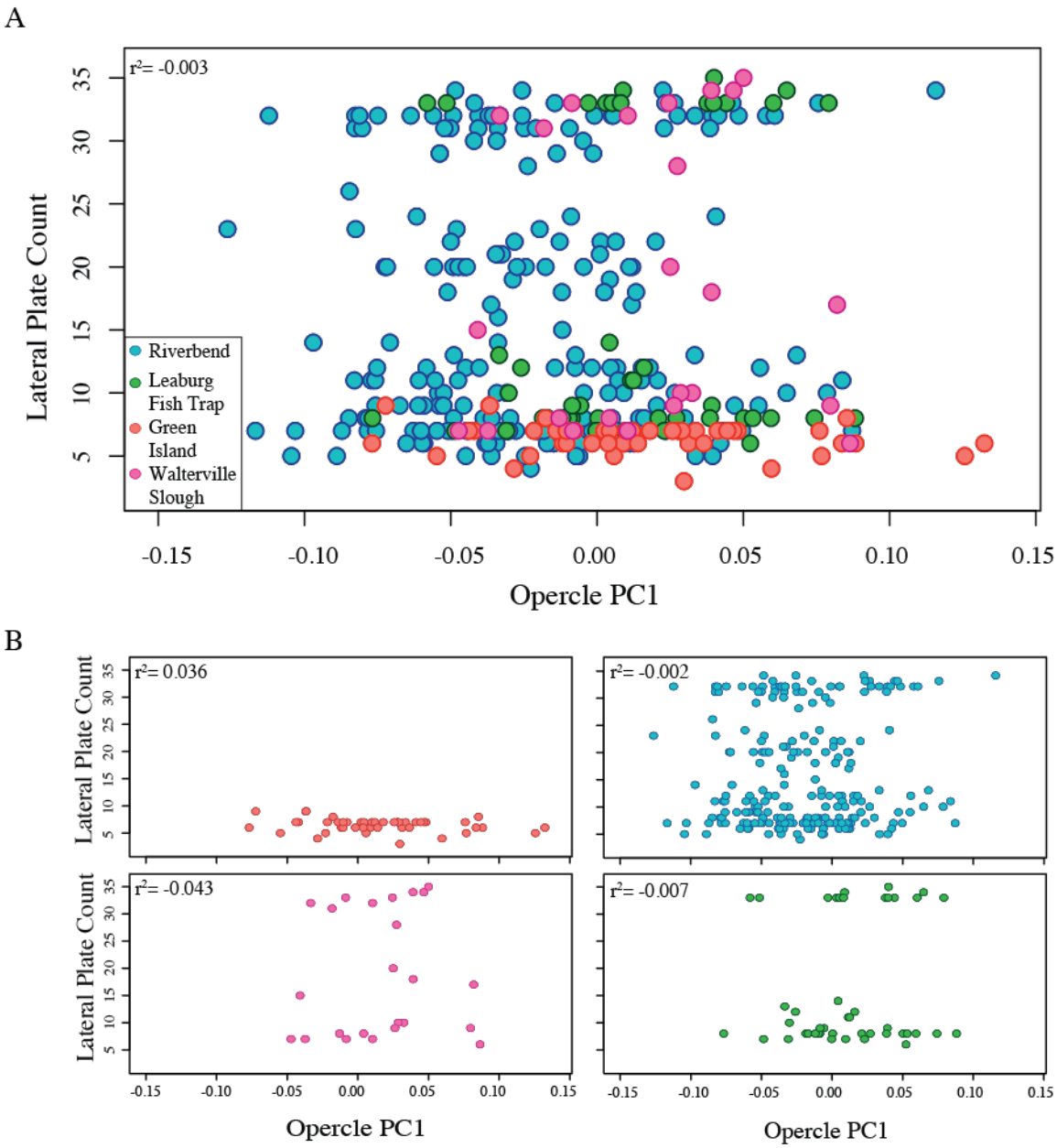

Figure 2.5 Correlation between lateral plate number and opercle PC1 scores among (A) and within (B) McKenzie River populations.

Population Genetic Variation Appears to be Generated Through Neutral Processes and Exhibits Spatial Structure along the McKenzie River

To investigate the patterns of genetic variation segregating among McKenzie River populations, we assessed population structure using 1000 randomly selected markers and PCA (see Methods). We found evidence for population structure and saw that genetic variation mirrored the population's physical location along the McKenzie (Fig. 2.6A). The first major axis explained 35.15% of the genetic variation (PC2 explained only 2.55%). Individuals from Green Island and Leaburg Fish Trap, representing the downstream and upstream ends of the sampling locations, respectively, tightly clustered in their respective groups on opposite sides of PC1 ordination space. Riverbend and Walterville Slough, which are the geographically intermediate populations, fell between Green Island and Leaburg Fish Trap along PC1, and covered a wider range of the ordination space (Fig. 2.6A,B).

The population structure observed may be explained by isolation-by-distance caused by spatial separation of the populations, local adaptation, or some combination of both. To begin to identify if spatial differentiation is due to selective or neutral processes, we used all pairwise combinations of markers between all individuals and calculated genome wide linkage disequilibrium (LD) as measured by r^2. This method allows us to identify patterns of genomic correlation both within and between linkage groups. Because selection acts heterogeneously across the genome, we expect that if selection is the major driver of population structure, a portion of the genome would be in very high LD - some of which would be across linkage groups - where as other genomic regions would show little LD (see Chapter III, Middleton Island for a good example). We also expect that the blocks of high LD within linkage groups would display between linkage group LD as a product of producing an artificially admixed population (see Chapter III, Middleton Island). If, however, neutral processes, which largely act homogeneously across the genome, were primarily responsible for the population structure along the McKenzie, when we pooled populations we would expect to see an overall increase in LD across the genome with little evidence of between linkage group LD.

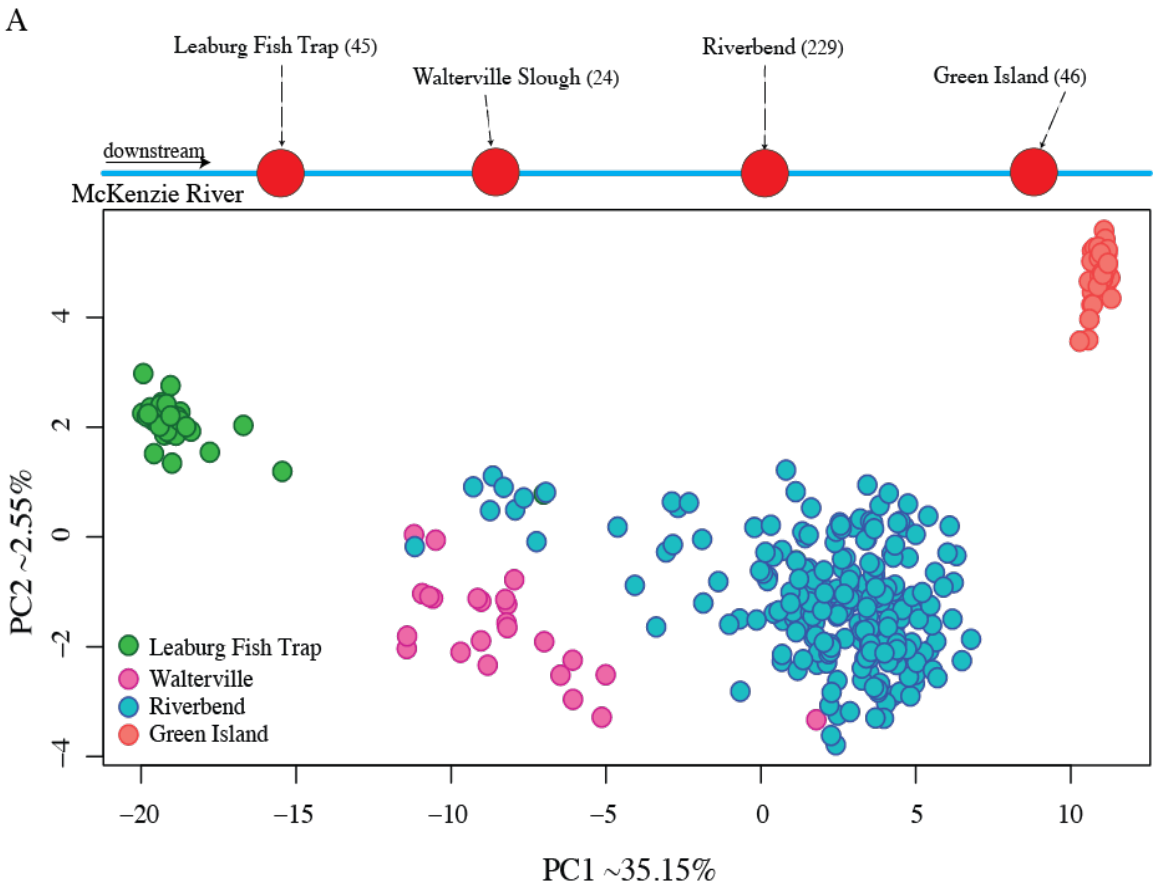

Figure 2.6 Population structure along the McKenzie River reflects proximate physical locations. A) Principal Component Analysis (PCA) of 1000 randomly selected loci across genome shows that population location on the McKenzie River is the primary axis along which variation is partitioned (35.15%). PC2 (2.55% variation explain) and beyond account for much less of the variation among individuals. Individuals from Leaburg Fish Trap (green) and Green Island (orange) are clustered tightly, but individuals from Walterville Slough and Riverbend occupy a larger phenotypic area. B) Boxplot and distributions of each population shows differences in clustering of PC1 scores. The group of Riverbend individuals which occupy Walterville Slough's genetic space could indicate a set of recent migrants into the Riverbend population.

Visualization of genome wide LD patterns show blocks of high LD within linkage groups (average LD within linkage groups $r^2 = 0.17$) and an overall elevation LD across the genome ($r^2 = 0.10$). Although the average whole genome r^2 value was elevated, we did not find any systematic patterns of genomic correlation between linkage groups (Fig. 2.7A). These results suggest that the population structure observed with PCA is due to neutral divergence that acts globally across the genome.

Population structure at any scale can impede one's ability to identify the genetic variants that contribute to phenotypic variation (Marchini et al. 2004). However, populations whose structure is primarily created by neutral processes are more amenable to GWAS because it is easier to control for spurious associations but not remove the signal that contributes to the phenotypic variation of interest (Price et al. 2010). The lack of selection driven genetic variation among populations from the McKenzie River, together with phenotypic variation, provides an attractive system to pursue a search for the genomic and genetic bases of lateral plate and opercle shape variation.

Patterns of Relatedness Vary between Individuals from Different Populations

Calculating the pattern of relatedness between pairs of individuals (often summarized by PCA) has become an essential step to control for population structure in a GWAS (Astle and Balding 2009). We, therefore, calculated and visualized average relatedness among individuals in the McKenzie River. Unlike our PCA, we used all markers available and employed GEMMA to calculate the matrix of relatedness in all pairwise combinations of individuals. Figure 2.8 shows the mean centered relatedness coefficients between all individuals colored by individuals within or between populations. Because the Riverbend sample size is larger than other populations examined, within comparisons of Riverbend individuals are predominantly responsible for defining the mean relatedness coefficient.

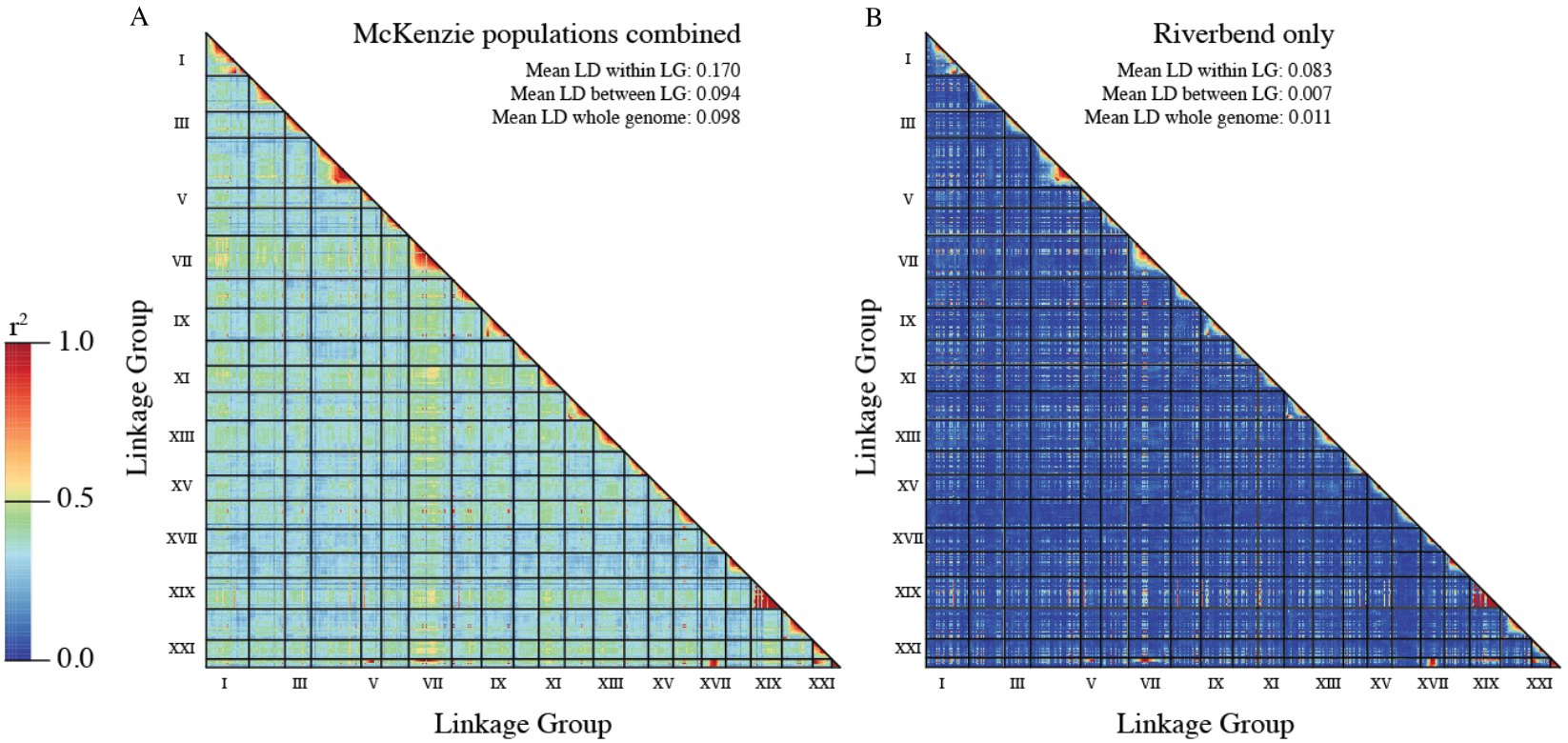

Figure 2.7. Comparison of genome wide linkage disequilibrium between a pooled sample of the four populations on the McKenzie River (A) and only the Riverbend population (B). Genome wide linkage disequilibrium is calculated as r^2 in PLINK (see methods). Linkage groups are displayed I-XXI and the five largest scaffolds are also included at the end. The diagonals are r^2 comparisons within linkage groups and the off diagonals are comparisons between linkage groups. The mean linkage disequilibrium within linkage groups, between linkage groups, and across the whole genome is noted.

Overall, we found that individuals chosen between populations were less related to each other than they were between individuals within populations. Two exceptions are the comparison between Leaburg Fish Trap:Walterville Slough and Riverbend:Green Island. These population pairs are more related to each other than on average across the McKenzie. Increased relatedness and proximate locations of population pairs suggests that the pairs may experience gene flow. The complex relationships of individuals from very closely to distantly related individuals highlight complicated population structure along the Mckenzie. Because appropriately controlling for population structure is known to be a challenge (Price et al. 2010; Sul and Eskin 2013), pooling individuals along the McKenzie likely presents a difficultly for interpreting GWAS results in this system. An alternative is to focus within one McKenzie population which shows phenotypic variability but which has a simpler population structure.

Figure 2.8 Mean centered relatedness coefficients between all pairwise combinations of individuals along the McKenzie River. A mean center of zero is indicated by the gray dashed line. Within and between population comparisons are denoted by color and abbreviation, and location along McKenzie River shown in river cartoon. GI, Green Island; Rb, Riverbend; Wv, Walterville Slough; LFT, Leaburg Fish Trap. A) Density distributions for all populations in stacked barplot. B) Density distributions separated by population.

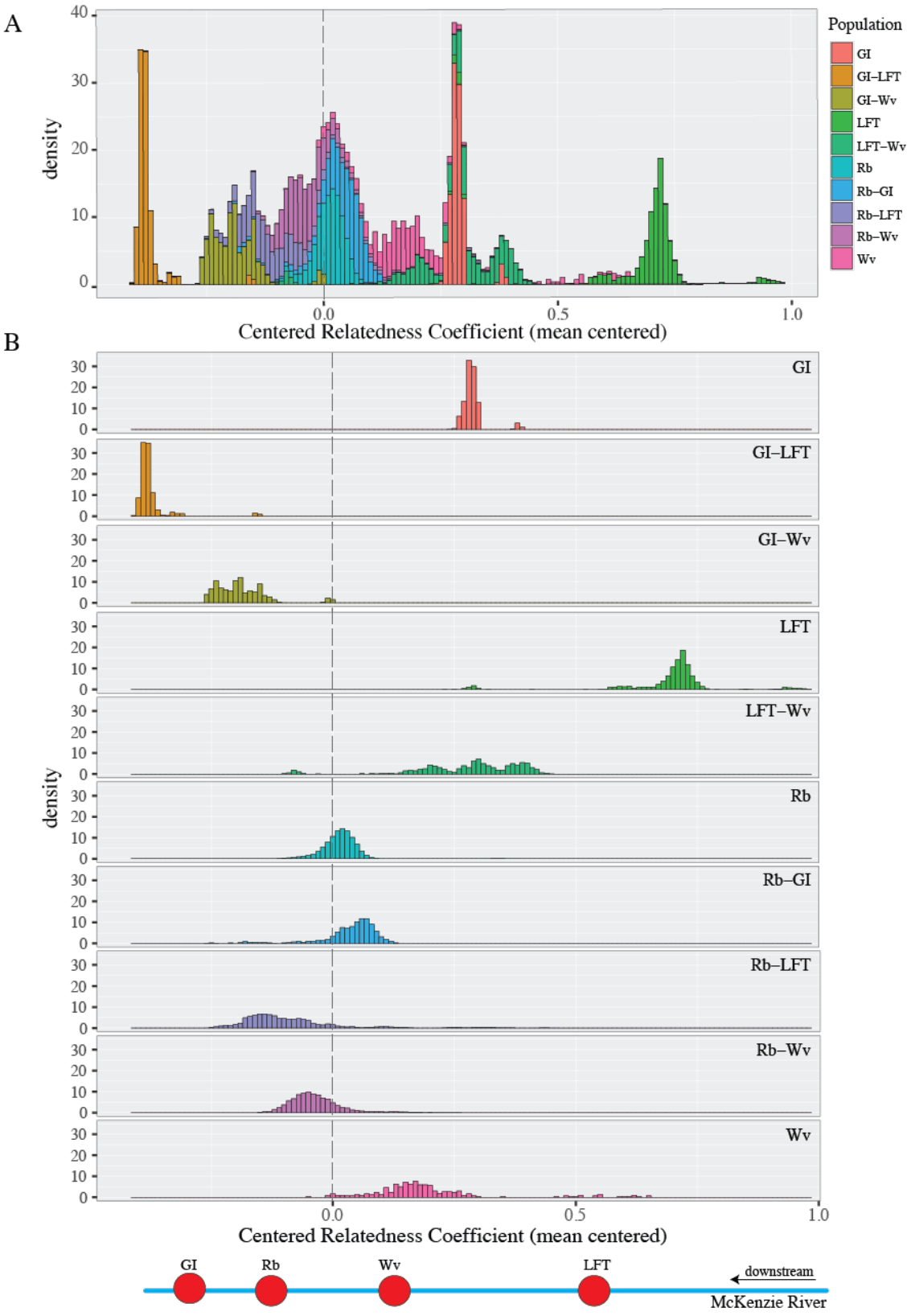
A
B
density
Centered Relatedness Coefficient (mean centered)
Population
GI
GI–LFT
GI–Wv
LFT
LFT–Wv
Rb
Rb–GI
Rb–LFT
Rb–Wv
Wv
0.0
0.5
1.0
GI
Rb
Wv
LFT
downstream
McKenzie River

The Riverbend Population is Phenotypically Variable with Little Genetic Structuring

Phenotypic variation among individuals collected from Riverbend reflect the phenotypic variation present among individuals collected along the McKenzie River. Stickleback with a low number lateral plates, typical of freshwater environments, dominate the population. However, individuals with intermediate and high numbers of lateral plates were also sampled revealing a trimodal distribution (Fig. 2.9B). Opercle PC1 shape (~47% variance explained with AK individuals included), like the McKenzie River collection, is normally distributed with the majority of individuals falling within the phenotypic space defined by individuals from the freshwater monomorphic Alaskan population (Fig. 2.9C).

Unlike individuals from the combined McKenzie River populations, individuals sampled from Riverbend display little population structure. The first factor (PC1) of an analysis between collection dates which span a three-year period only explained 5.62% of variation (PC2 explains 3.23% of variation), suggesting that a large proportion of variation among individuals cannot be projected onto any one ordination axis (Fig. 2.10). Although, notably, 10 individuals from the most recent collection date clustered away from the other 219 individuals. Overall, genomic correlation genome-wide is lower in the Riverbend population (average r^2=0.01) compared to the combined McKenzie populations (average r^2=0.10). Analysis of genome-wide linkage disequilibrium within the Riverbend population shows that blocks of high LD are present within linkage groups, similar to combined McKenzie populations, but that LD among linkage groups is lower than the combined McKenzie populations. The Riverbend population is nearer equilibrium (Fig. 2.7B). Finally, individuals in Riverbend do not show complex patterns of relatedness, but rather are normally distributed about the mean (Fig. 2.11). Taken together, phenotypic variability and little underlying population structure suggest that stickleback from Riverbend comprise an ideal population for GWAS.

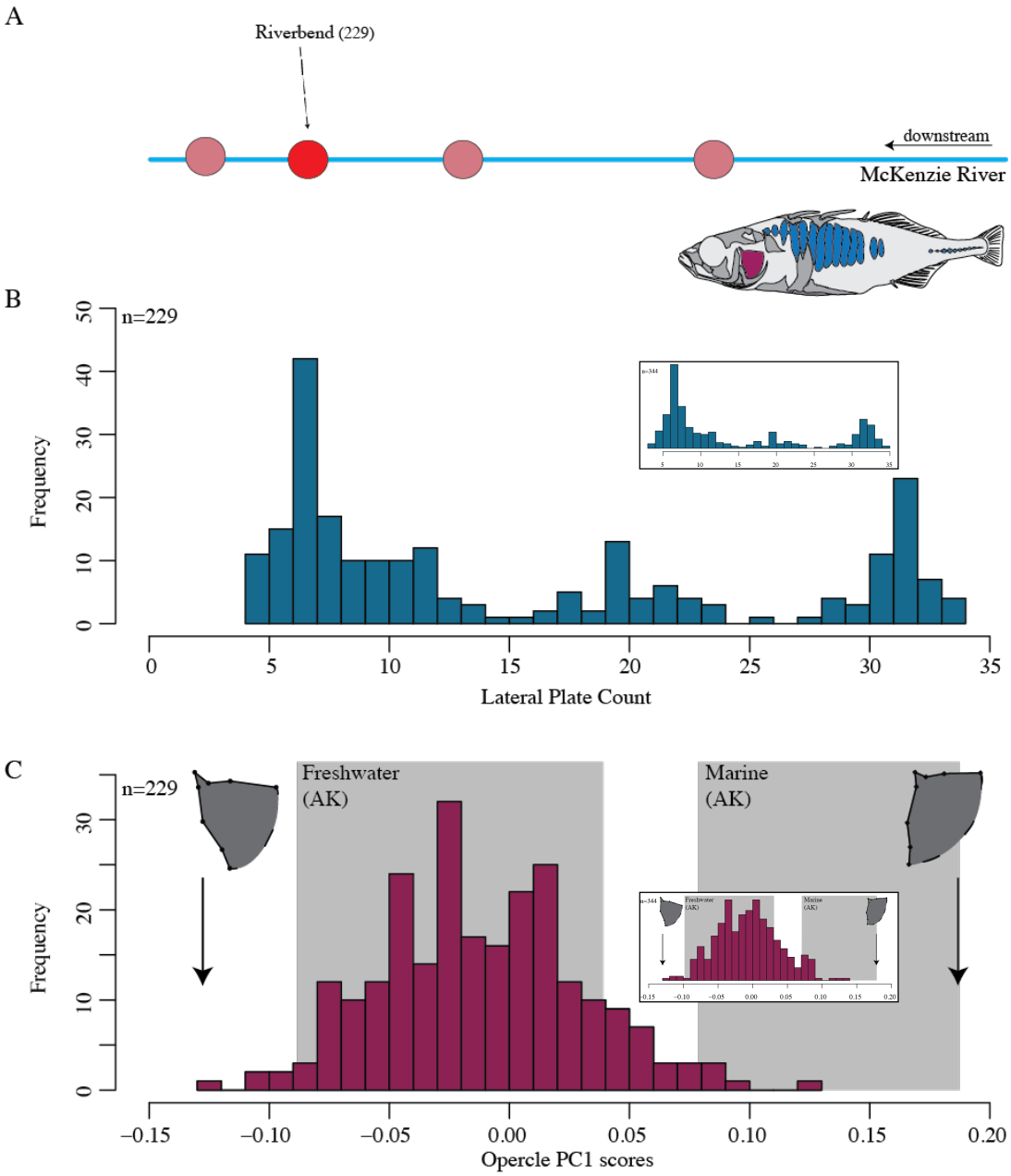

Figure 2.9 Phenotypic distributions of lateral plate count and opercle shape in Riverbend reflect the discordant distributions observed across all McKenzie River populations. A) Location of Riverbend with respect to other McKenzie River populations. Stickleback line drawing highlights the location of lateral plates and the opercle bone. Colors for lateral plates (blue) and opercle (purple) are used in B and C, respectively. Sample size is indicated for the Riverbend population, n=229. Frequency distribution of lateral plate count (B) and opercle shape (C) in stickleback collected from the Riverbend population. Frequency distribution in Riverbend reflects frequency distribution for pooled populations along the McKenzie (inset). C) Gray boxes indicate morphospace occupancy of post-glacial, divergent marine and freshwater Alaskan stickleback included in PCA to help anchor the morphospace. Opercle shapes at the extremes of PC1 are shown.

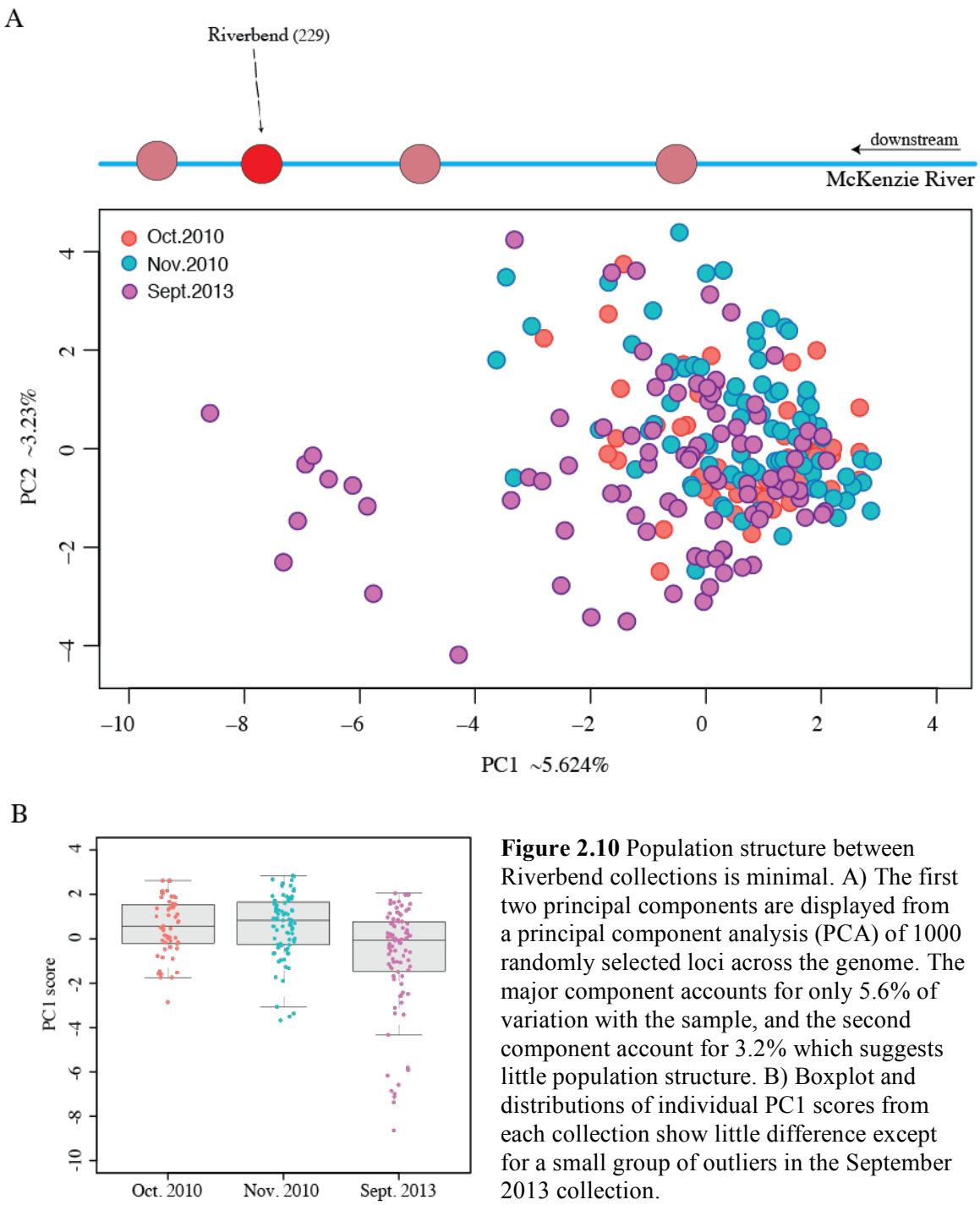

Figure 2.10 Population structure between Riverbend collections is minimal. A) The first two principal components are displayed from a principal component analysis (PCA) of 1000 randomly selected loci across the genome. The major component accounts for only 5.6% of variation with the sample, and the second component account for 3.2% which suggests little population structure. B) Boxplot and distributions of individual PC1 scores from each collection show little difference except for a small group of outliers in the September 2013 collection.

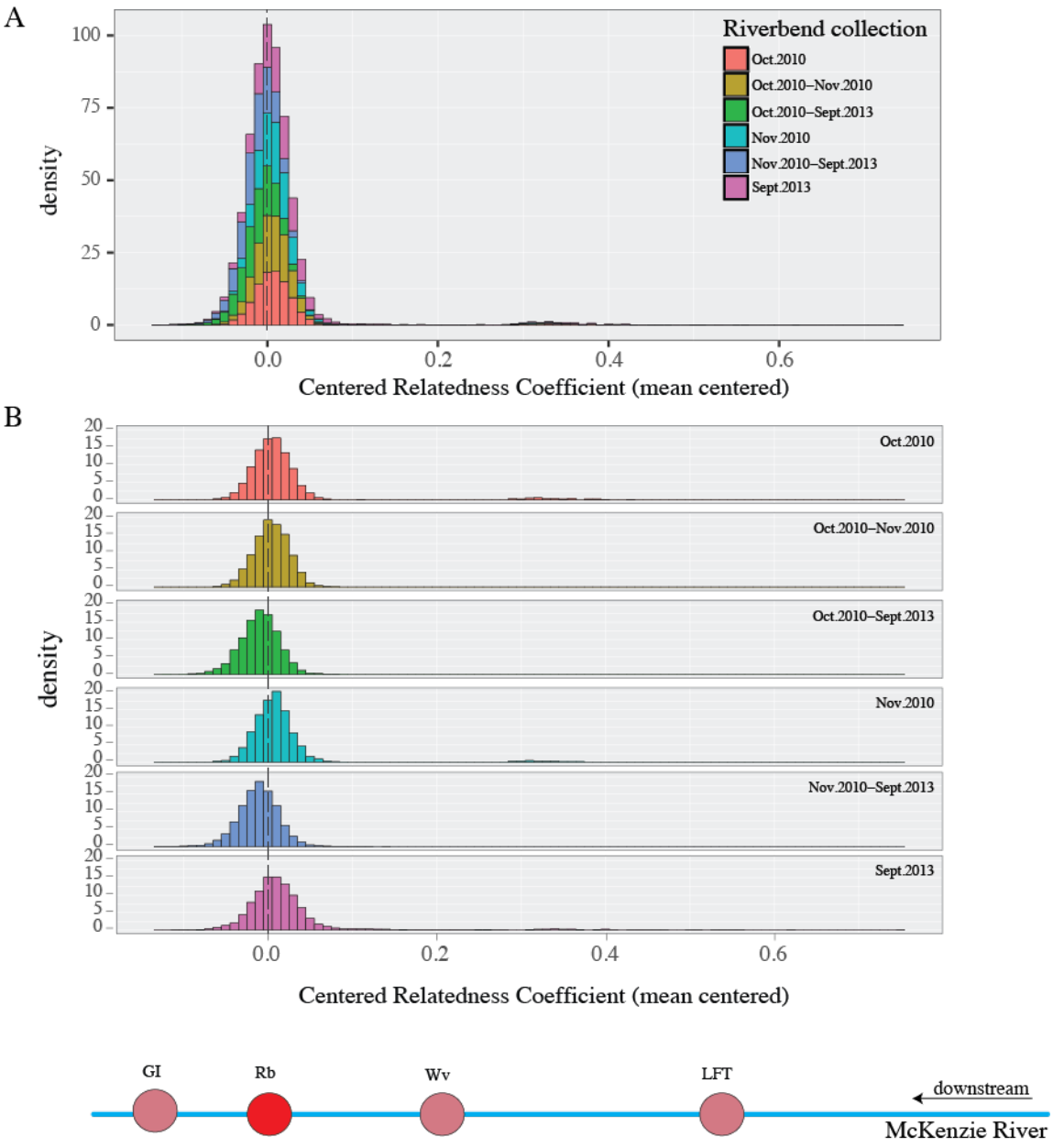

Figure 2.11 Mean centered relatedness coefficients between all pairwise combinations of sampled individuals in Riverbend. A mean center of zero is indicated by the gray dashed line. Within and between population comparisons are denoted by color and collection date. Location along McKenzie River shown in river cartoon. A) Density distributions for all collections in stacked barplot. B) Density distributions separated by collection date.

GWAS Uncovers Multiple Genomic Regions Associated with Variation in Lateral Plate Count and Opercle Shape

Using individuals from the Riverbend population, we conducted a GWAS using the software GEMMA (Zhou and Stephens 2012) to determine the genomic regions, and potentially genes, that are associated with phenotypic variation of lateral plate count and opercle shape while controlling for population structure and limiting spurious associations using a mean centered relatedness matrix. For lateral plate count, we expected to find genomic regions that had previously been implicated in loss of lateral plates such as the major effect locus, ectodysplasin (*eda*), and potentially additional modifier loci. For opercle shape, we expected to find variants that contribute primarily to freshwater variation and less to the marine-freshwater transition. Although opercle shape is thought to be polygenic (Kimmel et al. 2005), it remains unclear if the architecture includes a locus of major effect or if the loci that contribute are all of small effect.

Two Genomic Regions are Associated with Lateral Plate Count

Following permutation tests to generate a genome-wide significance level, ($p < 4.38 \times 10^{-06}$, see Methods), we identified two genomic regions associated with lateral plate count variability. A large peak on LG 4 spans a genomic region that encompasses ectodysplasin (*eda*), the gene previously identified as the major effect locus for lateral plate loss in the marine-freshwater transition (Colosimo et al. 2005). Because we expect that the genomic region containing *eda* should be associated with lateral plate number, these results give us confidence that GWAS in the Riverbend population is informative (Fig. 2.12).

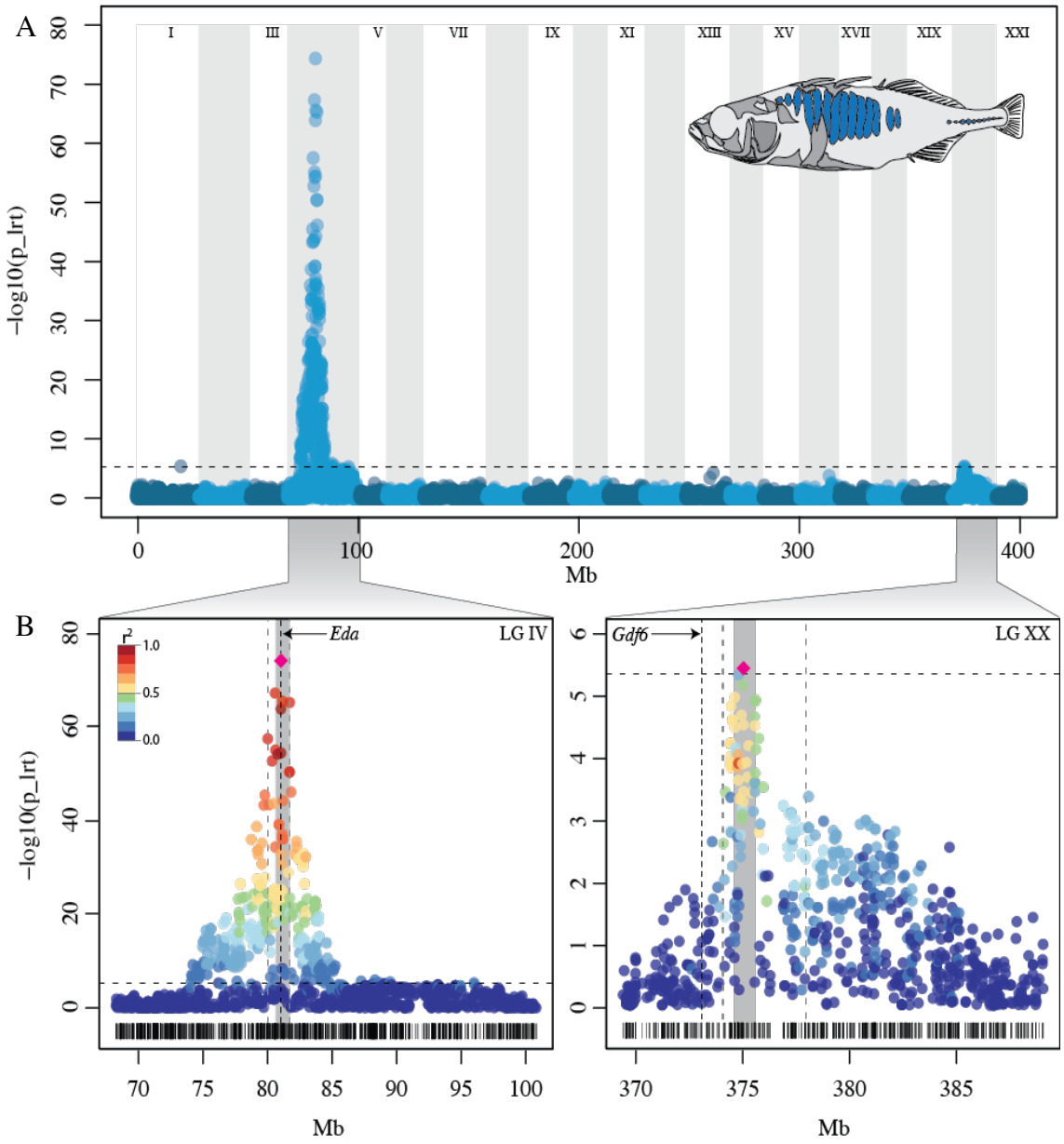

Figure 2.12 Manhattan plot visualizing genomic regions of association between genotype and lateral plate number variation. LMM GWAS identifies two genomic regions associated with the phenotype on linkage group IV and linkage group XX. Genome wide significance level shown by horizontal, dashed black line determined through phenotypic specific permutations. -$\log_{10}$(*p*-vals) show significance of association and were calculated through the likelihood ratio test (LRT) in GEMMA software. A) Genome wide Manhattan plot. Alternating gray bars depict linkage group boundaries. B) Single linkage group view of associations on LG IV and LG XX. Vertical black bars below Manhattan plots show position of RAD markers along the linkage group. Magenta diamond shows the top associated SNP. Linkage decay of every other SNP to the top SNP was calculated with r^2 correlations and visualized by a red-blue color palette. Credible interval calculated by linkage decay bounded by vertical gray dashed lines. Candidate genes from credible interval are reported from the small gray box surrounding the top SNP for simplicity (Table S2.1). Vertical black dashed lines indicate the location of previously identified genes of interest with lateral plate phenotypes (*eda*, *gdf6*).

We examined the genotypic effect of the most highly associated SNP on the number of lateral plates. Few individuals had the AA genotype (Fig. 2.13A), but all individuals displayed high lateral plate counts (mean = 31.5; Fig. 2.13A; Fig. 2.14A). The majority of individuals had the alternative homozygous genotype, GG, and had significantly fewer lateral plates (mean = 8.7; Tukey HSD, $p<0.05$). Unlike the plate count for AA homozygote individuals, the distribution of plate count for GG homozygote individuals was larger. These results suggest that either other loci contribute, or that the environment can influence variability observed within individuals with reduced lateral plate counts. Mean plate count of the AG heterozygotes appears to have incomplete dominance (Fig. 2.14A; mean = 26.6), however, because the distribution is bimodal (Fig. 2.13D). One group of AG fish are completely plated, similar to individuals with the AA genotype, but a second group of fish are largely intermediate between the two alternative homozygote individuals (Fig. 2.13A, D). These findings are of interest because in most mapping studies the heterozygous genotype shows complete or nearly complete dominance for high lateral plate counts (but see Erickson et al. (2016)). Our results, therefore, suggest a role for modifier loci.

Figure 2.13. Genotypic effect of most highly associated SNP on chromosome 4 and chromosome 20 on lateral plate count phenotype. (A-C) Boxplots and distributions of individuals with available genotypes at each locus and the corresponding lateral plate count. Genotypes are organized from left to right to show the higher, or more "oceanic" (Oc), lateral plate number to the lower, more "freshwater" (F), lateral plate number genotype. A) Genotypic effect on lateral plate number at chromosome 4. B) Genotypic effect on lateral plate number at chromosome 20. C) Interaction between genotypes of the most highly associated SNP on chromosome 4, labeled by dark blue (AA), green (AG), and light blue (GG) colors, and genotypes of the most highly associated SNP on chromosome 20, indicated by left to right order. No individuals have both the chr4(AA) and chr20(CC) genotype. D) Lateral plate number frequency distribution of individuals with the heterozygote (AG) at the chromosome 4 SNP. Representative line drawings of stickleback within the two groups are shown.

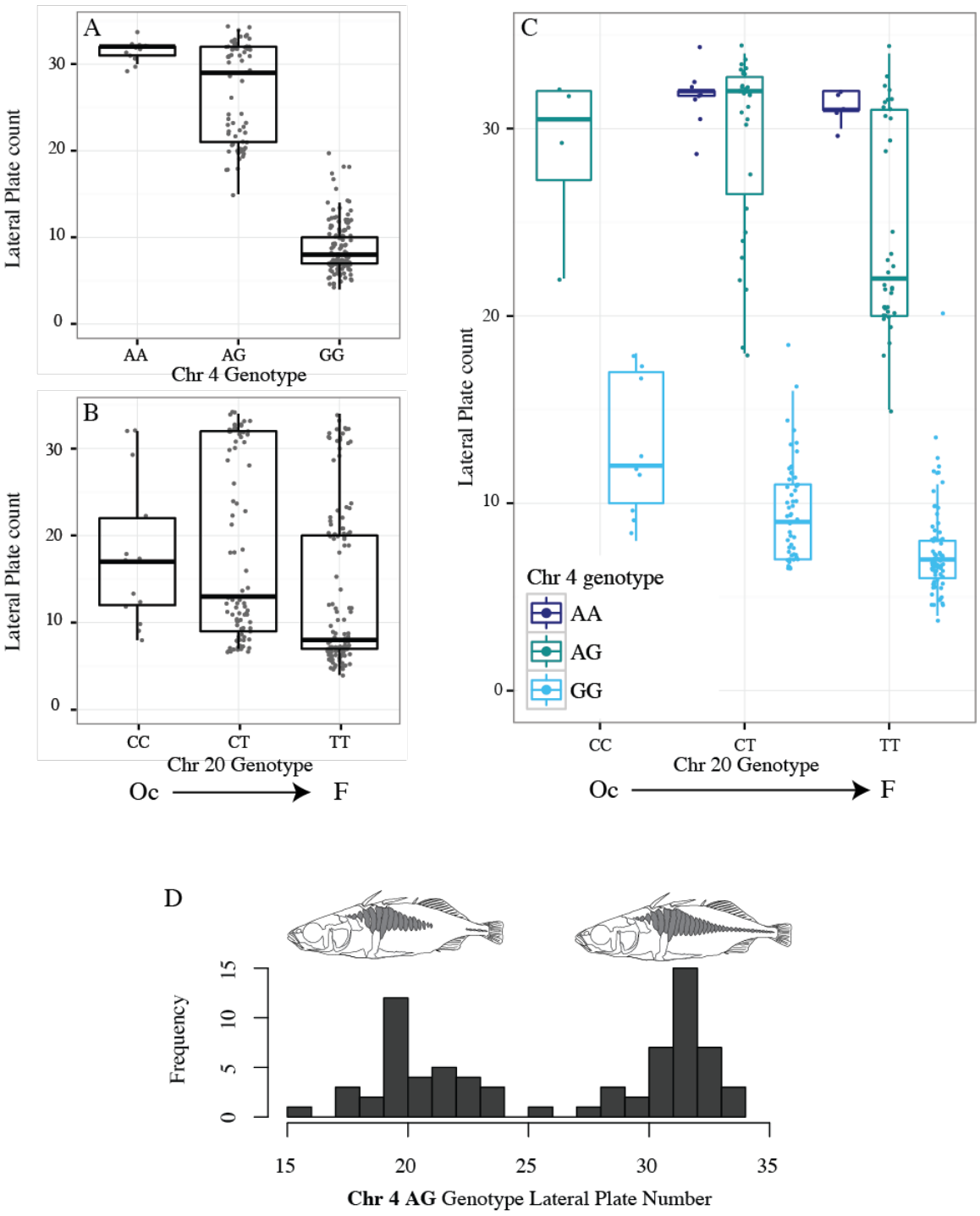
A
Lateral Plate count
30
20
10
0
AA
AG
GG
Chr 4 Genotype
B
Lateral Plate count
30
20
10
0
CC
CT
TT
Chr 20 Genotype
Oc
F
C
Lateral Plate count
30
20
10
0
Chr 4 genotype
AA
AG
GG
CC
CT
TT
Chr 20 Genotype
Oc
F
D
Frequency
0
5
10
15
15
20
25
30
35
Chr 4 AG Genotype Lateral Plate Number

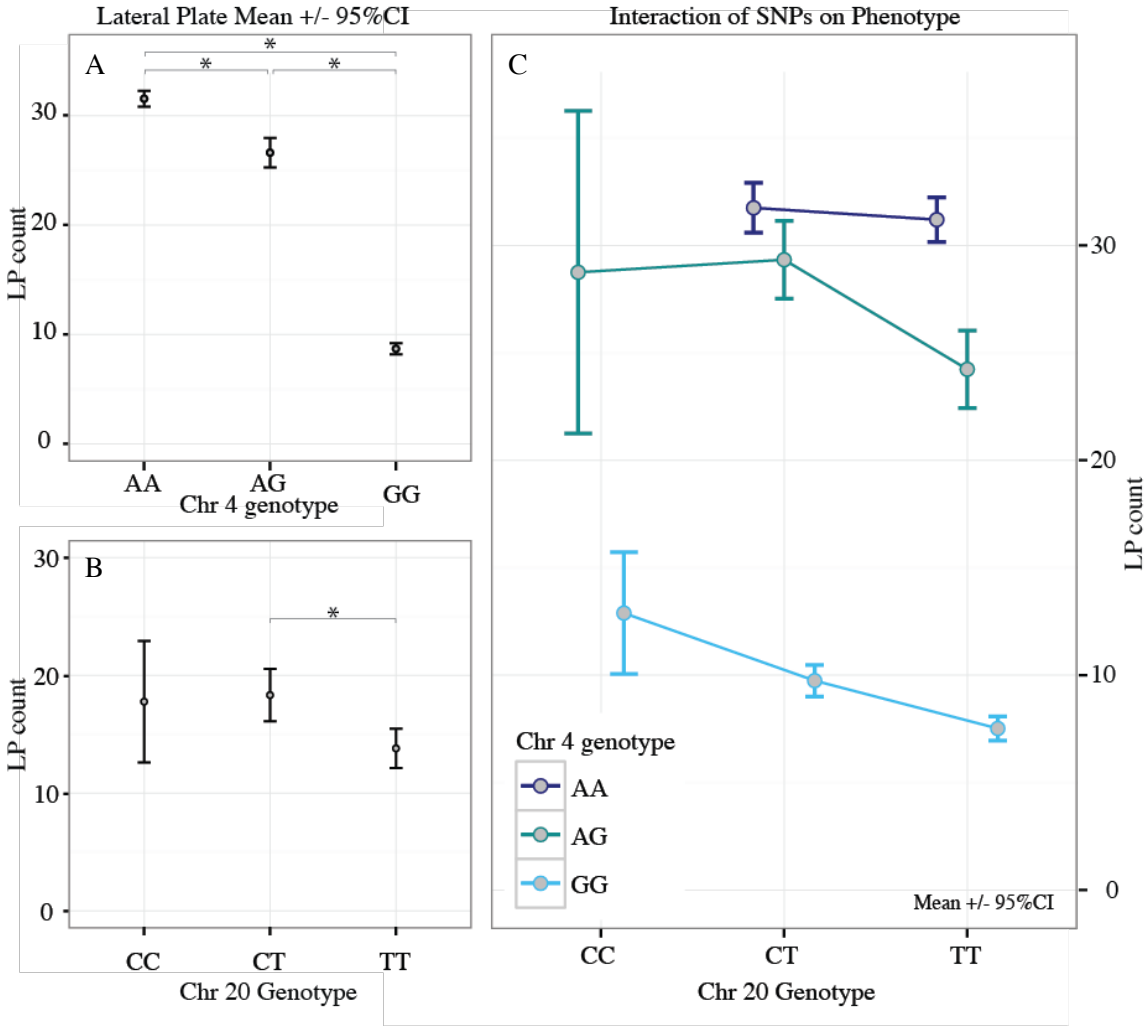

Figure 2.14 Mean lateral plate count (+/- 95% CI) of the most highly associated SNP genotype at chromosome 4 and chromosome 20 (A, B) and the interactions among genotypes (C). In each panel, genotypes organized from more "oceanic" to more "freshwater", left to right. Pairwise comparisons show if genotype had a significant effect on mean lateral plate number depicted by * (Tukey HSD; $p<0.05$)

We identified a second peak of association on LG 20 (Fig. 2.12) which has not previously been shown to be associated with lateral plate loss (Colosimo et al. 2004; Cresko et al. 2004; Colosimo et al. 2005; Conte et al. 2015). This peak is smaller and more narrow than the genomic region on LG 4, with only two SNPs at or above significance. The genotypic effect of the most highly associated SNP on the lateral plate phenotype was less clear than the effect of the top SNP on LG 4, with high, low, and intermediate lateral plate numbers associated with each of the homozygote and heterozygote genotypes (Fig. 2.13B). Like LG 4, one homozygote genotype (CC) was more rare than other genotypes, but the mean lateral plate count was not significantly greater than mean plate count of the two other genotypes (Fig. 2.14B; Tukey HSD $p>0.05$). Both the heterozygote (CT) and alternative homozygote (TT) tend to include more fish with low and intermediate numbers of lateral plates. Although groups of individuals with high and intermediate plate count were present for each CC and TT genotype, in a pairwise comparison, these genotypes had a significant effect on mean lateral plate count (Tukey HSD $p< 0.05$). The loci on linkage group 4 and 20 were in Hardy-Weinberg Equilibrium (HWE).

Genotypes at Loci on Linkage Group 4 and Linkage Group 20 May Interact

To determine if an interaction exists between the SNP on LG 4 and on LG 20 we first looked, and found no evidence, for long distance LD between the pair of SNPs (r^2 =0.002). This confirmed that the association on LG 20 was independent and not a spurious association caused by genomic correlation with LG 4. Next, we identified the effect of the multi-locus genotypes on lateral plate phenotype. Interestingly, no genotyped individual was a double homozygote for the AA (LG 4) and CC (LG 20) multi locus genotype (Fig. 2.15C). These homozygote genotypes would correspond to the highest plated genotypes at each locus on LG 4 and LG 20 and may indicate that this multi locus genotype combination has a low fitness in the freshwater environment.

We do not expect that genotypes on LG 20 interact with either the homozygote high plated genotype (AA) or the heterozygote LG 4 genotypes (AG) (Fig. 2.13C, Fig. 2.14C). However, the genotypes on LG 20 do appear to interact with the LG 4

homozygote low plated genotype (GG), modifying plate variation within the low plated LG 4 genotype (Fig. 2.13C, Fig. 2.14C,). This suggests a potential epistatic effect between the loci.

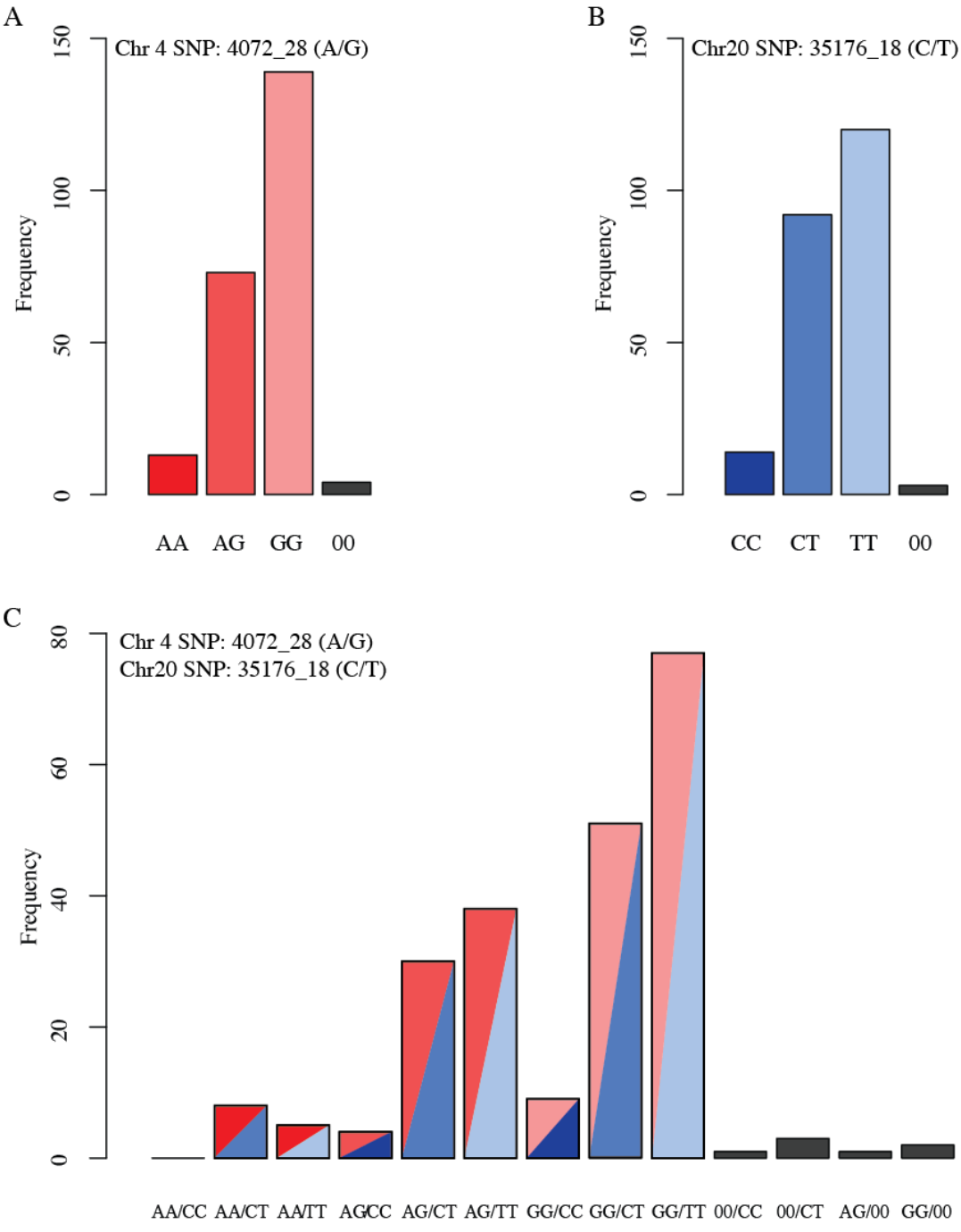

Figure 2.15 Genotype frequencies at each significantly associated locus (A, B) and multi-locus frequencies (C). Gray bars indicate missing genotypes. Both single locus genotype frequencies are in HWE. 00=individuals not genotyped at the locus

Genomic Intervals Are Defined by Decay of Linkage and Reveal a Potentially Novel Genomic Region that Contributes to Lateral Plate Variation

To identify the genomic region that we expect will include the causative locus, we attempted to define the genomic interval. Common practice in GWAS defines the interval in terms of local LD, and identifies the putative genomic region as that which includes SNPs in tight linkage ($r^2 \geq 0.8$) with the most associated SNP (see Methods). With these criteria, we identified an approximately 2 Mb genomic region on LG 4 that includes a known major effect locus of lateral plate number, *eda*, although we did find it interesting that the genomic region containing SNPs above the genome-wide significance level is >10Mb (Fig. 2.12). The credible interval region also encompasses two other candidate loci, *pdlim7* and *anxa6*, identified in an F_2 mapping family between lake and stream stickleback (Berner et al. 2014). *Pdlim7* was also identified as a candidate gene in an F_2 mapping family between ocean and freshwater stickleback (Hohenlohe et al. 2010). Notably, however, the gene closest to the most highly associated SNP is, indeed, *eda*.

While defining the genomic interval according to local LD was appropriate for the peak on LG 4, using this method for the peak on LG 20 was more difficult because few SNPs were in tight linkage ($r^2 \geq 0.8$) with the most associated SNP (Fig. 2.12). We attempted to remedy this problem in two ways. In the first, we converted *p*-values derived from the likelihood ratio test, generated in GEMMA (Zhou and Stephens 2012), into LOD scores to determine the 2-LOD interval (see Methods). This interval, however, spanned nearly the entire linkage group. We, therefore, considered this method too conservative. In the second method, we used a criterion to include any SNP correlated at a value of $r^2 \geq 0.4$ with the most highly associated SNP. The resulting interval included the narrow peak that rises to significance as well as a portion of the elevated shoulder to the right of the peak (Fig. 2.12). While the causative locus could be located anywhere in this interval, *ctnnb1* (β-catenin) is one of the genes that flanks the second most significant SNP on LG 20. This gene is particularly interesting because of *ctnnb1*'s role in canonical and non-canonical Wnt signaling and key function in skeletal development and bone mass accrual (Westendorf et al. 2004; Kramer et al. 2010). Notably, the second most associated SNP failed to be genotyped in ten individuals while the top SNP was only

missing in three individuals. Because the sample size is small, this genotyping discrepancy could contribute to subtle differences in *p*-value.

Two Linkage Groups Are Independently Associated with Opercle Shape

We identified two genomic regions associated with opercle PC1 shape (Fig. 2.16A). The first, on LG 8, is significantly associated with opercle PC1 shape, and the second genomic region on LG 7 is just shy of the genome-wide significance level ($p < 6.19 \times 10^{-06}$). We found no evidence for long distance LD between the two top SNPs at each locus ($r^2=0.005$) which suggests that the associations are real (i.e. no spurious associations caused by correlation). The phenotypes for all genotypes at both loci on LG 8 and LG7 were normally distributed except the TT homozygote on LG 7 (Fig. 2.17A,B). On LG 7, only 7 individuals were identified with the TT genotype but they fell into two distinct groups. The opercle PC1 shapes of heterozygote individuals on both linkage groups were intermediate with respect to the homozygotes. Interestingly, the genotypes of the loci at LG 7 and LG 8 appear to have phenotypic effects in directions different than one would expect by their frequencies (Fig. 2.18A,B). As expected, the genotype on LG 8 with the most individuals corresponds to the most freshwater phenotype. The opposite is true on LG 7 (Fig. 2.19). However, the distribution of all genotypes is shifted towards freshwater as compared to the distribution of phenotypes on LG 8. Both loci are in HWE, and there appears to be no interaction between the loci (Fig. 2.17C, Fig. 2.18C).

Genomic Intervals Reveal Candidate Genes Not Previously Implicated in Opercle Shape

We identify several candidate genes within the credible interval determined by linkage decay (see Methods). On LG 8, the *EPHB3* (*Eph receptor* B3) gene flanks the most highly associated SNP with opercle PC1 within the interval. *EPHB3* has recently been implicated as a regulator of bone growth in mice (Kamath et al. 2016) and is critical for cell-cell interactions during development (Matsuo and Otaki 2012). The region on LG 7 also contained several genes of interest including *b3gat3* that encodes glucuronyltransferase 1, an enzyme suggested to play a role in bone density (Jones et al.

2015), and *rcor2* which has recently been implicated in regulating osteoblast differentiation (Tarkkonen et al. 2016) (Fig. 2.16).

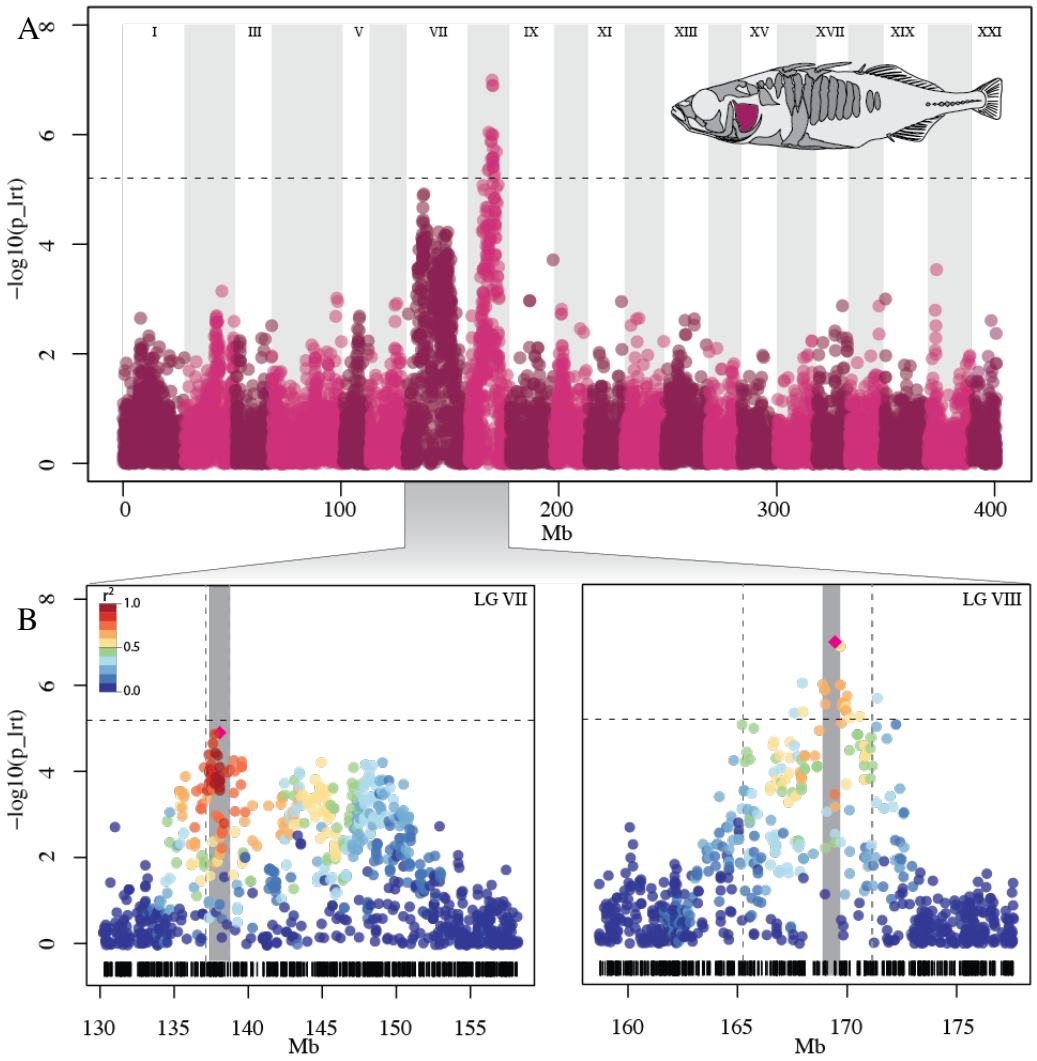

Figure 2.16 Manhattan plot visualizing genomic regions of association between genotype and opercle PC1 variation. LMM GWAS identifies a genomic region on LG VII that is suggestive of an association and another region of LG VIII that is significantly associated with the phenotype. Genome wide significance level (horizontal, dashed black line) is determined through phenotypic specific permutations. -$\log_{10}$(*p*-vals) show significance and were calculated through the likelihood ratio test (LRT) in GEMMA software. A) Genome wide Manhattan plot. Alternating gray bars depict linkage group boundaries. B) Single linkage group view of associations on LG VII and LG VIII. Vertical black bars below plots show position of RAD markers along the linkage group. Magenta diamond is the top associated SNP. Linkage decay of every other SNP to the top SNP was calculated with r^2 correlations and visualized by a red-blue color palette. Credible interval calculated by linkage decay bounded by vertical gray dashed lines. Candidate genes from credible interval are reported from the small gray box surrounding the top SNP for simplicity (Table S2.2).

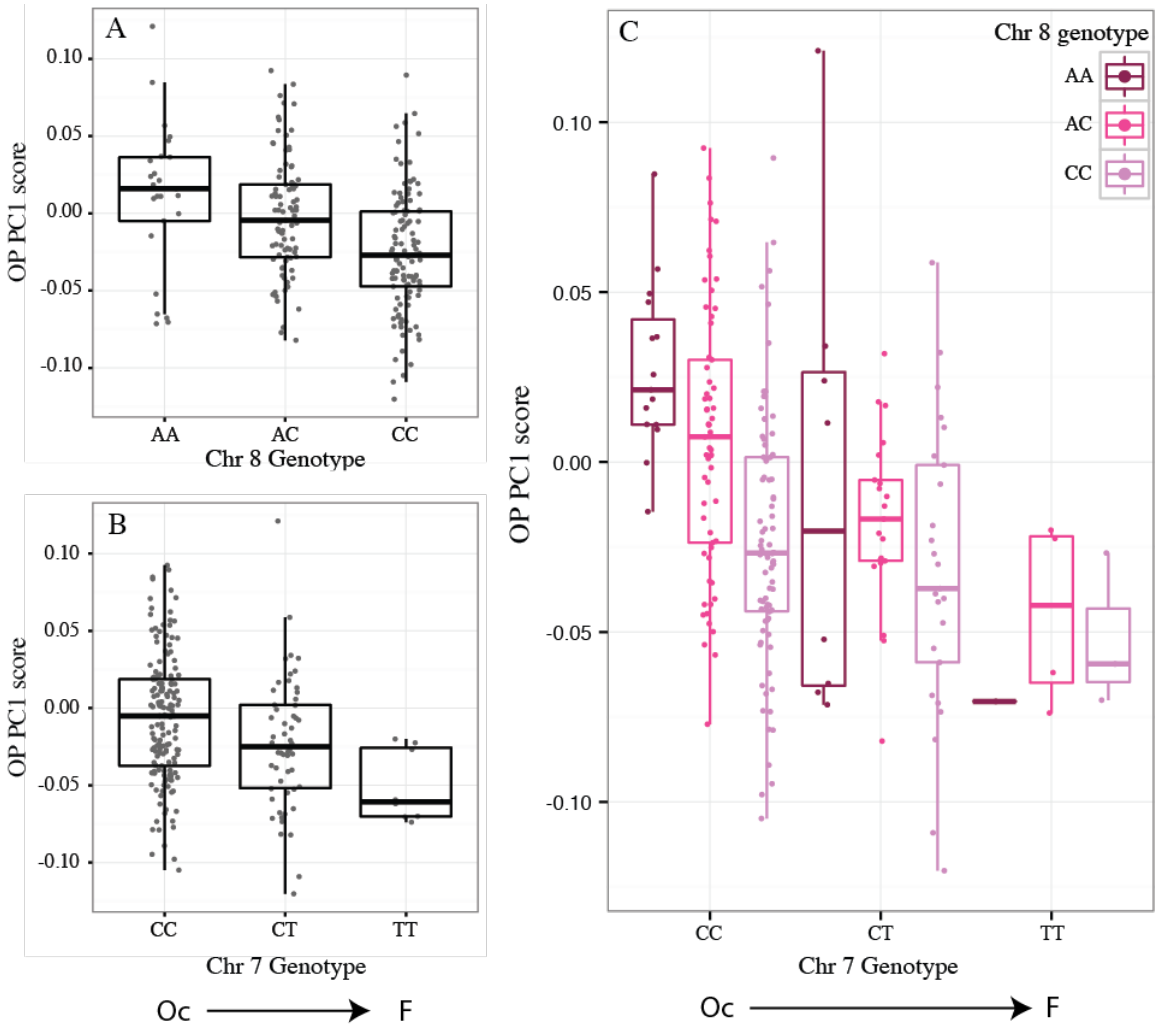

Figure 2.17 Genotypic effect of most highly associated SNP on chromosome 8 and chromosome 7 on opercle PC1 variation. (A-C) Boxplots and distributions of individuals with available genotypes at each locus and the corresponding lateral plate count. Genotypes are organized from left to right which show more "oceanic" (Oc) to "freshwater" (F), opercle shapes. A) Genotypic effect on opercle PC1 score at chromosome 8. B) Genotypic effect on opercle PC1 score at chromosome 7. C) The multi locus genotype effect on opercle PC1 score.

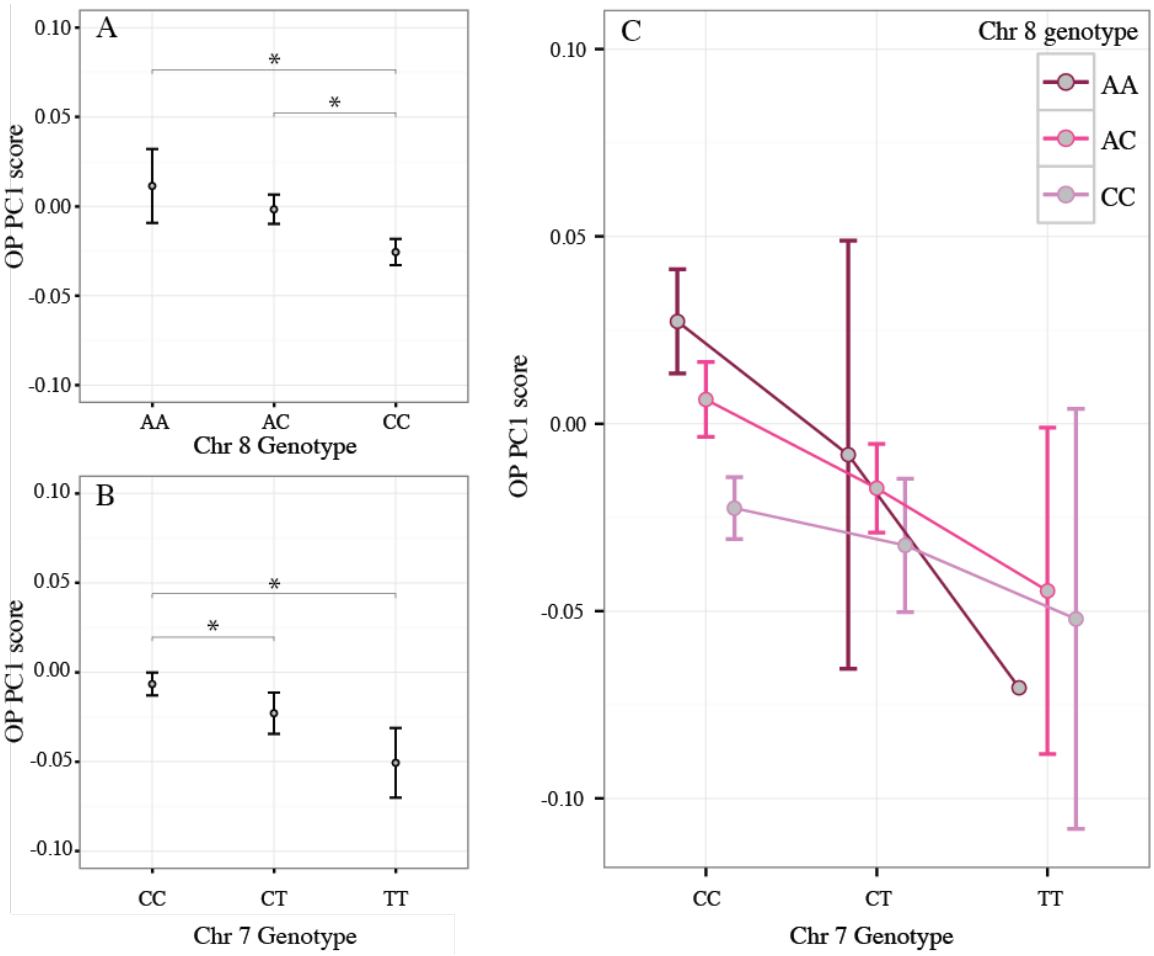

Figure 2.18 Mean opercle PC1 score (+/- 95% CI) of the most highly associated SNP genotype at chromosome 8 and chromosome 7 (A,B) and the interactions among genotypes (C). In each panel, genotypes organized from more "oceanic" to more "freshwater", left to right. Pairwise comparisons show if genotype had a significant effect on mean lateral plate number depicted by * (Tukey HSD; $p<0.05$)

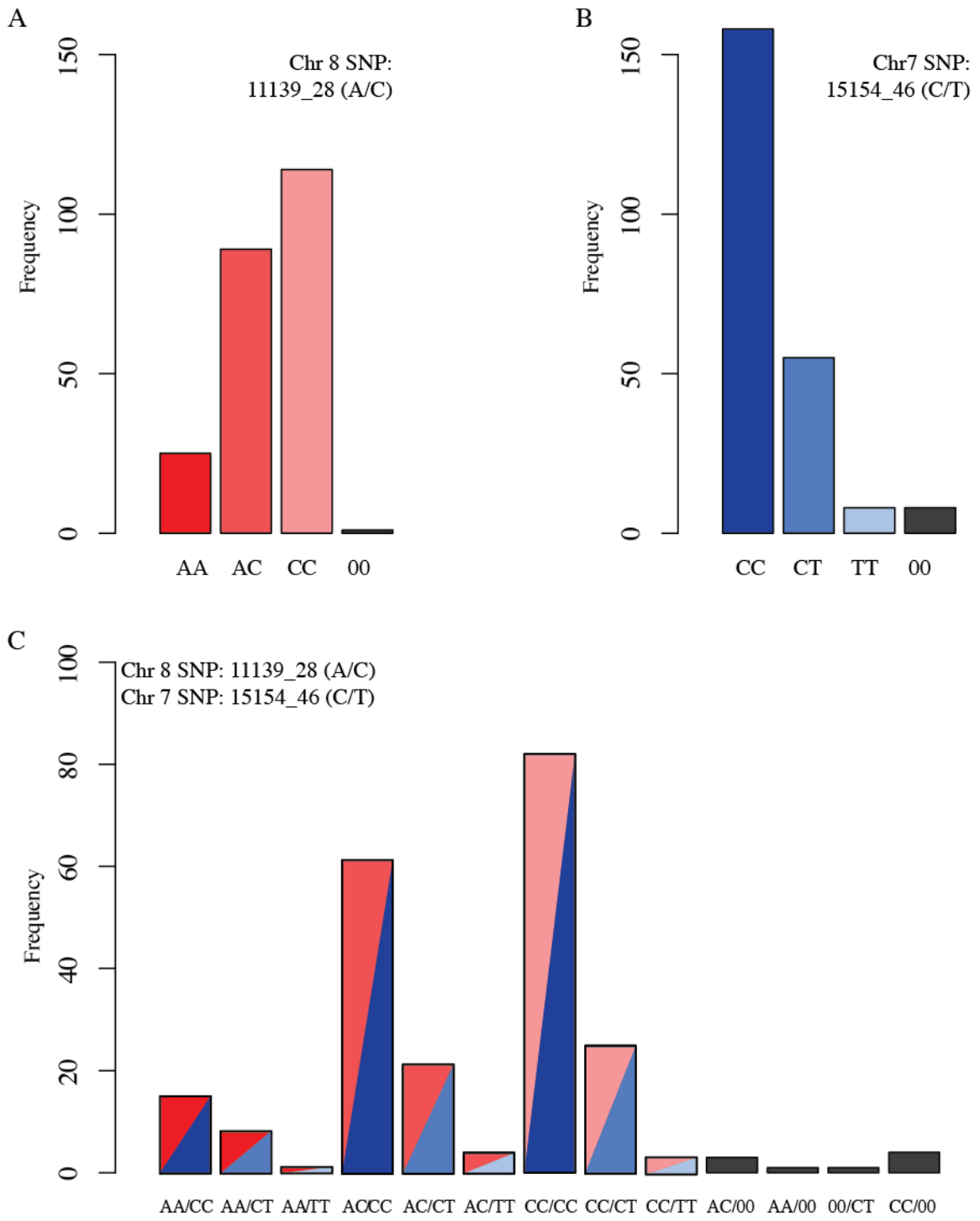

Figure 2.19 Genotype frequencies at each significantly associated locus (A,B) and multi-locus frequencies (C). Gray bars indicate missing genotypes. Both single locus genotype frequencies are in HWE. 00=individuals not genotyped at locus

DISCUSSION

In this study, we genetically mapped two traits that are classically associated with marine to freshwater divergence in stickleback, and for which we have *a priori* expectations about the nature of the genetic architectures, using a phenotypically variable population in Oregon. We show that opercle shape and lateral plate number likely have independent genetic underpinnings in this population. We identified genomic regions associated with each trait using a linear mixed model GWAS. For lateral plate count we clearly identify one major effect locus at *eda*, as expected, as well as a novel second locus that has not previously been identified that appears to modify variability in the low plated morph. For opercle shape, we identified two genomic regions associated with freshwater variability that map to genomic regions that have been implicated in previous QTL mapping studies. Within those, we identify at least one gene underlying these associations which has not been previously identified to contribute to opercle shape, but which could be an interesting candidate. Analysis of these two traits makes us confident that the genomic associations we find in the Riverbend stickleback population are real. Notably, we identify narrow genomic regions even with a relatively limited sample size, demonstrating the utility of using natural populations to connect genotype to phenotype.

Hybrid Stickleback Populations Are a Powerful Tool for Evolutionary Genomics

Significant progress in identifying the genetic basis of phenotypes in stickleback has occurred through QTL mapping studies (Miller et al. 2007; Albert et al. 2008; Arnegard et al. 2014). Although interest in utilizing natural populations to address these questions has grown, only a few such studies have been undertaken in stickleback. In two prominent examples, researchers in one study used admixture mapping and in the other used QTL analysis of F_2 populations in semi-natural ponds. Malek et. al. (2012) used bulk segregant analysis (BSA) in a recently admixed stickleback population from Enos Lake to identify genomic regions that contribute to nuptial color and body shape. Arnegard et. al (2014) mapped niche differentiation using benthic-limnetic F_1 hybrids allowed to breed freely in semi-natural ponds that comprised both habitats. These studies, though successful in moving analyses out of the laboratory and into natural

environments, are still limited in resolution by the small number of meioses from a recently admixed population used in Malek et. al. (2012) and from an F_2 cross Arnegard et. al. (2014). Using natural systems with many more generations of recombination would be ideal.

An optimal scenario for genetic mapping in natural systems are phenotypically variable populations with little cryptic relatedness or population structure, and low, but still measurable, LD within linkage groups that will link genetic markers with the traits of interest. In this study, we show that Riverbend is such an ideal system in stickleback. Even among collection dates that span three years, and using several genome-wide approaches, we find little population structure. PCA of genetic variation broadly detects population structure contained within genome-wide SNP data (Abraham and Inouye 2014; Raj et al. 2014; Li and Ralph 2016). Within the Riverbend population, PCA among several combinations of 1000 randomly selected markers was largely spherical across the first several principal components followed by small reductions of percent variation explained (Fig. 2.10). In contrast, PC1 from a PCA that included individuals from four populations along the McKenzie River explained nearly 35% of the genetic variation, followed by a steep reduction in percent variation explained by the remaining PCs. This analysis largely grouped individuals by geographic location along the river, but identified little within group stratification. Furthermore, the distribution of mean-centered kinship matrix relatedness coefficients in Riverbend lacks a systematic pattern, and the values are normally distributed about the mean. In contrast, extensive patterns of relatedness seen among individuals from different populations along the McKenzie River supports the presence of population structure along the river.

Long-range genomic correlation, due to a significant amount of contemporary gene flow (Slatkin 2008) or strong natural selection, can be problematic for GWAS (Pritchard et al. 2000b; Slatkin 2008) (see Chapter III, Middleton Island). Our genome-wide correlation analysis shows that within the Riverbend population there is little evidence for long range LD, and that between linkage group LD is nearly at equilibrium. These data give confidence in the veracity of the GWAS results and provide some insight into the still opaque origins of the Riverbend population. The lack of large blocks in long-range LD suggests that Riverbend is not a young hybrid zone, that contemporary gene

flow and selection are not strong enough to create LD, and any genomically distant genetic correlations quickly succumb to recombination. Together with our PCA and relatedness results, these LD data support our hypothesis that individuals sampled from Riverbend represent a population with little genetic structure across geography or the stickleback genome, and is therefore ideal for GWAS.

The Lateral Plate and Opercle Phenotypes Are At Least Partially Independent Genetically

As stickleback adapt to freshwater environments, correlated armor and body shape changes occur repeatedly across independent populations, prompting decades of investigation about the mechanisms for such correlated evolution (Reimchen 1983; Schluter and McPhail 1992; Marchinko and Schluter 2007; Purnell et al. 2007). Does selection target each trait independently, or does genetic linkage or pleiotropy facilitate a correlated response? QTL mapping studies between marine and freshwater stickleback, between benthic and limnetic stickleback, and between lake and stream stickleback have shown that similar genomic regions are implicated in contributing to suits of traits including lateral plate loss and head/body shape (Berner et al. 2014; Liu et al. 2014; Miller et al. 2014; Conte et al. 2015; Glazer et al. 2015; Erickson et al. 2016) but that QTL contributing to trait variation are not always identical between populations (Erickson et al. 2016). Although previous laboratory QTL studies have suggested that lateral plate number and opercle shape variation are not genetically linked (Kimmel et al. 2005), the environment in which individuals were raised may affect both the phenotypic variation present and the contribution of alleles to the traits (Hermida et al. 2002; McGuigan et al. 2011). Genetic correlations not observed in laboratory environments may therefore be revealed in analyses of natural populations of stickleback in their native environment.

We addressed the possibility of linkage and pleiotropy shaping phenotypic variation in wild stickleback populations experiencing a natural environment by assessing the correlation between opercle shape and lateral plate variation within the Riverbend population, and among populations along the McKenzie River. We found little evidence

for within population correlation which suggests that linkage or pleiotropy is likely not a major driver in defining phenotypic variation or co-variation in lateral plate number or opercle shape (Paaby and Rockman 2013). We suspect that phenotypic variation of the traits is controlled an independent genetic basis.

GWAS of Lateral Plate Number Variation in the Riverbend Stickleback Population Provides Novel Understanding of this Classic Trait

Riverbend stickleback range from completely plated to low plated fish, covering the marine to freshwater transition both in phenotypes and underlying genetic variants. Confirming this hypothesis we identified the strongest association with a genomic region on LG 4 only approximately 3 kb upstream of *eda,* the major effect locus identified previously for lateral plate loss (Colosimo et al. 2004; Colosimo et al. 2005). This finding instills confidence that a second peak on LG 20, although just above the genome-wide significance threshold, was also a real association. Previous QTL mapping studies found associations on LG7, 10, and 21 as well as LG4 and LG20 (Colosimo et al. 2004; Erickson et al. 2016), indicating that these variants are not segregating in Riverbend. Alternatively, it is possible that our study was underpowered and unable to detect variants on the linkage groups previously identified, or that our markers were not in linkage disequilibrium with the segregating variants. We do not suspect this is the case because though the effect sizes of lateral plate number QTL were small in previous studies (Colosimo et al. 2004), we saw no elevation in significance in these regions even though markers were well distributed across the linkage groups. While variants at *eda* are certainly a major factor, the variance in genomic regions identified might highlight nuances in the genetic architecture of the trait among populations (Bell 2001; Aguirre et al. 2004).

Since the 1950's, several lateral plate morph inheritance models have been proposed that employ one or few loci of large effect (Münzing 1963; Banbura and Bakker 1995; Bell 2001). Recently, findings from QTL studies hint at a model in which a major effect locus is critical to establish the overall lateral plate morphotype (high, partial, low) with minor effect additive loci to fine tune the number of plates (Aguirre et al. 2004;

Colosimo et al. 2004; Cresko et al. 2004). Aguirre and colleagues (2004) argue that in Loberg Lake, however, the alleles contributing to low and high lateral plate morphs are likely polygenic and independent. Our results largely support the classical models with some role for epistasis. The alternative homozygote genotypes on LG 4 determine high and low morph. However, the plate morph for heterozygotes is variable suggesting the role of yet to be identified interacting loci and/or environmental variance only affecting the LG 4 heterozygotes. We did identify, however, a locus on LG 20 that acts epistatically with the LG 4 locus by modifying variation only within the low lateral plate morph (Fig. 2.13C, Fig. 2.14C). These results suggest the role of other modifiers acting epistatically on the high and partially plated genotypes at the major effect locus. Larger GWAS studies will continue to identify these genes.

The genomic intervals we identified on LG 4 and LG 20 harbored both anticipated and interesting novel candidate genes. The 2 Mb region identified on LG 4 contained *eda,* the most likely candidate, which has been implicated previously in QTL and transgenic studies as a major effect locus of lateral plate loss (Colosimo et al. 2005; O'Brown et al. 2015). The association window in Riverbend, determined by the decay of linkage with the most highly associated SNP, however, also included genes *pdlim7* and *anxa6* which have been labeled as additional candidates in a QTL study between stream and lake stickleback from Central Europe (Berner et al. 2014) and population genomic studies between ocean and freshwater fish (Hohenlohe et al. 2010). *Pdlim7* and *anxa6* play a role in de novo bone initiation and bone calcification, respectively (Berner et al. 2014).

Within the identified genomic region on LG 20, the nearest gene to the second most highly associated SNP was *ctnnb1*. This gene encodes β-catenin, which has not been previously implicated in lateral plate variation in QTL studies. It is a particularly interesting candidate gene because of its obligatory role in the Wnt/β-catenin signaling pathway known to be critical in bone formation and resorption (Kramer et al. 2010; Chen and Long 2013). Additionally, Wnt signaling is known to act upstream of *eda* (Arte et al. 2013), and O'Brown et al (2015) showed that, in laboratory manipulations, the Wnt signaling can alter *eda* expression. Although LG 20 has often been identified as a linkage group that harbors QTL associated with many aspects of skeletal variation, this LG has

not been previously implicated in lateral plate count. However, Colosimo et al. (2004) did identify QTL for lateral plate height and width which fell on LG 20 (then LG 25). More recently, two distinct QTL were fine mapped to a region between 3.2-4.0 Mb on LG20 containing the gene *gdf6* (Indjeian et al. 2016). Transgenic experiments revealed that expressing freshwater *gdf6* cDNA in marine stickleback led to a loss of plates or a reduction in the size of the plates (Indjeian et al. 2016).

Based on these previous findings for *gdf6* affecting lateral plate shape, we initially hypothesized this gene would be in the credible region. It is not. However, if *gdf6* were associated with lateral plate variation we would likely miss it due to low LD in the genomic area (Fig. 2.20). Markers do flank *gdf6*, but because LD in that region is low, without a marker within the gene itself, any association would go undetected. Instead we saw a clear association at ~5.6Mb that pinpoints β-catenin as a strong candidate gene. A closer look at the RAD markers identified on LG 20 show that marker coverage is lower than on LG 4 (on average 1 RAD locus per 27kb LG 20 vrs. 1 RAD locus per 23kb LG 4), and a large group of markers immediately to the right of our association is missing. Thus, there is also a possibility that our association points to a gene contained in the region with missing data and not *ctnnb1*. Without additional markers, we would be unable to see a potential peak in that area, although the pattern of LD decay does not suggest that this is the case. Considering the association that we identified on LG 20 in addition to the potential association missed due to lack of markers or linkage, it is possible that we were unable to detect other real associations. We, therefore, consider our GWAS for lateral plate number variation to be a conservative estimate.

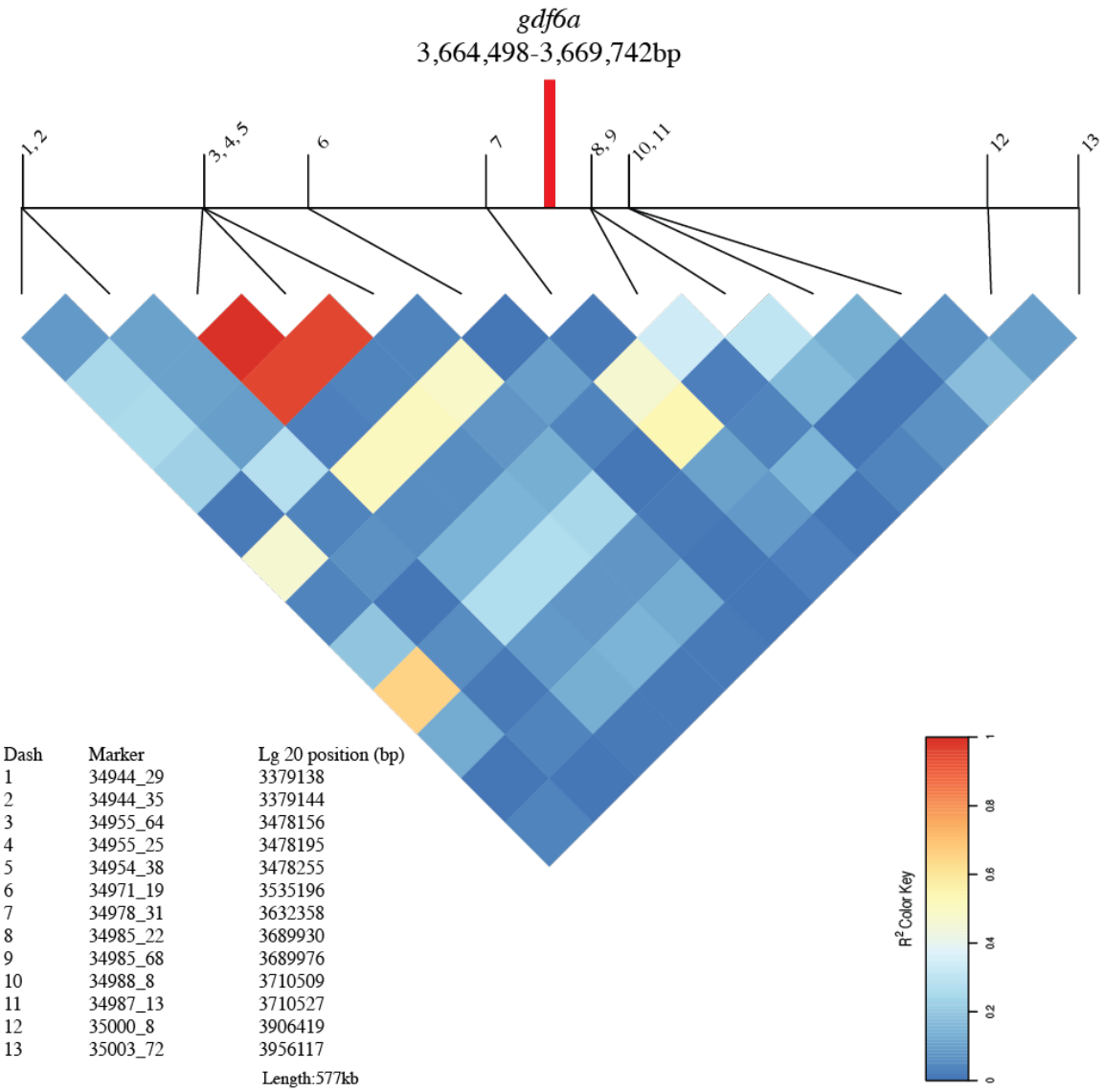

Figure 2.20 Thirteen RAD markers and SNP locations in a 577kb window around *gdf6a* location on LG 20. All pairwise SNP combinations of local linkage disequilibrium depicted by r^2 values in heatmap.

GWAS of Opercle Shape in Riverbend Advances Craniofacial Genomic Understanding

Opercle shape distribution, in contrast to lateral plates, primarily occupied freshwater morphospace. As such, we expected to identify genomic regions that contribute primarily to within freshwater variation and perhaps some to marine-freshwater divergence. Little is known about the genetic architecture of opercle shape, and previous mapping studies suggest that it is polygenic (Schluter et al. 2004; Kimmel et al. 2005; Miller et al. 2014; Conte et al. 2015; Erickson et al. 2016). Our GWAS may support this hypothesis and significantly extends this previous work.

We identified one genomic region on LG 8 that is significantly associated with opercle shape. We are encouraged by this association because LG 8 has for the first time recently been implicated in changes to the width of the opercle in QTL mapping crosses between a marine fish and three independent benthic populations from British Columbia (Erickson et al. 2016). A peak on LG 7 has also been previously identified in multiple QTL studies in crosses between marine-freshwater and benthic-limnetic individuals (Miller et al. 2014; Conte et al. 2015).

Additionally, Kimmel et. al. (2005) identified LG 19, the sex-determining locus, as a potential major effect locus associated with opercle shape differences between marine and freshwater individuals, but Albert et. al. (2008), who also identified an opercle associated peak on LG 19 between a marine-benthic cross, noticed that the shape differences between the sexes and between the divergent populations were quite similar prompting them to hypothesize that having a male-like opercle shape was important in the adaptation to benthic environments. Because we did not identify LG 19 with opercle PC1, this suggests that opercle shape sex differences do not contribute to the primary axis of variation within freshwater variation.

Certainly, we are not capturing all the genomic regions associated with opercle shape, and with present methodologies, identifying all loci is impossible. However, the fact that we identified two genomic regions with a relatively moderate sample size of 229 individuals is encouraging. Moving forward, we predict that increasing the sample size and marker density, as well as capturing and mapping different aspects of opercle (and other head bone) shape variation, will be informative. Current efforts to increase the

sample size should narrow the existing associations and identify more genomic regions. Our data already indicate that this genetic vein is not tapped. Because the linear mixed model assumes that each genetic variant will have some effect on the trait of interest, the model is able to produce an estimate of the percent phenotypic variation explained (PVE) by all genotyped markers (Zhou and Stephens 2012; Pallares et al. 2014). For opercle PC1 the PVE was only ~36% (compared to ~99% for lateral plate count), indicating that our ~16,000 SNP markers were only sufficient to explain approximately one third of the opercle shape variance captured by PC1. Unless all the unexplained variation is environmental, another explanation is that more markers are required to link to causative loci (see *gdf6* example given above). Future studies would include more markers through RAD-seq with a more frequent cutter, targeted re-sequencing of particularly interesting genomic regions, or whole genome sequencing.

Unlike lateral plate number, the inheritance of opercle shape is far less understood and likely more complex. Of the two genomic regions we identified, it is unclear why the most "freshwater" genotype on LG 7 would be observed in the fewest number of fish. But the genotypes of the loci at the two linkage groups clearly have distinctive and opposite effects on the phenotypes. Based on developmental studies in zebrafish (Kimmel et al. 2010; Huycke et al. 2012; Kimmel et al. 2012b), the opercle develops in a modular fashion which appears to be genetically independent. The fact that we see no interaction between the genotypes at the two loci could suggest that they are operating on independent modules. Further investigation of how each locus affects the opercle shape change will be important.

Comparing the genes in these associated regions with previous work already sheds light on a fundamental question: Are genes identified through mutagenesis studies in developmental model systems the same genes used by evolution to contribute to adaptive phenotypes (Mackay et al. 2009)? In some cases, major developmental genes are implicated in adaptive changes. For example, both in African cichlid fishes and in Darwin's finches, *bone morphogenetic protein 4* (*Bmp4*) appears to regulate aspects of head shape through mechanical advantage of the jaw and depth and width of the beak, respectively (Abzhanov et al. 2004; Albertson et al. 2005). Although several QTL studies have addressed opercle shape in stickleback, no candidate genes from these crosses have

been identified for further study likely because the mapping intervals are quite large. Given our limited sample size, the genomic interval for our significantly associated region on LG 8 is also still large (~5Mb). However, the *EPHB3* gene flanking the most associated marker is an interesting candidate because of its role in palate formation in mice (Risley et al. 2009; Matsuo and Otaki 2012). Eph receptors and their ephrin ligands, in general, are important for cell-cell adhesion, a process which helps to regulate migration, proliferation, and differentiation, all of which are critical for bone cells to properly make bone (Matsuo and Otaki 2012). So far *EPHB3* has not been implicated in opercle shape regulation.

The opercle in zebrafish has been long studied as a model for bone shape development which is hypothesized to be regulated by a genetically modular system (Huycke et al. 2012). Opercle bone ossification is initiated as a small, linear spur surrounded by osteoblasts, the cranial neural crest-derived cells primarily responsible for bone formation in the head. The dorsal end of the spur becomes the joint ('j' Fig. 2.1C) and the ventral end becomes fan-shaped ('v','p' Fig. 2.1C). Development largely occurs through differential elongation along the 'vp' edge (fan) caused by spatiotemporal patterning of osteoblast deposition of mineralized matrix that appears to be regulated by a genetically modular, spatially specific system (Kimmel et al. 2010; Huycke et al. 2012). Members of the endothelin 1 signaling pathway, Dlx genes, and *mef2ca* were identified through mutagenesis studies of opercle shape development (Kimmel 2003; Talbot et al. 2010; DeLaurier et al. 2014). In addition, Huycke et. al. (2012) showed that mutants identified in the Hedgehog (Hh) signaling pathway, including *indian hedgehog a* (*ihha*) and *patched 1* (*ptch1*), are required for appropriate outgrowth of the ventral region of the opercle, but that they do not affect the development along the dorsal region. They hypothesized that the mechanism by which Hh signaling is involved likely lies in the regulation of pre-osteoblasts proliferation along the growing edge of the fan.

Interestingly, the changes in opercle shape we see in stickleback from Riverbend along PC1 include modifications of the ventral portion of the opercle similar to shape changes identified through mutagenesis studies in zebrafish (Huycke et al. 2012). This shape change is even more pronounced in the stickleback transition from marine to freshwater (Kimmel et al. 2008; Kimmel et al. 2012a). We therefore tested if the regions

associated with opercle in our Riverbend GWAS included the members of developmental pathways previously identified critical in normal opercle development in zebrafish such as *ihha*, *edn1*, *mef2ca*, or dlx genes. The genomic regions identified on LG 8 and 7 do not appear to contain members of these signaling pathways. In fact, *ihha* is encoded on LG 16, a linkage group which, to our knowledge, has not been associated with changes in opercle shape in any QTL study, nor a major contributor in genome wide scans for signatures of selection (Hohenlohe et al. 2010). It is possible that with increased sample size and density of markers, we or others may uncover genes previously identified in opercle developmental studies in the laboratory. Clearly further genetic analysis of these genomic regions in stickleback will provide novel and complementary understanding to the laboratory work in zebrafish.

Genetic Analysis of Traits in an Ecological Context Provides Deeper Understanding

Lateral plate variation is often used to distinguish marine and freshwater stickleback. Especially in post-glacial populations of western North America and western Mediterranean, a strong correlation exists between habitat (marine/freshwater) and plate count (Bell 2001) arguing that selection may target lateral plate variation (Hagen and Gilbertson 1972, 1973b). The environmental factors shaping lateral plate variation are hypothesized to include both abiotic factors, such as ion concentration and salinity tolerance, and biotic factors, such as predation. This previous work and the identification of the major plate QTL has led to investigations about the fitness consequences for the *eda* alleles (Barrett et al. 2008; Le Rouzic et al. 2011). Artificial pond studies show strong selection for the e*da* low allele in freshwater.

The distributions in lateral plate number and opercle shape in the McKenzie River suggest, however, that the selective pressures on these traits may be more complicated. It is worth noting again that a suit of skeletal, physiological, and behavioral traits all shift in response to freshwater adaptation (McKinnon and Rundle 2002; Barrett et al. 2009; Barrett 2010). The phenotypic distributions from our data show that lateral plate count varies across the range of phenotypes between what is thought of as classically marine and freshwater phenotypes, but that opercle shape largely varies within the freshwater

range. While with our data we cannot explicitly test the strength of selection on each phenotype, we would expect that if each were under the same selection strength that the phenotypes would vary concordantly. To this end, we wonder if trophic morphology, such as opercle bone shape which has a distribution predominantly within freshwater variation, experiences stronger selection than armor traits which has a distribution which covers the marine-freshwater range.

We suspect that the sharp divergence between completely plated marine stickleback and low plated freshwater stickleback may not be a largely global pattern, but that lateral plate number may be correlated with other traits experiencing strong selection. This hypothesis fits into observations of stickleback populations found particularly in Western and Central Europe along North America's Atlantic Coast which show weaker correlations between marine-freshwater divergence and lateral plate count (Bell 2001; Raeymaekers et al. 2014). Notably, many of these freshwater populations are not completely isolated from brackish or marine environments leaving open the possibility that gene flow occurs and reduces the response to selection. In the populations along the McKenzie River that we examined, natural gene flow from anadromous fish from the sea is unlikely. It is more likely that marine stickleback were reintroduced upstream at the Leaburg Fish Trap and that gene flow has occurred downstream, but more work is required to establish the source of the marine phenotype.

The genomic findings on both opercles and lateral plates shows that our understanding of traits that we investigate through the lens of developmental genetics, can be facilitated by looking to evolutionary genetics in natural populations (Albertson et al. 2009). In traditional forward genetic screens researchers, by necessity, identify mutants for which there is a visible phenotype. In the interest of time and physical space, these mutants often have a robust phenotype that is observed early in development. In natural populations, the mutations that are not lost to selective forces are typically more subtle, especially for quantitative traits, and can be analyzed at many different stages of development. Using GWAS or other genome wide approaches in natural populations will likely be a productive route to identify genes and broaden our understanding of gene interactions within known developmental genetic networks.

Conclusion

QTL studies in the laboratory have significantly advanced the genetic understanding of stickleback evolution. However, a major impediment to subsequent progress has been the broad genomic regions identified. In addition, some traits are simply not amenable to analysis via crossing in the laboratory (Korte and Farlow 2013). Lastly, the common laboratory environment itself may directly affect the genetic architecture of traits that are being identified (McGuigan et al. 2011). Here we demonstrate the power of using GWAS in a naturally occurring, phenotypically variable population to efficiently begin to identify narrow genomic regions contributing to adaptive phenotypes that have developed in a natural environment.

With a limited sample size, we identified anticipated and novel genomic regions and candidate genes which contribute to lateral plate count and opercle shape. These findings have extended our current knowledge about the transmission genetics of lateral plate count, the genetic basis of low plated variability, and the nature of the genetic architecture of opercle shape. Our research demonstrates a fruitful intersection between evolutionary genetics and developmental genetics by using variation seen in nature to complement mutagenesis and transgenic studies in the laboratory.

Of course, identifying a population with the kind of phenotypic variability one wishes to study without the problems of population structure can be challenging. However, we demonstrate that these populations exist in Oregon and will likely be available across stickleback habitats in their holarctic distribution. In addition to identifying the genomic regions which contribute to phenotypic evolution, and because we examined wild caught individuals, using the Riverbend population we can begin to think about the selective forces and population dynamics which contribute to organismal fitness and link the genome, phenome, fitness map. These resources will continue to help this stickleback ‘supermodel’ (Gibson 2005) become even more superb.

BRIDGE

In Chapter II, we showed that GWAS can be an effective method to determine narrow genomic regions that contribute to phenotypic variation in the context of environmental and selective forces, even given a relatively small sample size. Although lateral plate number phenotypic variation spanned the morphospace between plate number expected from marine to freshwater stickleback, in the Riverbend population, we were only able to capture freshwater variation. Identifying the loci that contribute to the rapid divergence from marine to freshwater stickleback, however, is a long-standing goal of the field. Therefore, in Chapter III, we use GWAS to investigate the loci contributing to phenotypic divergence in a population of stickleback fish which span the range of phenotypic and habitat space of the most divergent populations. These populations however, only diverged from their marine ancestors within the last 50 years and possibly provide a unique system to utilize GWAS to uncover the genetic basis of phenotypes which are in the process of adapting to new freshwater environments.

CHAPTER III

GENOMIC COVARIANCE FUELS VERY RAPID EVOLUTION OF COORDINATED PHENOTYPES IN STICKLEBACK

The stickleback fish used in this chapter were collected from ponds on Middleton Island by E. A. Lescak and F. A. von Hippel. E. A. Lescak prepared DNA to be used for further sequencing preparation by S. L. Bassham. The sequences were aligned and first processed by J. Catchen. I subsequently processed the sequences again based on the specific needs of my study. E. A. Lescak previously phenotyped lateral plates, and, under my direction, S. Sichel performed much of the opercle bone phenotyping. I performed all data analysis and writing. W. A. Cresko was the principal investigator for this study.

INTRODUCTION

Multicellular organisms are often phenotypically modular (Klingenberg 2008), with traits being more highly correlated within than among modules (Olson and Miller 1958; Berg 1960; Armbruster et al. 2014). Phenotypic modularity can be molded by evolution (Clune et al. 2013), and once evolved can lead to coordinated change of traits within a module, while still facilitating independent evolution of suites of phenotypes in different modules (Wagner and Altenberg 1996; Wagner et al. 2007). The definition of modularity is context dependent and can be investigated at multiple levels (Armbruster et al. 2014). Modular phenotypes may be defined by their functional interactions. Levers of the cichlid lower jaw (Albertson et al. 2005; Albertson and Kocher 2006) provides one example. Similarly in blind cavefish, hyperactivity of the gene sonic hedgehog (Shh) promotes increased jaw size and number of taste buds, but simultaneously inhibits eye development (Yamamoto et al. 2009).

Evolutionary modularity refers to those traits which evolve in a correlated fashion due to any combination of functional, genetic or developmental mechanisms for correlation (Armbruster et al. 2014). Identifying the mechanisms for observed evolutionary modularity in natural populations is a goal of evolutionary biology.

Independent phenotypes may covary because selection acts on both traits independently in the same direction (Melo and Marroig 2015), leading to covariance across populations and sometimes individuals. Phenotypic modularity may also be due at least in part to genetic or genomic factors (Pepper 2003). Correlated phenotypes may have independent genetic loci that are correlated through either physical linkage or gametic phase linkage disequilibrium. As a result, selection on one trait will lead to a correlated response to selection on other traits via linked selection (Wagner et al. 2007). Correlated phenotypic characters may also share a genetic architecture via pleiotropy or epistasis of traits that share aspects of developmental genetic networks (Cheverud 1988; Cheverud et al. 2004; Wagner and Zhang 2011). In this case, selection on one trait would lead to a correlated response on other genetically or developmentally integrated traits (Lande and Arnold 1983; Marroig and Cheverud 2001; Cheverud et al. 2004).

The genetic and genomic basis of phenotypic modularity has been investigated from a variety of perspectives (Berg 1960; Lande 1979a; Cheverud et al. 1983; Phillips and Arnold 1989; Schluter 1996; Mezey et al. 2000; Magwene 2001; Marroig and Cheverud 2001; Wagner and Zhang 2011). Quantitative geneticists became interested in how the response to selection on multiple traits can be affected by genetic correlations, and initially assumed a large number of loci of small effect acting in a largely additive fashion (Santiago 1998; Orr 2005). This theoretical framework was subsequently extended to account for linkage disequilibrium (Bulmer 1971), but epistatic effects and linkage were assumed to be relatively weak and transitory (Barton and Keightley 2002; Carter et al. 2005; Barton 2017). Quantitative genetics models capture these effects via the genetic variance-covariance matrix, **G**, which is a statistical summary of genetic correlations among traits (Lande 1979b, 1980; Lande and Arnold 1983; Roff 2000). These models are largely agnostic, however, as to whether the correlations are due primarily to linkage or pleiotropy; discriminating between tight linkage and pleiotropy in natural populations is difficult (Conner 2002). Thus, the relative roles of genetic and genomic architectures are still unclear for evolutionary modularity in natural populations.

More recently, developmental biologists discovered a surprisingly conserved genetic toolkit for the development of even long diverged animals (Carroll 2008). The observation of ‘master regulatory genes’ re-ignited an interest in the possible role of

pleiotropy on phenotypic modularity, and created a new appreciation for how genetic correlations may impact the trajectory of evolution (Arnold 1992; Cheverud 1996; Gehring 1996; Wagner and Zhang 2011). Because a phenotype is the product of genetic effects translated through development, phenotypic modularity may be strongly affected by a trait's genetic and genomic architectures. By genetic architecture we mean the number of genes and alleles and their interactions which contribute to trait variation (Wagner and Altenberg 1996; Hansen 2006). We define genomic architecture as the location, distribution, and covariation of loci within a genome (Hohenlohe et al. 2012a). Interestingly, because it is now known that gene families often grow by tandem gene duplication and functional divergence, the structure of developmental genetic networks may link genetic and genomic modularity as the gene families evolve (Amores et al. 1998; Cresko et al. 2003; Force et al. 2005). These modern developmental genetic discoveries have renewed attention on the potential role of genetic and genomic correlations in affecting evolutionary change, primarily at the macroevolutionary scale. For example, an area of focus has been the relative use of (presumably) less pleiotropic cis-regulatory changes than more consequential coding mutations for macroevolutionary change (Carroll 2008).

The genetic and genomic basis of very rapid evolution of correlated phenotypes in natural populations has been less explored (Hendry and Kinnison 1999). Recent studies reveal that the tempo of evolution can be much faster than previously appreciated and can, in fact, occur on contemporary timescales (Stockwell et al. 2003; Hendry et al. 2007) via adaptive changes in many phenotypes. For example, Grant and Grant (2002) showed that the sizes and shapes of beaks and bodies of Darwin's finches were modified several times over a 30-year period in response to selective pressures. Reznick et al. (1997) showed that in fewer than 11 years, the descendants of guppies transplanted from high- to low-predation sites in natural river systems evolved life histories similar to guppies naturally adapted to low-predation, and Roels and Kelly (2011) found that when pollinators were removed in an experimental population of *Mimulus guttatus*, the ability of the population to self-fertilize improved after only 5 generations and a variety of traits, ranging from floral characters to life-history, also diverged. Threespine stickleback also show evidence that adaptive evolution from marine to freshwater environments can occur

at the level of the phenotype and genotype in several decades (Bell et al. 2004; Terekhanova et al. 2014; Lescak et al. 2015).

In these and many other cases, the rapid evolution involves coordinated changes in so-called syndromes of traits (Protas et al. 2008; Roels and Kelly 2011). In many of the cases the evolution of these modular syndromes occurs repeatedly in a stereotypical fashion (Sicard and Lenhard 2011). In the present study, our goal is to document the patterns of phenotypic, genetic and genomic architectures in very rapidly evolving natural populations. To achieve this goal we use the threespine stickleback (*Gasterosteus aculeatus*), which is an ideal system to investigate questions about the rapid and repeated evolution of coordinated phenotypes (Bell and Foster 1994). This small, common fish is distributed along coastlines across the Northern Hemisphere as a marine and freshwater ecotype. The marine ecotype is phenotypically and genetically similar throughout its range and gives rise to the freshwater ecotype after it invades freshwater environments (Bell and Foster 1994). Molecular data support that freshwater populations in many high latitude regions are often the result of multiple, independent colonization events after the retreat of glaciers at the end of the Pleistocene era ~18,000 yrs ago (Bell and Foster 1994). However, despite these multiple, independent invasions of freshwater habitats, stickleback have repeatedly evolved towards a freshwater form which more closely resembles other independently derived freshwater lineages than the common marine ancestor both at the level of the phenotype and genotype (Hohenlohe et al. 2010). These observations provide compelling evidence for the adaptive nature of the derived suites of phenotypic traits which include modifications to body shape, trophic morphology, behavior, and reduction of bony armor (Barrett 2010; Barrett et al. 2011; Aguirre and Bell 2012; McGee et al. 2013). What is still unclear is the degree to which the evolutionary modularity of the freshwater and oceanic syndromes of traits are underlain by genetic and/or genomic modularity, or are simply the product of selection acting independently on numerous different traits and their myriad underlying genetic loci.

We focus on the contemporary evolution of threespine stickleback on Middleton Island, AK (Gelmond et al. 2009; Lescak et al. 2015). After the Great Alaskan Earthquake of 1964, islands in the Gulf of Alaska were uplifted resulting in the formation of new ponds, and oceanic stickleback invaders quickly evolved freshwater phenotypes to

provide a unique natural experiment to investigate the genetic and genomic architecture of correlated phenotypes (Lescak et al. 2015). We concentrate on the coordinated phenotypic evolution between two well-studied skeletal traits in sticklebacks— opercle shape and lateral plate number— that are integrated within a larger evolutionary module which incorporates many traits, including skeletal, behavioral, and physiological components, that contribute to the stickleback "freshwater syndrome" (Conte et al. 2015). We use these two traits for several reasons. First, both traits are ecologically relevant. Lateral plate number is thought to be adaptive in avoiding predation (Barrett 2010), and the shape of the opercle is important in the kinetics of the stickleback jaw (Jamniczky et al. 2014). Second, the traits are skeletal structures derived from dermal bone and therefore may share aspects of their genetic architectures (Colosimo et al. 2005; Kimmel et al. 2010). Third, opercle shape is a continuous trait while lateral plate count is a meristic phenotype, therefore it is also plausible that the genetic architecture of the variation of these traits differs (Schluter et al. 2004; Kimmel et al. 2005).

To understand the genetics and genomics of rapidly evolving phenotypes, we integrated phenotypic and genomic analyses of lateral plate and opercle traits in natural populations. Traditional forward genetic approaches in the laboratory, such as quantitative trait locus (QTL) studies, are a powerful tool to identify the genetic and genomic architectures of phenotypes of divergent populations (Slate 2005). In the stickleback system alone, QTL mapping has led to the discovery of the genetic basis of divergent traits such as lateral plate loss (*eda*), lateral plate size (*gdf6*), pelvic structure reduction (*pitx1*), and pigmentation changes (*kitlg*) (Colosimo et al. 2004; Shapiro et al. 2004; Miller et al. 2007; Indjeian et al. 2016). QTL for many skeletal traits have been found to localize to similar genomic regions (Conte et al. 2015; Glazer et al. 2015). However, QTL mapping is challenged by the number of recombination events which determines QTL resolution, and many laboratory F_2 mapping families are small leading to relatively large linkage blocks which severely limit our ability distinguish pleiotropy from linkage (Haggard et al. 2013). Moreover, the genetic variation of phenotypes in laboratory crosses is often a small subset of that in the wild, and the laboratory environment itself can influence trait development and modularity (McGuigan et al. 2011).

Genetic analyses of phenotypes in natural environments allows us to interrogate the genetic and genomic architectures of phenotypes present within natural environments. This general approach has long been largely inaccessible for studies of all but humans and a small handful of model organisms in the wild (Korte and Farlow 2013). However, as genomic technologies rapidly advance, a promising new approach is to use next generation sequencing (NGS) combined with genome wide association studies (GWAS) to connect genome to phenome, and to elucidate the contributions of evolutionary processes to the genetic and genomic architectures of rapid and coordinated phenotypic evolution in the wild. In this study, we have applied NGS and GWA approaches to our study on opercle shape and lateral plate number. We first ask if these traits covary because of a shared genetic or developmental basis. We do this by assessing correlations within and among individuals collected from two freshwater ponds and two marine habitats. Next, we use genome wide association (GWA) mapping in this natural population to uncover the genetic architecture of each of the traits. Finally, we assess the extent of genomic covariation in these recently diverged populations of stickleback.

METHODS

Sample Collections

We compared pre- and post-1964 maps as well as aerial imagery of Middleton Island to identify ponds on a terrain that were submarine prior to the 1964 earthquake (Fig. 3.1). During the summers of 2005, 2010, and 2011 we collected stickleback from several these ponds using minnow traps (Table 3.1). Some ponds contained freshwater (salinity 0.1-1.4 ppt); others were marine (salinity 21.4-26.4 ppt). We sacrificed fish on site with an overdose of MS-222 anesthetic, and preserved them in 95% ethanol using protocols described previously (Lescak et al. 2015).

Sample Preparation

Briefly, as per Lescak et. al. (2015), we clipped the caudal and pectoral fins for DNA extraction using the Qiagen DNeasy kit and assigned unique identification numbers to associate genotyped DNA with soma in downstream analysis. We fixed the samples in

10% neutral buffered formalin, bleached in a 0.05% hydrogen peroxide solution, and stained with a 0.1% Alizarin red S solution to identify skeletal structures, followed by 1% KOH destain and preservation in 70% ethanol.

Phenotyping of Lateral Plates and Opercle

Lateral plate counts and standard length measures (anterior tip of upper jaw to posterior end of hypural plate; Fig. 3.2A) were collected using a tripod-mounted Canon digital SLR camera and Canon EOS ViewerUtility software. Only fish that were longer than 32 mm standard length were included to ensure we were consistently measuring adult phenotypes.

Analysis of the opercle bone shape required a more detailed view of the head, so we also imaged the left side of the head with an Olympus SZX16 dissecting microscope equipped with an Olympus DP71 microscope digital camera and processed the image with Olympus DP Controller version 3.3.1.292. We measured opercle shape by digitizing the positions of eight landmarks, previously identified by Kimmel et al. (2008) and shown in Fig. 3.2, using the 'tps' software package from the State University of New York at Stony Brook [tpsDig vrs. 2.1 software; (Rohlf 2006)]. Using the `geomorph` R package (Adams and Otárola-Castillo 2013), we treated landmarks 1, 2, 4, and 8 as fixed and landmarks 3, 5, 6, and 7 as sliding semi-landmarks (Fig. 3.2B) (Bookstein 1997b). Landmarks 1 and 8 and semi-landmark 2 capture the opercle joint and the region where the opercle connects to the hyomandibula. Semi-landmark 3, 5 and landmark 4 show the curvature of the anterior edge of the bone which is nestled with the reciprocal curvature of the adjacent subopercle bone. Semi-landmarks 5 and 6 denote the points at the far ventral and posterior edges, between which is the opercle fan (dotted line). Semi-landmarks 6 and 7 show the dorsal edge of the bone and the edge to which the elevator opercular muscle attaches to rotate the opercle, an important function in the opening of the jaw (Hulsey et al. 2005; Kimmel et al. 2008; Anker 2010).

To eliminate variation imposed due to size, location, or orientation, we performed a Generalized Procrustes Analysis (GPA) with the digitized landmark configurations. Following the GPA, a new dataset was generated which reflected entirely shape variation called the "Procrustes Coordinates" (Klingenberg 2010).

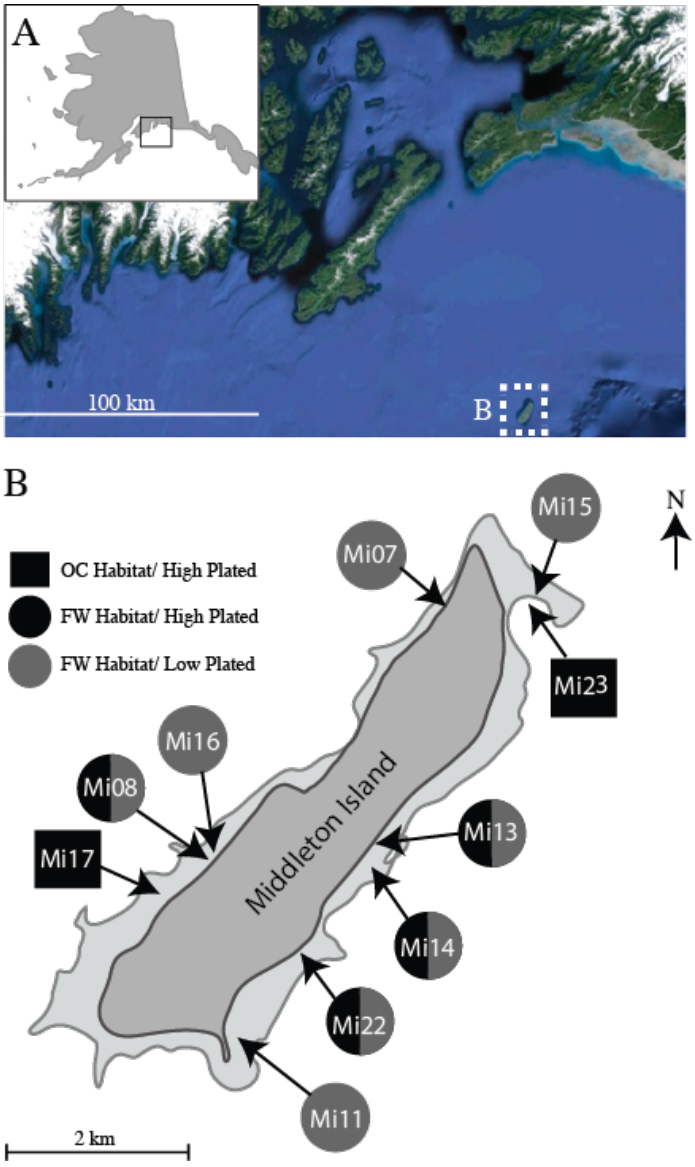

Figure 3.1 Middleton Island, AK sampling locations. A) Alaska with box around sampling site (*inset*). Prince William Sound and the Gulf of Alaska with Middleton Island (*B*) surrounded with white dotted line. B) Middleton Island collection sites coded by whether the site was an oceanic (OC) or a freshwater (FW) habitat and by the dominant (high or low) lateral plate ecotype. Darkly shaded, inner Middleton Island shows approximately the shoreline prior to the 1964 earthquake. Figure modified from (Lescak et al. 2015b)

Table 3.1 Sample collection data, including site name (Mi=Middleton Island), coordinates, habitat type based on water chemistry (FW = freshwater, OC = oceanic), freshwater grouping (FW-1, FW-2, based on Lescak et. al. (2015) population genomic analysis), if freshwater and marine stickleback were sympatric, and whether the population was included in GWAS.

Site	Island	Latitude	Longitude	Habitat- Group	Sympatry	GWAS
Mi07	Middleton	59.448	-146.325	FW-1	N	N
Mi11	Middleton	59.412	-146.338	FW-2	N	**Y**
Mi15	Middleton	59.463	-146.299	FW-1	N	N
Mi16	Middleton	59.429	-146.349	FW-2	N	**Y**
Mi17	Middleton	59.427	-146.359	OC	N	**Y**
Mi23	Middleton	59.461	-146.296	OC	N	**Y**
Mi08	Middleton	59.426	-146.357	FW-2	Y	N
Mi13	Middleton	59.432	-146.314	FW-2	Y	N
Mi14	Middleton	59.437	-146.311	FW-1, 2	Y	N
Mi22	Middleton	59.412	-146.333	FW-2	Y	N

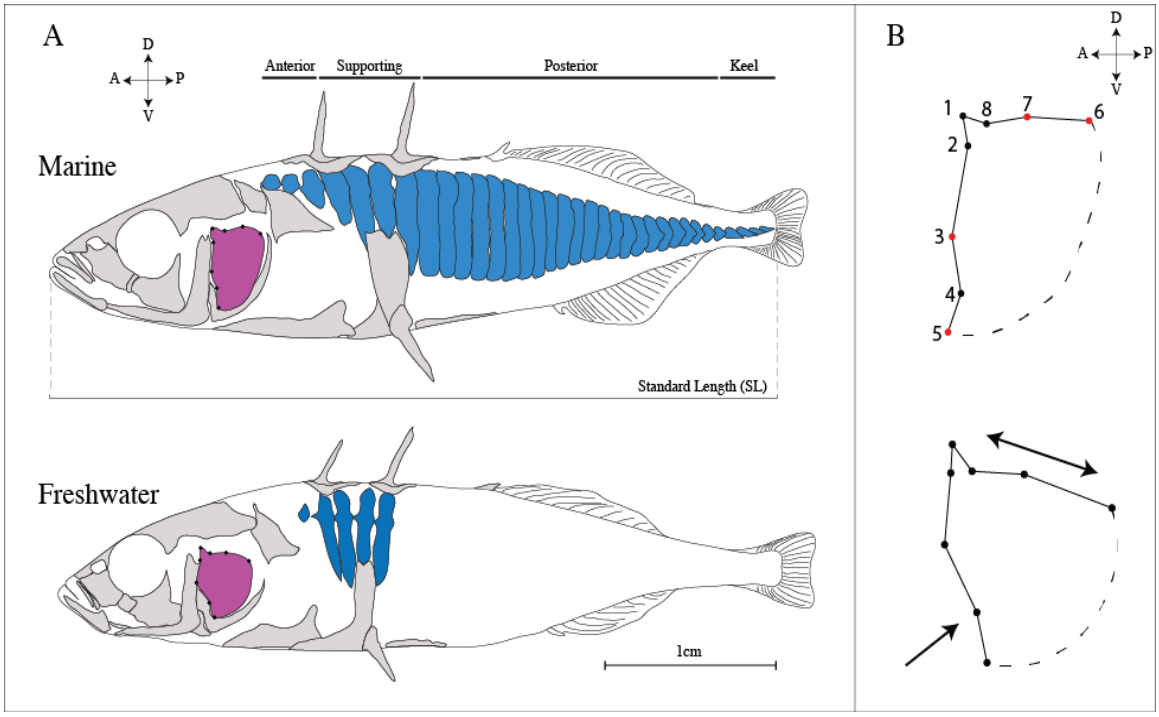

Figure 3.2. Stickleback phenotypes measured and morphological differences. A) Gross morphological differences between collected marine and freshwater stickleback on Middleton Island. Most anterior, posterior, and supporting lateral plates (blue) are lost during the marine-freshwater transition. The opercle bone (purple) also undergoes shape changes, and the positions of digitized landmarks are shown in context of the head. Standard length (SL) was collected for all fish. B) Opercle principal component 1 (PC1) captures the major shape changes during the marine-freshwater transition. Characteristic is a widening of the dorsal edge and reduction of the ventral region (arrows). Numbered landmarks are depicted on the marine opercle shape. Black landmarks are fixed, red landmarks are sliding, dotted line represents the shape of the fan which was not captured by our landmarks. See text for further details about landmark position and principal component analysis (PCA).

Phenotypic Statistical Analyses

Principal component analysis (PCA) was used in the `geomorph` R package (Adams and Otárola-Castillo 2013) to uncover the major axis of variation of opercle shape among individuals from Middleton Island with the Procrustes Coordinates. Included in this PCA were forty individuals from two post-glacial populations formed approximately 10,000-15,000 years ago in South Central Alaska. Twenty individuals were from a marine population and represented the ancestral oceanic population and the other twenty individuals were from a freshwater lake nearby. These South Central Alaska post-glacial populations were used to anchor the morphospace because the populations are monomorphic for divergent marine and freshwater opercle shapes. Thus, by overlaying opercle shapes from Middleton Island we were able to assess the extent of phenotypic space covered by individuals from a newly formed population. PCA was performed with the `plotTangentSpace` program (Adams and Otárola-Castillo 2013). When we treated different sets of landmarks as fixed or as sliders, the results of downstream analyses were not affected.

To assess if opercle shape and lateral plate number were correlated, we used a model I linear regression. Because lateral plate number had a bimodal distribution we performed a square root transformation. Opercle shapes were normally distributed and therefore we did not perform any transformation. All statistical phenotypic analyses were performed in R (R Development Core Team 2015).

RAD Library Preparation and Sequence Analysis

All sequences we used for this study were from individuals collected from sites Mi07, Mi11, Mi15, Mi16, Mi17, Mi23 on Middleton Island (Fig. 3.1, Table 3.1) and the loci were generated as described previously (Lescak et al. 2015). Briefly, genomic DNA was digested with restriction enzyme SbfI-HF (NEB) and RAD-seq libraries were created as reported previously (Baird et al. 2008; Hohenlohe et al. 2010; Etter et al. 2011). The individuals used for the present study were a subset of a larger study by Lescak et. al. (2015) where the uniquely barcoded samples were sequenced in a total of 12 lanes on an Illumina HiSeq2500 platform. Each lane contained between 76-96 individuals, and on

average we retained approximately 72% (113 million) of a total of approximately 157 million single end, 101 nucleotide long reads. The 101 nucleotide long reads each included a 6 nucleotide in-line barcode to identify individual fish. Raw reads were demultiplexed with `process_radtags` program in *Stacks* software suite (Catchen et al. 2011; Catchen et al. 2013) and aligned against the stickleback reference genome (version BROADs1, Ensembl release 64) using GSnap (Wu and Watanabe 2005). Aligned sequences were processed and genotypes at each locus called using the `pstacks`, `cstacks`, and `sstacks` programs from *Stacks* (Catchen et al. 2011; Catchen et al. 2013). Using the *Stacks* program populations, we calculated population genetic measures of divergence at each SNP (F_{st}, Phi_{st}) across all loci with a minor allele cut off of 10%.

Genome Wide Association (GWA) Mapping

To utilize SNP data for genome wide association studies, we used the populations program in *Stacks* to output filtered SNP data (minor allele frequency cutoff, 10%; required at least 75% of individuals in population to possess a locus) formatted for PLINK from the 21 linkage groups and five largest scaffolds (Purcell et al. 2007). We used PLINK, along with our generated phenotype files, to prepare a binary PED file from the PED and MAP output files from *Stacks,* which is compatible with the Genome-wide Efficient Mixed-Model Association (GEMMA) software package (Zhou and Stephens 2012).

We used lateral plate count and the first principle component of opercle shape PCA for association mapping with the SNPs that passed quality control filters in *Stacks* (Catchen et al. 2011; Catchen et al. 2013). We completed association mapping for each trait using the univariate linear mixed model (LMM) implemented in the GEMMA software package (Zhou and Stephens 2012), in which each SNP is assumed to have some effect on the trait. The LMM accounts for population structure by using a relatedness matrix as a covariate.

We controlled for population structure in our GWAS by using one of four relatedness matrices: 1) A mean centered relatedness matrix generated within GEMMA (Zhou and Stephens 2012). By default, GEMMA filters out SNPs with a minor allele

frequency (MAF) above 1%, missingness below 5%, and correlation with a covariate above r^2=0.9999. Because quality filtering was previously done in *Stacks* (Catchen et al. 2011; Catchen et al. 2013), we modified the defaults to ensure that all SNPs were used both in building the relatedness matrix and in the subsequent association. 2) A relatedness matrix calculated from a PCA based on a 1000 randomly selection SNPs. We performed the PCA in the program GenoDive (Meirmans and Van Tienderen 2004) and extracted the first principle component. We followed Sul and Eskin (2013) and used the outer product of the PC1 vector to create a square relatedness matrix. 3) A relatedness matrix in GEMMA (Zhou and Stephens 2012) only from SNPs extracted from linkage group 4, a linkage group highly divergent between marine and freshwater populations (Hohenlohe et al. 2010). 4) A relatedness matrix in GEMMA only from SNPs extracted from linkage group 15, a linkage group with little divergence between marine and freshwater populations (Hohenlohe et al. 2010). We visualized all relatedness matrices to assess the population structure used by the LMM to control for spurious associations in R (R Development Core Team 2015).

We performed all associations in GEMMA (Zhou and Stephens 2012), again adjusting parameters to ensure that all SNPs were included in analyses as above. In order to account for 'proximal contamination', the phenomenon where the power to identify a causative SNP is reduced because the causative SNP is fitted to the model twice, once in the relatedness matrix and again in the association, we used a 'leave one chromosome out' method where we created relatedness matrices for all linkage groups except for the linkage group used in the association (Listgarten et al. 2012; Pallares et al. 2015).

Determining Genome-Wide Significance Thresholds via Permutations

To account for multiple testing, we determined the genome-wide significance threshold for each phenotype by permutation. We performed association mapping on 1,000 permuted datasets. In these datasets, phenotypes were randomized but the genotypes were kept intact. We recorded the minimum *p*-value for each statistical test (Wald, LRT, Score), and we used the 95% quantile from the *p*-value distribution as the genome-wide significance threshold (Pallares et al. 2014).

Analysis of Linkage Disequilibrium

We tested all pairwise combinations of SNPs for genotypic linkage disequilibrium (LD) by calculating the squared correlation coefficient (r^2) in PLINK 1.07 (Purcell et al. 2007). We used the *Stacks* populations program to output a reduced dataset for LD analysis with only one SNP per RAD locus. This reduced the number of pairwise comparisons and the number of SNPs with r^2 values of 1 due to tight physical linkage. We did not remove all pairwise SNPs across the genome with high r^2 values because we wanted to identify long distance genomic correlations.

RESULTS

Middleton Island Stickleback Display Extensive Phenotypic Variation across the Ocean-Freshwater Phenotypic Range

We analyzed wild caught stickleback (n=480) from ten populations on Middleton Island, a subset of those described in Lescak et al. (2015) (Fig. 3.1). We analyzed two populations (Mi17, Mi23) from marine habitats that contained only individuals classified as marine based on phenotype and genotype. Four populations (Mi07, Mi11, Mi15, Mi16) were collected from freshwater habitats that contained only individuals classified as freshwater based on phenotypic and genotypic data. The remaining four populations (Mi08, Mi13, Mi14, and Mi22) from freshwater habitats contained both freshwater and marine stickleback in sympatry. They were only used in phenotypic analysis (Table 3.1).

Interestingly, multiple population genomic analyses from Lescak et al. (2015) - including STRUCTURE, pairwise F_{st}, and Principle Component Analysis (PCA) - supported the presence of two distinct clusters of freshwater stickleback from the ponds which contained only freshwater individuals. These analyses showed that Mi07 and Mi15 were distinct from freshwater populations Mi11 and Mi16. Therefore, for the rest of this paper, we follow the convention presented in Lescak et al. (2015) and analyze individuals collected from Mi07 and Mi15 as Freshwater group-1 (FW-1), and individuals collected from Mi08, Mi11, Mi13, Mi14, Mi16, and Mi22 as Freshwater group-2 (FW-2). More recent analyses showed that in ponds containing both freshwater and marine ecotypes, the

marine stickleback are likely recent migrants from the ocean, and that the freshwater fish are the older, resident population that has rapidly adapted to the freshwater environment in fewer than 50 years (Lescak et al. 2015).

The majority of stickleback we analyzed from marine habitats on Middleton Island had a full set of lateral plate armor. As expected, individuals from freshwater habitats, and not sympatric with marine stickleback as defined by phenotype or genotype (Table 3.1), displayed stereotypical lateral plate loss. These freshwater individuals have lost the majority of their keel and posterior lateral plates and display a reduction of the number of the anterior and supporting plates (Fig. 3.2).

We found that of the 479 individuals we analyzed, the distribution of lateral plate counts was bimodal, and very few individuals had intermediate numbers of plates (Fig. 3.3A). Across all phenotyped populations used in this study, we assume that plate count is a good measure for a marine or freshwater genotype. Despite the presence of high plated fish in sympatry with low plated fish in freshwater habitats in several ponds, lateral plate count still appears to correlate with a fish's marine or freshwater genotype (see above).

We assessed opercle shape change with geometric morphometrics using previously identified landmarks (see Methods), and we reduced shape dimensionality using PCA. We captured the marine-freshwater transition largely with PC1 (62% of the variation; Fig. 3.3B) which is defined by a characteristic widening of the dorsal region and reduction of the ventral region (Fig. 3.2B). The PCA with Middleton Island individuals included a marine and freshwater population from South Central Alaska which are thousands of years old. These older populations occupied the extremes of the phenotypic space along PC1 and did not overlap, (Fig. 3.3B, shaded rectangles). By contrast, opercle shapes from Middleton Island individuals spanned the entire phenotypic space between older marine and freshwater Alaskan populations with many individuals occupying the intermediate space (Fig. 3.3B).

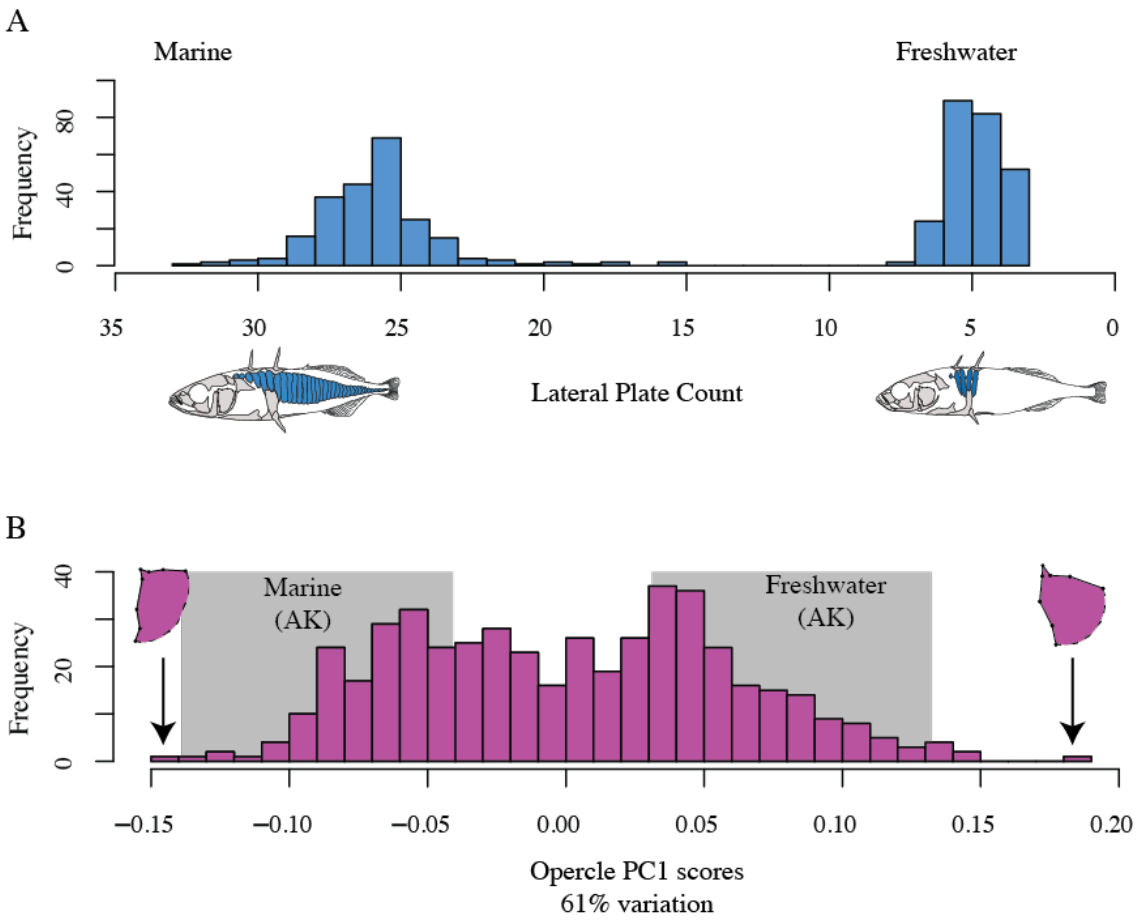

Figure 3.3 Distribution of lateral plate count and opercle PC1 phenotypes across 480 stickleback on Middleton Island. A) Distribution of lateral plate count is bimodal. Individuals with fewer plates (low ecotype) were considered resident freshwater, while individuals with a nearly complete set of lateral plates (high ecotype) were considered marine. In some cases, it appeared that marine fish were the product of very recent introductions into freshwater habitats and had not yet adapted to the freshwater environment (Lescak et al. 2015). Line drawings of lateral plate morph (blue) stereotypical marine and freshwater stickleback below the extremes of the phenotypic range. B) The distribution of opercle shape along PC1 spans the phenotypic range between stereotypical marine and freshwater shapes and includes intermediates. Included in the PCA were individuals from 10,000-15,000 year old post glacial marine and freshwater populations which are divergent and monomorphic for opercle shape to facilitate visualization of the boundaries of opercle shape, marine-freshwater divergence (gray boxes, see methods). The most extreme PC1 shapes are shown, opercle PC1 account for approximately 61% of variation among these individuals.

Coordinated Dermal Bone Evolution of Stickleback Occurs in Decades

Stereotypical and coordinated phenotypic evolution of skeletal, physiological, and behavioral traits is observed during the marine to freshwater transition comprising a freshwater syndrome (Bell and Foster 1994). We focused on two of these traits, a marked reduction in the number of lateral plates and changes in opercle shape along the PC1 axis which are wider in the dorsal region and reduced in the ventral region than the marine ancestors. We used a linear regression model and measured the correlation between lateral plate and opercle PC1 shape across all individuals on Middleton Island (n=480). Because phenotypically marine and freshwater individuals were present in sympatry in several freshwater sites, we classified individuals as marine or freshwater based on lateral plate number rather than the habitat from which they were sampled (Table 3.1). We found that opercle shape and lateral plate number were correlated across phenotypically marine (high plated) and freshwater (low plated) individuals (r^2=0.526) but weakly correlated within groups of only high or only low plated individuals (r^2=0.116, r^2=0.008 respectively) (Fig. 3.4, Table 3.2).

We used marine individuals from Mi23, Mi17 and freshwater individuals from FW-2 (n=154) for subsequent analyses to reduce population structure imposed by pooling individuals from different freshwater populations. To ensure that phenotypic correlations in the marine and FW-2 subset reflected phenotypic correlations found across all individuals on Middleton Island, we compared the correlations between the groups. We found that like all individuals sampled on Middleton Island, correlations between opercle shape and lateral plate number in this subset were strong among high and low plated individuals (r^2= 0.594) and weak within only low or high plated individuals (r^2= 0.013, r^2= 0.126; Fig. 3.4, Table 3.2)

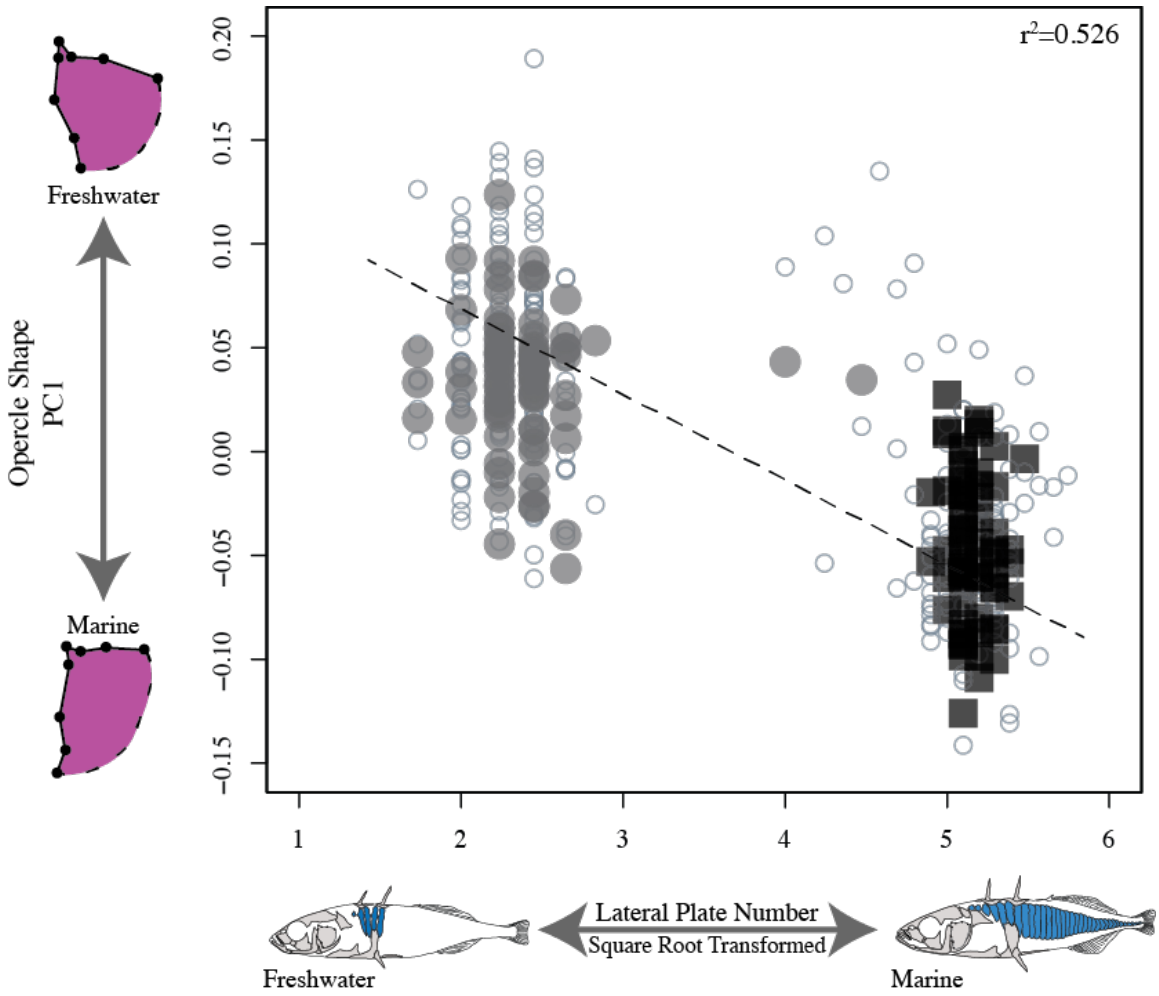

Figure 3.4 Correlation between lateral plate number (square root transformed) and opercle PC1 scores. All individuals from Middleton Island included in regression analysis are represented by open circles, filled gray circles, and black squares. Individuals represented by filled gray circles (FW-2 individuals captured from freshwater environments) and filled black squares (individuals captured from marine ponds) represent those individuals used subsequently in GWAS. Regression line plotted and r^2 value was determined using all the individuals phenotyped on Middleton Island. For details about regression analysis within and among populations see Table 3.2)

Table 3.2 Model II regression analysis (Major Axis): lateral plate count (square root transformed) and opercle PC1 scores. Within group regressions were with individuals with either high or low plate morphologies. Among group regressions grouped together all plate morphologies. Populations include all individuals on Middleton Island and only those used for GWAS

Populations	n	r	r^2	Intercept (-\+ 97.5% CI)	Slope (-/+ 97.5% CI)
All: Middleton Island Among - high/low	480	-0.725	**0.526**	**0.109** (0.100,0.119)	**-0.029** (-0.032,-0.027)
All Middleton Island Within- low plated morph	249	-0.093	**0.008**	**0.081** (0.027,0.136)	**-0.017** (-0.041,-0.005)
All Middleton Island Within- high plated morph	231	-0.341	**0.116**	**0.281** (0.165,0.398)	**-0.063** (-0.086,-0.040)
GWAS: Middleton Island Among - high/low	154	-0.771	**0.594**	**0.056** (0.048,0.064)	**-0.038** (-0.004,-0.003)
GWAS: Middleton Island Within- low plated morph	81	-0.116	**0.013**	**0.078** (-0.003,0.160)	**-0.018** (-0.053,-0.016)
GWAS: Middleton Island Within- high plated morph	73	-0.356	**0.126**	**0.319** (0.093,0.545)	**-0.070** (-0.115,-0.026)

Relatedness among Individuals on Middleton Island Reveals Strong Population Structure

We evaluated population structure by calculating a mean-centered relatedness matrix in GEMMA. Pairwise comparisons among FW-2 individuals showed that they are closely related, as did similar comparisons in the marine populations. The pairwise relatedness coefficients were normally distributed within populations, however, several pairs of individuals sampled from each of the marine and freshwater ponds appeared to be more closely related than others and likely reflect individuals sampled within a family. Because we use a mean centered relatedness matrix, the relatedness coefficients are not the realized relatedness between individuals. Rather, they are a scaled coefficient based on mean centering and therefore should not be interpreted as actual relatedness coefficients among individuals. Pairwise comparisons among marine and freshwater individuals revealed a distribution of negative relatedness coefficients. This indicates that individuals sampled from marine and freshwater environments were more distantly

related to each other than they were from individuals sampled from the same environment which reveals the structured nature of the populations used for GWAS (Fig. 3.5A).

We also evaluated relatedness and population structure with a second method that uses a PCA of 1000 randomly selection genotypes (see Methods). This method of analysis yielded a distribution of relatedness coefficients that was similar to those obtained by the mean-centered relatedness matrix. However, unlike the relatedness matrix generated in GEMMA, the PCA analysis did not appear to show the familial relationship between a few individuals (Fig. 3.5B).

Controlling for Population Structure Created by Strong Divergent Selection in GWAS

Controlling for population structure is critical in GWAS, and if not done sufficiently can lead to spurious associations. While the general need to control population structure is well accepted for GWAS, the best way to do so is still unresolved. The chief reason is that population structure is often not generated equally across the genome (Charlesworth 2006) nor among species (Ellegren et al. 2012). Therefore, finding a single solution is now recognized as a significant challenge. If structure is primarily driven by drift, and the role of selection on specific genomic regions has been minor, then calculating average relatedness among individuals across the genome, is effective (Balding 2006; Astle and Balding 2009). However, if selection has played a prominent role in shaping genomes, controlling for population structure will be problematic because not only does the action of selection cause heterogeneity across the genome, but the mode of selection can create different kinds of population structure. In this scenario, calculating an average relatedness may be an ineffective method to control for structure (Price et al. 2010; Price et al. 2013; Sul and Eskin 2013). At present, the most common methods estimate across many loci to derive an average, and presumably, stable point estimate (Sul and Eskin 2013). We evaluate these below.

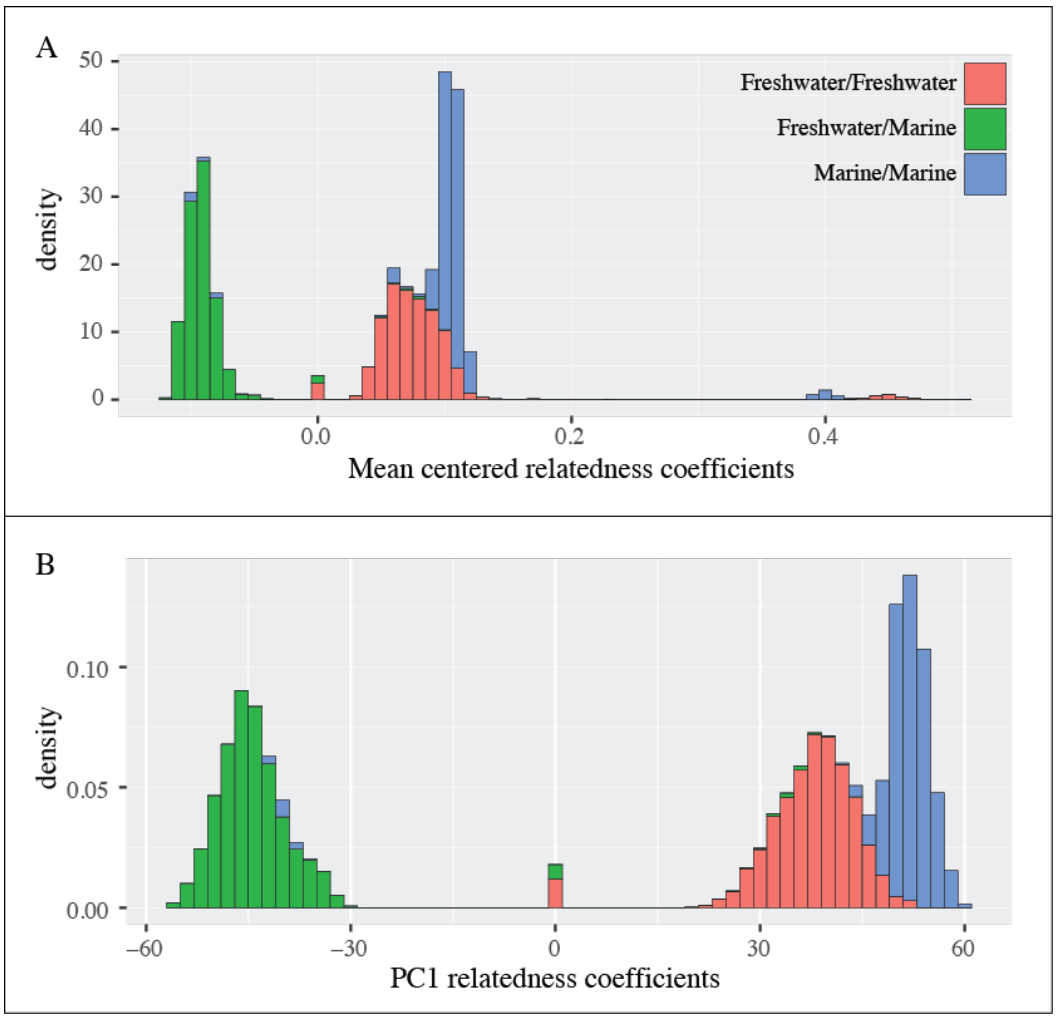

Figure 3.5 Stacked density bar plot of relatedness coefficients between all pairwise combinations of 155 individuals used for GWAS (marine and FW-2). Mean center is 0. Colors indicate from which environment the individuals were sampled. The freshwater individuals are from FW-2 population. A) Mean centered relatedness calculated within the GEMMA software (Zhou and Stephens 2012). B) Relatedness derived from PCA with 1000 random genotypes. The PC1 outer product was used to calculate the matrix (see Methods) (Sul and Eskin 2013).

As described in the above section, we visualized relatedness among individuals using a mean-centered relatedness matrix produced in GEMMA and an PCA based matrix formed from the outer product of PC1. These methods are widely used in GWAS (Pallares et al. 2014; Delmore et al. 2016). We tested each method to determine if either method was more suitable for our stickleback system on Middleton Island. With the mean-centered relatedness matrix, we used several approaches to generate matrices from a variety of SNP combinations. When we assessed population structure by visualizing relatedness matrices using either all SNPs across the genome, or SNPs from linkage groups that were divergent (i.e. LG 4) between marine and freshwater populations, we found that individuals compared within groups (marine v. marine; freshwater v. freshwater) were more closely related (positive relatedness coefficients) to one another than comparisons between marine and freshwater groups (negative relatedness coefficients) (Fig. 3.5). Associations with these matrices to control for population structure showed regions associated with lateral plate count on linkage groups 4, 7, 11, 12, 19, 20, 21 (Fig. 3.6C,E). Genomic regions associated with opercle PC1 shape were localized to linkage groups 4, 7, 11,12, 19, 20, and 21 (Fig. 3.7).

In contrast, when we used genomic regions where no population structure exists, the relatedness matrix was not effective in eliminating spurious associations. We evaluated population structure by visualizing a relatedness matrix generated only from SNPs in a genomic region where, based on F_{st} analysis, little divergence occurs. Using linkage group 15 we found that all combinations of comparisons among individuals and populations were normally distributed around a mean-centered relatedness coefficient of zero. This indicates that no population structure exists at this genomic region between the marine or freshwater populations (Fig. 3.6A,D). However, if this matrix is used to control for population structure in a GWAS, all divergent regions across the genome are strongly associated with lateral plate count. This suggests that using a genomic region which is not structured and does not reflect structure elsewhere in the genome is an inadequate control for GWAS in these stickleback populations.

Lastly, we assessed a relatedness matrix from the outer product of PC1 calculated from a PCA of 1000 randomly selected genotypes from all individuals. As described above, in visualizing this matrix we found that, like the ‘all SNP’ relatedness matrix

produced in GEMMA, the PC1 generated matrix nicely showed the lack of structure within populations (positive coefficients) and showed strong structure present between marine and freshwater populations (negative coefficients). When we used the PC1 matrix to control for population structure in a GWAS for lateral plate count we found that many of the more moderately associated peaks on linkage groups 11, 12, 19, and 20 fell away (Fig. 3.7).

Because we expected *eda* to be associated with lateral plate count, we were encouraged to see that the association at this genomic region on LG 4 was still present, and that the second two peaks on the right side of the linkage group had fallen away (Fig. 3.7). Peaks on LG 7 and 21 were still present. When we used the PC1 matrix to control for population structure in an association with opercle shape, we found a similar pattern as we saw with lateral plate association, that many of the more moderately associated peaks on linkage groups 11, 12, and 19 disappeared. Interestingly, however, of the SNPs that remained associated on linkage groups 4, 7, 20, and 21, clusters of SNPs grouped to approximately the same *p*-value.

We determined that controlling for population structure was effective using either a relatedness matrix generated with GEMMA using all SNPs across the genome, or using the PC1 outer product matrix from 1000 randomly selected loci. However, the PC1 matrix does appears to be more conservative.

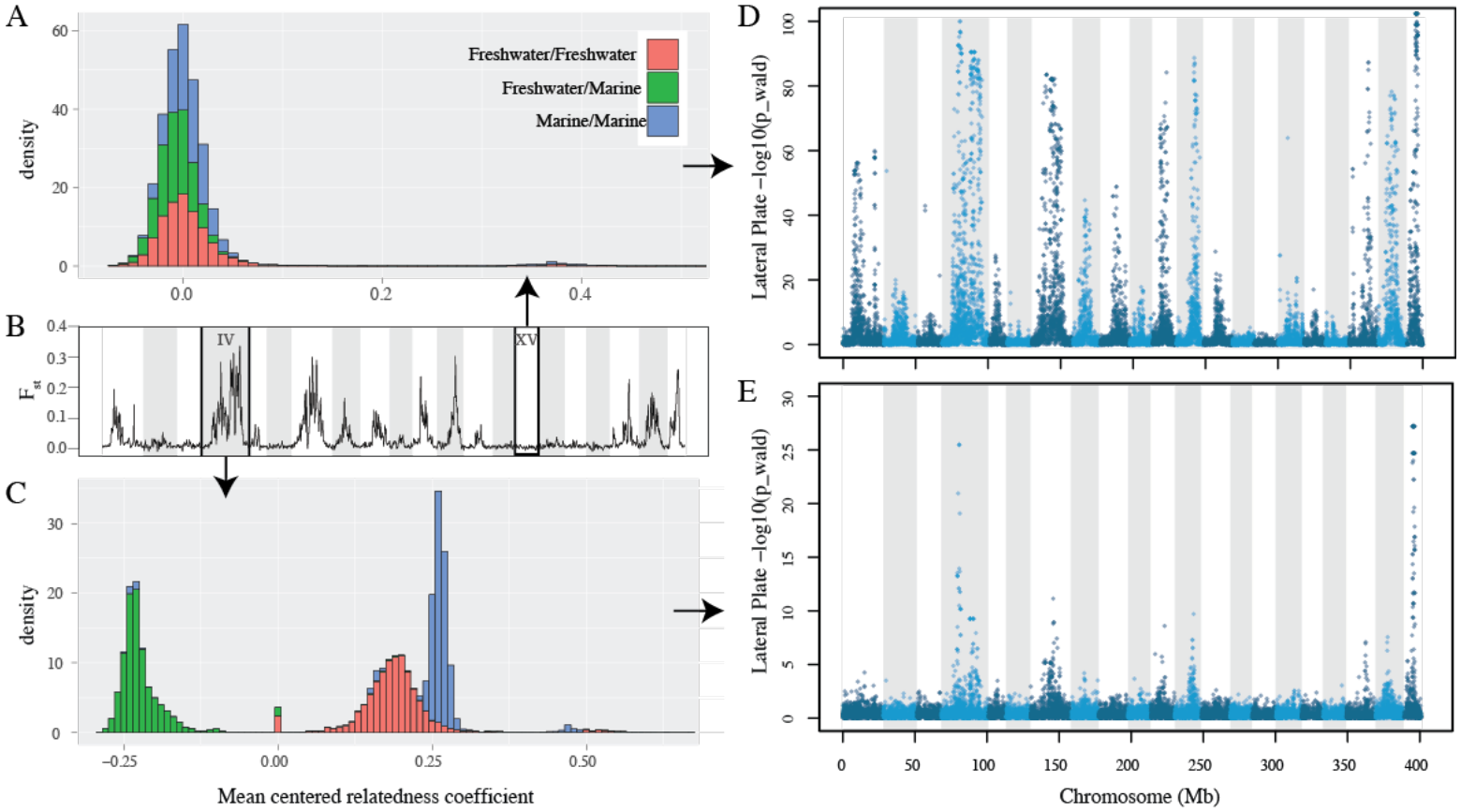

Figure 3.6 Effect of creating relatedness matrices from divergent or neutral genomic regions to control for population structure in GWAS. Lateral plate count is used as example phenotype. Mean centered relatedness coefficients using SNPs from LG 15 (A) and LG 4 (C). B) Genomic divergence between marine and FW-2 individuals (F_{st}). Boxes and arrows show the divergence at LG 4 and LG 15. Identifying genomic regions associated with lateral plate count using a relatedness matrix built from LG 15 (D) and LG 4 (E).

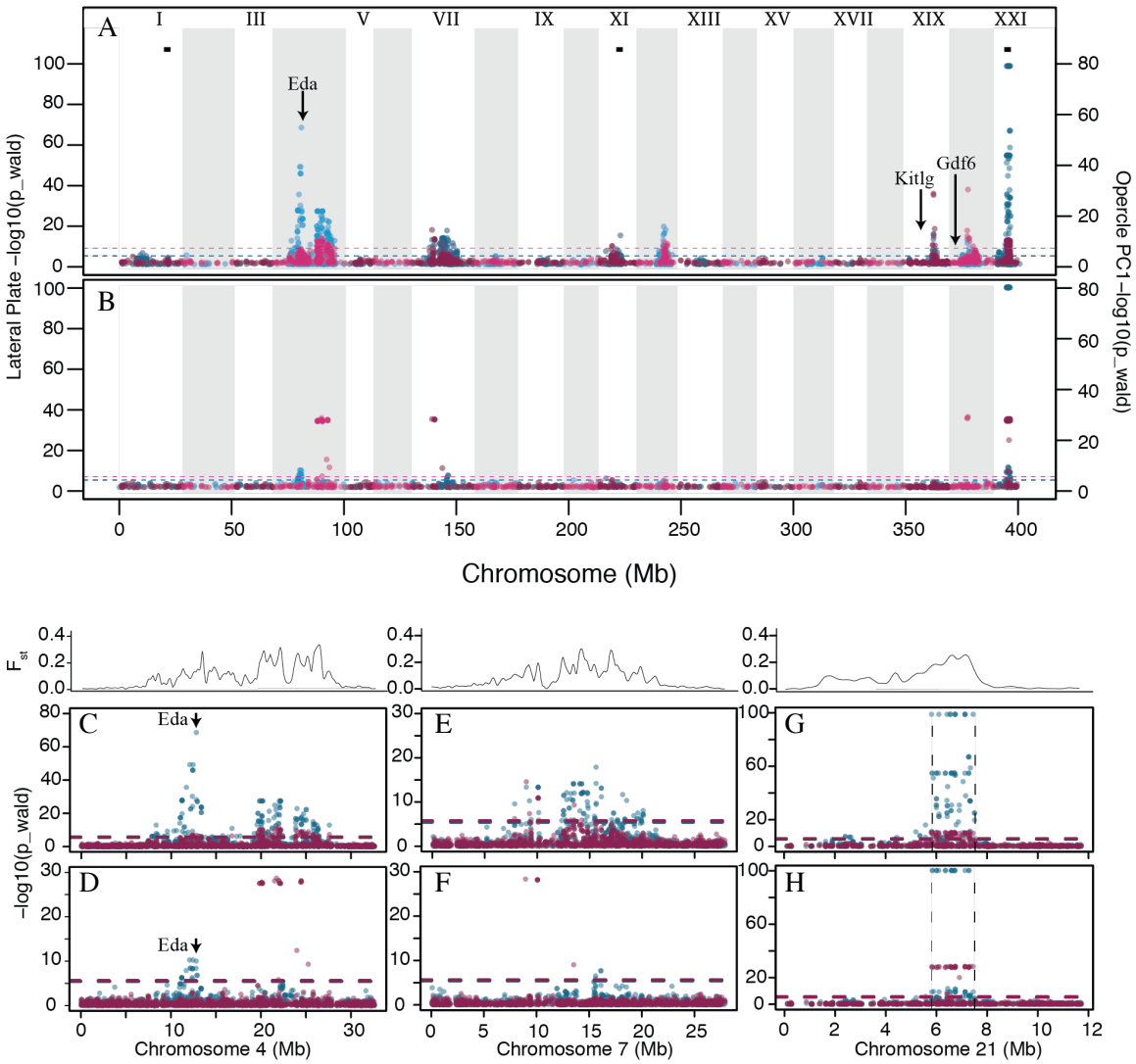

Figure 3.7 GWAS to identify genomic regions associated with lateral plate count (blue) and opercle shape (purple) using an "all SNP" relatedness matrix calculated in GEMMA (A, C, E, G) and a relatedness matrix derived from the PC1 outer product of a PCA on genotypes (B, D, F, H). Significance is reported as -$\log_{10}$ *p*-values from Wald's test. Genome wide significance line for each phenotype is represented as horizontal dashed lines (blue=lateral plate, purple=opercle shape). In (A), small horizontal black dashes represent the locations of known inversions (Jones et. al. 2012). Arrows identify genomic positions where previously identified genes have been implicated in traits contributing to the "freshwater syndrome" (see text for details). Alternating gray boxes represent chromosome boundaries with chromosome numbers identified. Individual chromosomes 4, 7, and 21 are shown to detail differences in GWAS results depending on relatedness matrix used. Genomic divergence (Fst) is shown above individual chromosomes. Horizontal dashed lines (G, H) depict large inversion on chromosome 21.

Genomic Regions Associated with Lateral Plate Number and Opercle Shape are Co-Localized

We identified significant associations for both lateral plate count and opercle PC1 shape after controlling for population structure using a GEMMA generated relatedness matrix with all SNPs and a proximal contamination approach. The genome-wide significance threshold for lateral plate count was determined to be $p < 3.74\text{x}10^{-06}$ through permutations (see Methods). In addition, SNPs above the defined significance level localize to linkage groups 1, 4, 7, 11, 12, 19, 20, and 21. Except for linkage group 1, genomic regions significantly associated with opercle PC1 shape variation ($p < 1.64\text{x}10^{-06}$) appear to co-localize with genomic regions associated with lateral plate count (Fig. 3.7).

For each SNP the significance of the association in a *p*-value from three tests can be calculated in GEMMA: the Wald test, likelihood ratio test (LR), and the score test. Wald's test consistently showed the most significant associations, followed by the LR test, followed by the score test which reported that no SNPs were significantly associated with either phenotype. The most highly associated SNPs were largely the same across tests, but the *p*-values fluctuated. We were concerned about which test statistic to report given the variation in number of, and degree to which, SNPs were associated with the phenotype, and because *p*-values can be unstable depending on effect size and sample size. We evaluated the $-\log_{10}$(restricted maximum likelihood estimates) and determined that these estimates were most congruent with *p*-values calculated with Wald's test (Fig. 3.8). *P*-values from Wald's test and the LR test are most commonly reported in GWAS (Pallares et al. 2014; Pirie et al. 2015), and based on the restricted maximum likelihood estimates, we report Wald's test.

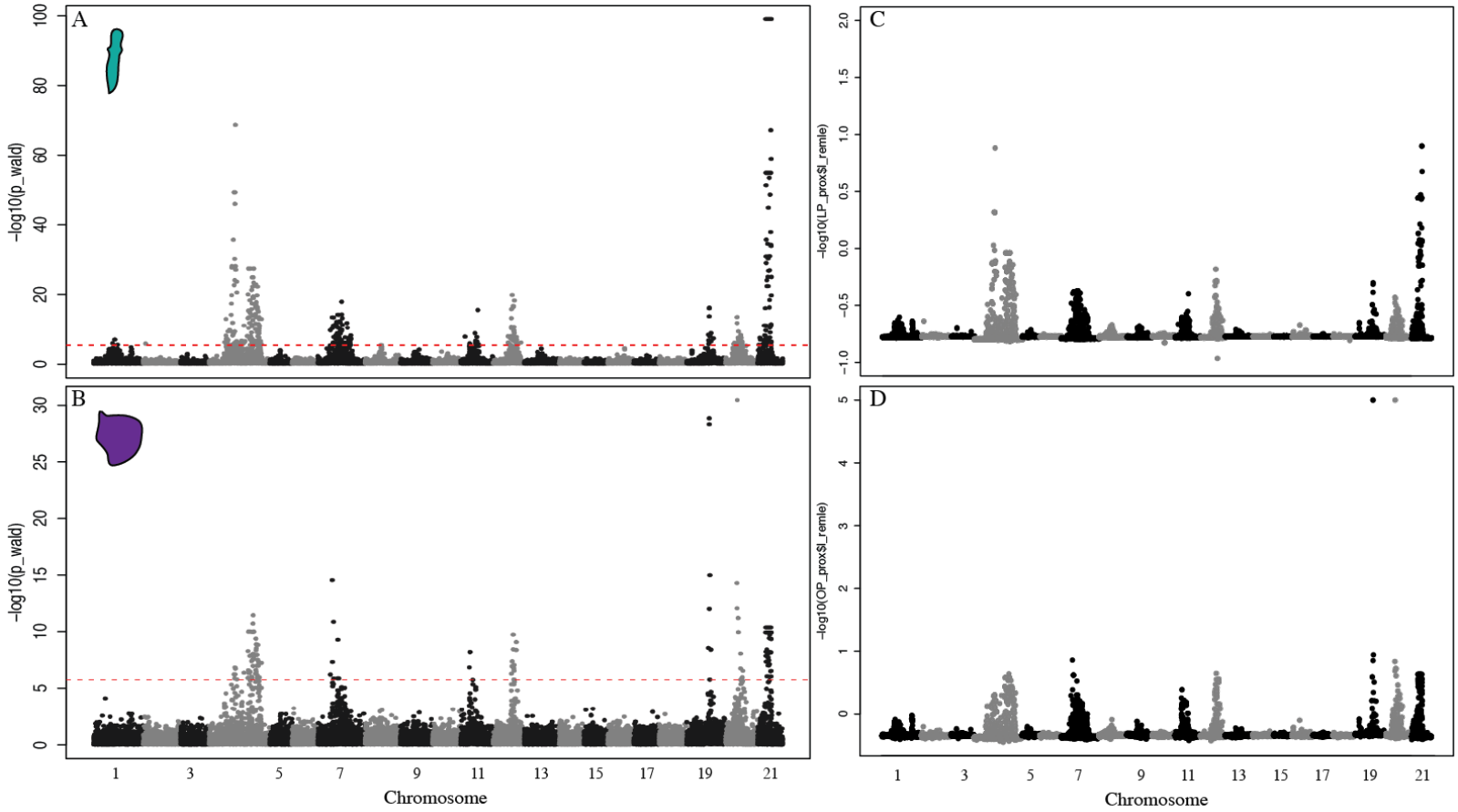

Figure 3.8 Genomic associations with lateral plate count (A, C) and opercle shape (B, D) controlling for population structure using a relatedness matrix calculated in GEMMA with all SNPs. Visual comparison of -$\log_{10}$(*p*-values) generated from Wald's test (A, B) and -$\log_{10}$(restricted maximum likelihood estimates(C, D). Red dotted line shows the genome wide significance level.

To determine if any genomic regions significantly co-varied between lateral plate count and opercle PC1 shape, we used a multivariate linear mixed model approach in GEMMA. We again controlled for population structure using the GEMMA generated relatedness matrix with proximal contamination control, and we found that genomic regions on linkage groups 4, 7, 11, 12, 19, 20, and 21 were significantly associated with covariation between lateral plate and opercle PC1 shape. This finding supports our previous finding that dermal bone evolution is correlated among marine and freshwater populations. Our result also extends our findings with univariate analysis to suggest that the genomic regions responsible for correlated dermal bone evolution corresponded to a subset of regions which are most divergent between populations as calculated by the population genetic differentiation statistic, F_{st} (Fig. 3.9).

Figure 3.9 Univariate (A, B) and multivariate (C) GWAS are colocalized to genomic regions of divergence (D). Lateral plate number (A) and opercle shape (B) variation individually map to genomic regions of divergence (F_{st}, D). Covariation between lateral plate number and opercle shape is also associated with genomic regions most divergent between the marine and freshwater populations (C).

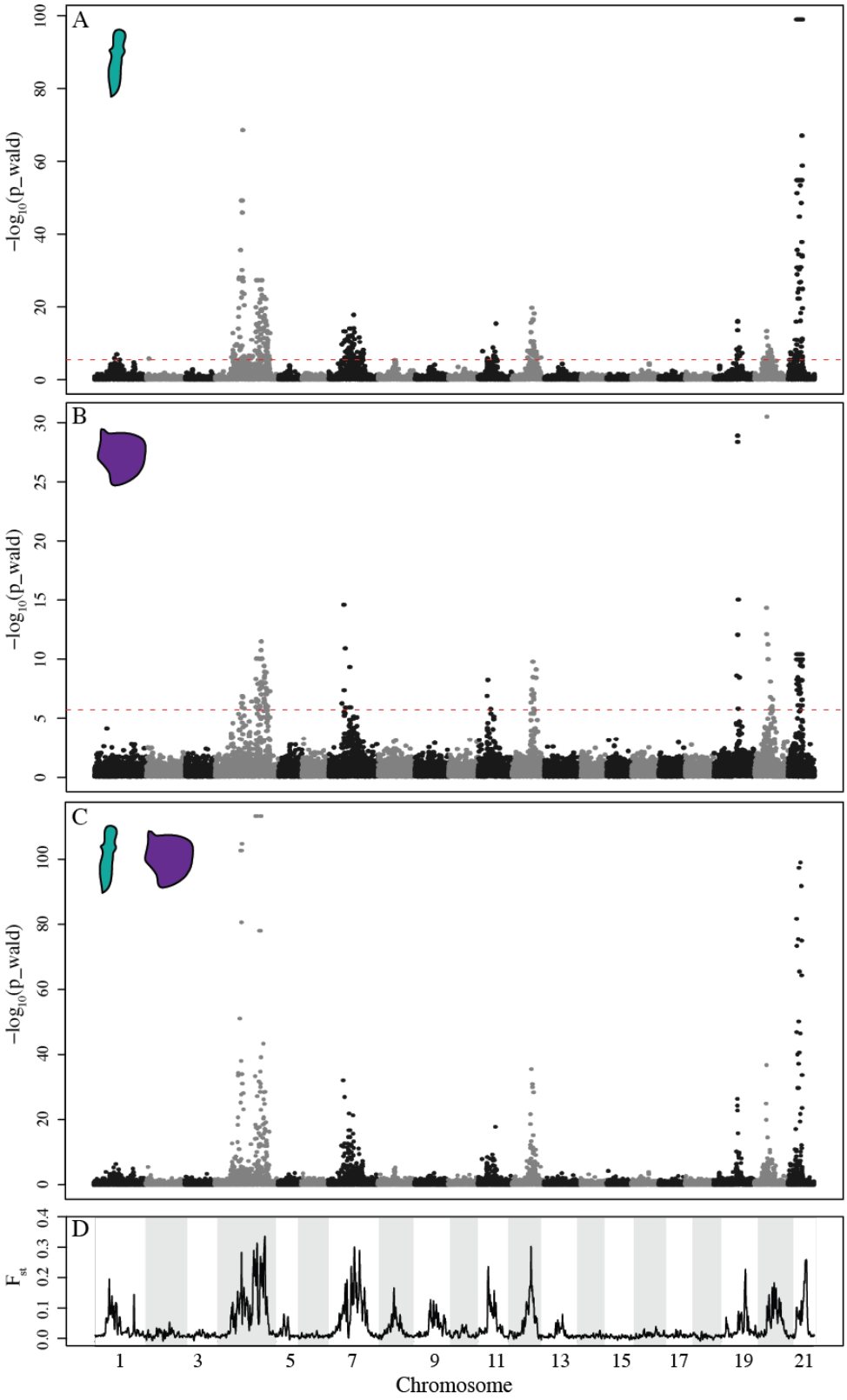
A
B
C
D
−log10(p_wald)
Fst
Chromosome
1
3
5
7
9
11
13
15
17
19
21

Extensive Genomic Covariation among Marine and Freshwater Populations

We tested for long-range linkage disequilibrium (LD) by calculating r^2 correlations between all pairwise combinations of SNPs across the genome (see methods). Within the group of individuals sampled from marine populations, we did not find evidence for widespread LD, however we did find a segment of LD within linkage group 19 in the non-recombining region which indicates the both males and females were present our sample. Furthermore, a portion of this block appeared to be in long-range LD with small regions on linkage group 7 and 9 and could suggest assembly error. LD was present within linkage blocks, but was minimal. Individuals from the FW-2 population were sampled from ponds on adjacent sides of the island and display slightly stronger genomic covariation within linkage groups than individuals from the marine population. Within linkage group LD may represent local adaption in each of the ponds, however, overall genome wide covariation was minimal except for long-range LD between linkage group 19 and linkage groups 7 and 9.

We also calculated long-range LD among individuals pooled from marine and freshwater populations which made up the sample population used for GWAS. Even within only 50 years of evolution, we found evidence for extensive genomic covariation, both short-range (within linkage groups) and long-range (across the genome), which highlights the dramatic and rapid creation of structure between marine and freshwater populations (Fig. 3.10). The blocked and heterogeneous nature of the LD between these populations strongly implicates natural selection as a major driver of population structure rather than drift which would largely affect the whole genome uniformly. Additionally, the large blocks of LD co-localize to regions of divergence, as measured by F_{st}, and house genomic regions of association with lateral plate number and opercle shape identified through GWAS (Fig. 3.10).

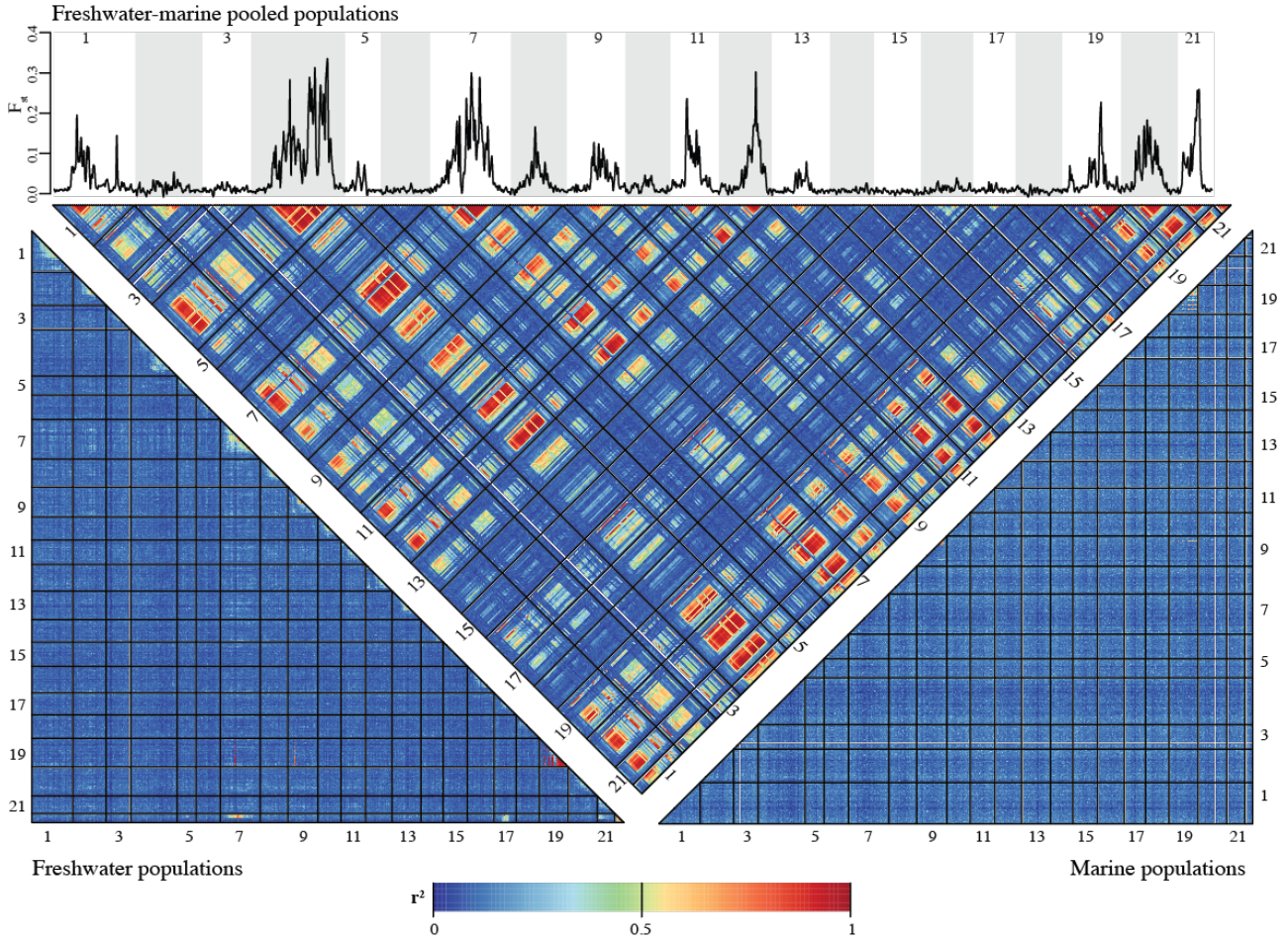

Figure 3.10 Genomic correlations within and among individuals from marine and freshwater populations on Middleton Island. Linkage disequilibrium measured between all pairwise combinations of SNPs with r^2 ranging from 0-1. Divergence (Fst) between individuals in marine and freshwater populations is shown. Alternating gray bars represent linkage group boundaries.

DISCUSSION

Opercle Shape and Lateral Plate Phenotypes Can Evolve in a Coordinated Fashion in Decades

Historically phenotypic evolution was thought to take many thousands of generations to generate discernible differences among populations or species of organisms (Bell 2001). More recently, that view has been challenged with numerous case studies of rapid evolution across a variety of taxa (Hendry and Kinnison 1999; Hendry 2000; O'Steen et al. 2002; Kopp and Matuszewski 2013; Lescak et al. 2015). The tremendous phenotypic diversification of marine stickleback into post-glacial freshwater environments has received considerable attention as a model system to study rapid evolution on the order of only about 10,000-15,000 years (Bell 2001; Peichel et al. 2001; Colosimo et al. 2004; Cresko et al. 2004). However, it is now known that nearly the same extent of phenotypic evolution seen in 10-15,000 years can actually occur on the order of decades (Bell et al. 2004; Aguirre and Bell 2012; Lescak et al. 2015). Several studies in stickleback have investigated the very rapid evolution of lateral plate loss, gill raker number, body shape change, cold tolerance, and opercle shape changes (Aguirre et al. 2004; Albert et al. 2008; Barrett et al. 2011; Kimmel et al. 2012a) that can occur over ecological time scales. Our findings, in which we show that lateral plate count and opercle shape are correlated across populations, integrate into this body of literature and show that a coordinated evolution of trophic morphologies and body armor can occur during a time frame of only decades. Although these are only two phenotypes, Lescak et. al. (2015) showed similar patterns of rapid evolution across many phenotypes in these population. These and other results in different populations of stickleback indicates that the phenotypes that comprise the freshwater syndrome, including trophic morphology and body armor, and likely physiological and behavioral traits as well, can evolve very rapidly. The degree to which this coordinated evolution over mere decades is facilitated by genetic and genomic modularity is largely unknown.

Independent Genetic Architectures Underlie Coordinated Phenotypic Evolution

Our data argue that rapid, coordinated phenotypic evolution of lateral plate number and opercle shape is not due to selection on completely independent loci, nor is it due to loci that exhibit pleiotropic effects for the genetic architecture of both traits. We showed that among marine and freshwater populations the correlation between lateral plate number and opercle shape was strong, but that within the marine or freshwater populations, the correlation was quite weak (Fig. 3.4). If pleiotropy were the primary contributor to correlated phenotypic variation, we would expect these correlations to be present both *among* and *within* populations (Armbruster and Schwaegerle 1996). Our findings may not be surprising when we consider that the way we measured the traits, meristic vs. morphometric, likely reflects aspects of the traits that may be regulated by fundamentally different genetic or developmental mechanisms.

Even within the same stickleback trait, the genetic basis can be different depending on the perspective from which the trait is analyzed. For example, stickleback laboratory mapping studies have identified the major effect locus of lateral plate count to be *eda* on chromosome 4 but that the major effect locus of lateral plate height and width is located on chromosome 20 and includes g*df6* (Colosimo et al. 2004; Colosimo 2005; Indjeian et al. 2016). Differences in the genetic architectures of meristic and shape phenotypes within lateral plates supports our interpretation that opercle shape is likely regulated by different mechanisms than lateral plate count.

While we argue that pleiotropy does not make a major contribution to the correlation of phenotypic variation present at the time of sampling, we recognize that pleiotropy may still play a role perhaps early in the process of phenotypic divergence. Because our correlation analysis only reflects phenotypic variation currently present, it is possible that some loci with pleiotropic effects on the phenotype were fixed between populations prior to sampling. Regardless, our results suggest that pleiotropy is not a predominate force facilitating rapid, correlated evolution on Middleton Island only 50 years after invasion of marine stickleback into freshwater ponds. Although such rapid, coordinated evolution could occur through the independent action of uncorrelated loci, another possibility is that loci for the two traits are genomically localized.

Genetic Architectures of Phenotypic Variation Co-Localize to Genomic Regions

Despite the finding of independent loci contributing to each trait, our GWAS show that the genetic architecture of the phenotypic variation clusters to similar genomic regions on LG 4, 7, 21 and additionally to LG 11, 12, 19, and 20 depending on how population structure is controlled (Fig. 3.7). Previous QTL mapping studies in threespine stickleback have generally implicated these linkage groups as housing genetic variation for the traits that comprise the freshwater syndrome (Colosimo et al. 2004; Miller et al. 2014; Conte et al. 2015; Erickson et al. 2016). However, these different mapping studies reveal that the observed relationship among linkage groups and these phenotypes varies geographically. This variability is probably due to a combination of differences in methodology - such as how the traits are measured and crossing design - as well as true biological differences such as the populations from which individuals were sampled for genetic crosses or the genetic variants captured in particular crosses. For example, QTLs associated with opercle shape changes, captured by linear measurements, localized to LG 19 and 3 in an F_2 derived from a cross between marine and freshwater individuals from South Central Alaska (Kimmel et al. 2005). However, QTLs associated with opercle shape captured by slightly different linear measurements than in Kimmel et. al. (2005), were identified on LGs 1 and 7 in an F_2 family derived from a cross between a Japanese Pacific marine and a Paxton Lake (British Columbia) benthic freshwater pair (Miller et al. 2014). Furthermore, when opercle shape was measured using a landmark based analysis in F_2 progeny from a cross between a freshwater benthic and a limnetic species pair in British Columbia, QTL were identified on LGs 2, 4, 6, 7, 9, and 13 (Conte et al. 2015).

These differences in QTL mapping results could reflect inter-population variability. Unlike lateral plate count, opercle shape is thought to be a more complex polygenic trait (Kimmel et al. 2005), and it is plausible that the contribution of each locus to shape may differ between populations. These data also suggest that different aspects of shape changes are governed by several different genomic regions (Huycke et al. 2012). Regardless, previous studies show the clear trend that QTL associated with multi-trait evolution are localized to similar LGs and often cluster to similar genomic regions within those LGs (Malek et al. 2012; Miller et al. 2014; Conte et al. 2015). Our GWAS data

extend previous research by showing that the loci identified in laboratory QTL studies also cluster and contribute to trait variation in natural populations.

Genetic Structure in These Young Populations is Created Primarily by Divergent Natural Selection

Both the pattern and the speed at which population structure (measured by LD quantified as r^2) is generated between marine and freshwater individuals on Middleton Island are striking. We found large LD blocks that are congruent with divergent regions (F_{st}) and span adaptive chromosomal regions known to harbor genes involved in repeated lateral plate loss (*eda*, LG 4) and pelvic structure loss (*pitx1*, LG 7) (Cresko et al. 2004; Shapiro et al. 2004). The speed at which these linkage blocks were created precludes the role of *de novo* mutation or drift as major drivers. Instead, extensive intra-chromosomal LD suggests that mechanisms that suppress recombination, such as inversions or translocations, may play an important role in coordinate phenotypic evolution via linked selection (Hohenlohe et al. 2012a). If alleles that contribute to multiple traits critical in the marine to freshwater transition are located in proximate genomic regions, reduced recombination would lead to these alleles being linked and allow them to segregate as a unit in the oceanic population (Hohenlohe et al. 2012a). For example, we showed in our GWAS that alleles that contribute to both lateral plate count and opercle shape may be harbored within a known 2Mb inversion on LG 21 which is encompassed by a large block of LD and which is divergent between marine and freshwater populations. Any mechanisms of reduced recombination, whether genetic or genomic, would serve to facilitate linked selection.

Unlike observations made by Hohenlohe and colleagues (2012a), we did not find evidence for intra-chromosomal or long-distance LD within the marine populations. Common to the stickleback system is that gene flow will occur from freshwater to marine populations (Hohenlohe et al. 2012a), constantly replenishing the panmictic marine population with freshwater alleles which aids in the maintenance of standing genetic variation (Barrett and Schluter 2008; Terekhanova et al. 2014). Similar to expectations expressed by Colosimo et. al. (2005) and Barrett et. al. (2008) that freshwater alleles are

present in the marine population, but at a very low frequency (estimated at ~1%), our results suggest that the frequency at which the freshwater alleles segregate in marine populations is remains low enough to go undetected in LD patterns. Given the relatively few fish sampled (20 individuals) by Hohenlohe et. al. (2012a), we suggest that LD found in marine populations in that study was the result of the stochasticity of sampling. The freshwater populations do show some intra-chromosomal LD patterns but nearly no long-distance LD (Fig. 3.10). LD at linkage group 19 indicates the non-recombining region of the sex chromosome and suggests the presence of both males and females in the sample.

GWAS Results for the Phenotypes Are Not Only due to the Underlying Population Structure

Correctly inferring genetic causation from GWAS depends on the appropriate control of underlying population structure to minimize spurious associations (Astle and Balding 2009). Examining stickleback populations that span marine-freshwater habitats and phenotypes is a strength of our GWAS design. However, because of the strong patterns of LD created by selection, one concern is that the associations we identified may only reflect the underlying population structure of pooled marine and freshwater populations and not the genetic architecture of the phenotypic variation of interest (Mezmouk et al. 2011). We addressed this concern by controlling for population structure in a variety of ways. These included using freshwater populations that cluster together on a neighbor joining tree to reduce within freshwater population structure (Lescak et al. 2015), a mean centered relatedness matrix generated within GEMMA which included all SNPs across the genome, a mean centered relatedness matrix generated from SNPs only within linkage groups that were heavily divergent (i.e. LG 4, 7) and alternatively from linkage groups with no divergence (i.e. LG 15) (Zhou and Stephens 2012), and a PC1 outer product relatedness matrix generated from 1000 random loci across the genome (for details see Methods) (Price et al. 2010; Sul and Eskin 2013).

If the associations identified in our GWAS only reflected population structure due to the marine-freshwater transition, we would expect that lateral plate count and opercle shape would associate with all genomic regions that are shown to be divergent between

stickleback in oceanic and freshwater habitats. In fact, when we control for population structure using only SNPs from a genomic region where we know there is little structure between marine and freshwater individuals (LG 15), we show that for each lateral plate and opercle shape phenotype, we identify significant associations that recapitulate divergence across all genomic regions that diverge between marine and freshwater populations (Fig. 3.6A). Conversely, when we control for structure using SNPs from a genomic region that we know to be highly divergent and displays population structure between marine and freshwater individuals, we show that only a subset of the peaks for each phenotype remain (Fig. 3.6B). Taken together, these results suggest that although it is challenging, by choosing the appropriate genomic regions we can control for underlying population structure and that we can minimize spurious associations.

Our GWAS results also contain one positive and several negative controls. Previous studies demonstrated that *eda* is the major effect locus for lateral plate count during the marine to freshwater transition (Colosimo et al. 2005). In our study, we identified a genomic region on LG 4 that is significantly associated with lateral plate count and that contains the *eda* gene (Fig. 3.7). Other traits associated with the marine to freshwater transition, such as pelvic structure loss, pigmentation changes, and differences in lateral plate width and height have been attributed to *pitx1*, *kitlg*, and a region containing *gdf6,* respectively (Shapiro et al. 2004; Miller et al. 2007; Indjeian et al. 2016). None of the genomic regions that contain these genes was significantly associated with either lateral plate loss or opercle shape change (Fig. 3.7). Together, these data provide additional strength to our argument that the genomic regions associated with lateral plate count and opercle shape reflect the underlying genetic architecture of the traits.

Variation in Method for Controlling Population Structure Subtly Affects Mapping Results

We found that using two different methods to control for population structure, mean centered relatedness matrix and PC1 relatedness matrix, provided differences in the number of genomic regions associated with each phenotype, as well as the width and

number of SNPs within those regions. When we used the centered relatedness matrices calculated within the program GEMMA (Zhou and Stephens 2012), and account for "proximal contamination" (Listgarten et al. 2012; Pallares et al. 2014; Yang et al. 2014), we identified seven large, wide peaks associated with lateral plate count and opercle shape which localize to similar genomic regions (Fig. 3.7). However, when we use a PC1 relatedness matrix, which Sul and Eskin (2013) argue more adequately corrects for population structure than a centered relatedness matrix in a linear mixed model with a highly structured population, only three of these peaks contained SNPs that reached our estimated genome wide significance level (Fig. 3.7). All of the peaks we identified using each relatedness matrix co-localize to regions of divergence between marine and freshwater populations (Fig. 3.7C-H). Furthermore, where we found large, wide peaks across genomic regions using a centered relatedness matrix, we found narrow peaks. We were still unable to untangle specific genomic regions associated with lateral plate count and opercle shape using a PC1 relatedness matrix, however.

We speculate these differences in the identified associations were due to how well population structure was controlled in each case. Our results suggest that Sul and Eskin (2013) were correct in their interpretation that a PC1 relatedness matrix may better control for highly structured populations, which may be particularly true in situations as we encounter here where the population structure and phenotypic divergence are both created by the actions of natural selection. Using a PC1 relatedness matrix, we found that many of the associations that we saw when using the mean relatedness matrix fall away and leave only the peaks at genomic regions with the strongest association. While the PC1 relatedness matrix appears to work better in structured populations, it still may not be adequate for situations where populations show very high genetic structure either due to neutral or adaptive processes.

Irrespective of the method used to control for population structure, the genomic regions we found to be associated with lateral plate count and opercle shape co-localize to a subset of divergent regions both across the genome and within chromosomes. These findings support the hypothesis that regions subject to divergent selection contain alleles that contribute to phenotypes important in the marine to freshwater evolution, and that the

alleles associated with lateral plate count and opercle shape are housed within a subset of those regions (Jones et al. 2012; Terekhanova et al. 2014).

We do not suggest that the identified genomic regions associated with the phenotypes are the only ones that contribute to the phenotypes. GWA studies are best able to identify associations with moderate to large effect (Korte and Farlow 2013). Thus, loci containing alleles that have small effects on the phenotype will often go undetected. We, therefore, conclude that associations we identified likely underrepresent the regions that contribute to the phenotypes. However, our phenotypic correlation data and our GWAS data together show that opercle shape and lateral plate phenotypes have largely independent, but clearly clustered, genetic architectures.

Not All Population Structure is Created - nor Can be Controlled - the Same Way

Our findings highlight an important consideration about the nature and extent of population structure to be controlled in GWA studies, particularly whether it is created by neutral processes or the action of natural selection. The way population structure is controlled experimentally can alter the associations observed if the phenotypic diversity and population structure are both created by natural selection. In fact, an alternative explanation for our GWAS findings, despite the evidence from positive controls, as mentioned previously, is that we have not adequately controlled for population structure. Support for this point comes from the observation that the remaining associated peaks coincide with the most highly divergent genomic regions as measured by Fst, and points to the need for new methods for appropriately controlling population structure created by very strong selection.

Performing GWAS in a system where some genomic regions are highly divergent while others are nearly identical, and using a mean relatedness matrix as a point estimate to control for the entirety of population structure between two individuals, can create a significant issue. The population structure point estimate will be unable to capture those genomic regions which are most highly divergent. If the causative loci for traits of interest reside within the most highly divergent genomic regions, the GWAS method would easily detect these regions. If the traits of interest, however, vary with population

structure, and the causative loci are located outside of the most highly divergent regions, the genetic signal that contributes to the traits will be removed because it is contained in the genomic signal that is controlled. The effect is that associations at the most highly divergent regions are spurious and the causative loci are unidentifiable. This will occur using either a mean relatedness matrix, a genetic PC1 matrix, or any matrix that controls for genome wide population structure with a point estimate. To determine if the associations we identified in our GWAS are due to inadequate control of population structure by current methods or if these regions do in fact contain the loci that that contribute to lateral plate loss and opercle shape change will require further study. One experiment might include simulations of structured genomic data with known causative loci to determine if the genomic regions could or could not be identified with current methods.

An alternative method to those employed here is to perform GWAS at local genomic regions for which population structure is controlled based on the genomically local population structure. It is becoming more clear that within a genome, various regions can have different evolutionary histories (He et al. 2011). An assumption made when employing genome wide relatedness matrices is that averaging over many evolutionary histories will produce a summary relatedness estimate that is stable and reflects the average population structure (Li and Ralph 2016). However, in populations such as those on Middleton Island, where population structure is clearly determined by the action of natural selection, there is no guarantee that selection is acting in the same way at each genomic region. It is likely not, and so, controlling for population structure in the same way across the genome may be insufficient. Further investigations about controlling local population structure should enhance our understanding about the genealogical histories and the role of selection at different genomic locations, which would be interesting on its own. Such work may also allow us to identify types of population structure which could be binned into categories and enable a more accurate and powerful GWAS approach (Li and Ralph 2016).

Transporter Hypothesis Revisited

Schluter and Conte (2009) proposed the 'Transporter Hypothesis': that repeated, independent, and relatively rapid evolution of ancestral marine stickleback to freshwater environments occurs through the influx of many independent freshwater alleles into the marine population. Each individual of the marine population harbors at most a small number of freshwater-adapted alleles. During adaptation, these myriad alleles must be transported and reassembled when marine fish colonize a new freshwater environment. The fundamental concept of the "transporter hypothesis" is in accord with our findings. However, our findings of clustered genetic architectures, co-localized genomic regions of divergence and statistical linkage disequilibrium, and extremely rapid evolution in freshwater suggests that freshwater-adapted alleles are not atomized into hundreds or thousands of individual alleles, but may persist as fewer, larger loci of cluster alleles that could facilitate such a rapid pace of freshwater adaptation that we see on Middleton Island. Still, rapid reassembly of freshwater-adapted alleles, in the correct combination, is likely difficult unless each pond were colonized by a large number of stickleback followed by significant mortality of unfit genotypic combinations in the first few generations. In fact, empirical work in artificial ponds (similar in size to those on Middleton) by Barrett et. al. (2008) showed that early in the F_1 generation after wild caught fish, heterozygote for the low plated *eda* allele were introduced into freshwater ponds, the frequency of the low plated *eda* allele declined from 50% to as low as ~25% in the first three months, most likely as a result of such significant mortality. However, only 8 months later, and at the approximate time of first reproduction, the low plated allele had increased to frequencies as high as ~70%. A similar case could occur in the freshwater ponds on Middleton Island where introduction of large numbers of fish followed by high mortality, could create a population of individuals with the correct combination of genomic building blocks to fuel adaptation in subsequent generations.

Conclusion

Stickleback on Middleton Island offer a unique, natural experiment of populations before and after selection. In this study, we investigated lateral plate loss and opercle shape change, two traits which are classically associated with threespine stickleback adaption to freshwater environments. Rather than using QTL mapping crosses to uncover

the developmental genetic basis of traits, the populations on Middleton Island combined into a GWAS framework provide a glimpse into the evolutionary genetic basis of traits that repeatedly undergo parallel evolution and the processes that act to shape the genomic architectures that may facilitate rapid evolution. We showed that lateral plate loss and opercle shape change exhibit correlated evolution even over a short 50-year period. Despite the patterns of phenotypic covariance in these traits across populations, we find that the two phenotypes are underlain by largely independent genetic architectures but which cluster to similar genomic regions. The genomic regions associated with the traits are nested within a larger set of genomic regions that tightly covary with one another, and which are divergent between marine and freshwater populations. The congruence between F_{st} divergence peaks and regions of high long-distance correlation (LD) on nearly homogeneous backgrounds within chromosomes suggests that these regions represent genomic archipelagos, potentially maintained by mechanisms which reduce recombination such as chromosomal rearrangements. When marine stickleback colonize freshwater ponds, combinations of freshwater loci may be rapidly produced through epistatic selection. Unfortunately, the very interesting rapid and extensive phenotypic and genomic evolution in these populations, most likely due to the action of natural selection, creates significant population structure that is difficult to control and which clouds our ability to identify the specific loci that contribute to rapid evolution of lateral plate loss and opercle shape change. Despite these difficulties, we have found that while these two key traits in the evolutionary syndrome of phenotypic changes to life in freshwater may not share genetic architecture, that they do share a genomic architecture may facilitate the action of natural selection to promote rapid adaptation to freshwater environments.

BRIDGE

In Chapter III, I used newly formed and rapidly evolving population of stickleback fish on Middleton Island to try to identify the genetic architectures of skeletal traits which are rapidly diverging. We showed that despite the genetic architectures of phenotypic variation being largely independent, also observed in Chapter II, the genomic regions which contribute to lateral plate number and opercle shape largely co-localize. Our analyses identify that the strong population structure among populations on Middleton Island, largely driven by selection, may hamper our ability to identify the genomic and genetic architectures of these traits. I conclude in Chapter IV with a summary of the findings presented in this dissertation and a discussion about when going after the genes to link the genotype-to-phenotype map may or may not be appropriate.

CHAPTER IV

GWAS OR: HOW I LEARNED TO STOP WORRYING AND EMBRACE POPULATION STRUCTURE IN LINKING GENOMES TO PHENOMES

Finding the Genes that Matter for Evolution When it Matters for Understanding Evolution

Understanding how phenotypes adapt to novel environments has persisted as a fundamental challenge for biologists since Darwin (Gardner 2009). We now know that realized phenotypes are the product of genes and the environment, and so inquiry into the genetics and genomics of phenotypic evolution provides insight into this enduring question (Pigliucci 2010). Natural genetic variation among populations is critical to provide the creative template upon which selective forces can act and shape phenotypic evolution (Rockman 2008). As such, there is a strong interest in the field to identify the genetic and molecular basis of evolving phenotypes in natural populations in the hopes of gaining further insight into the role of selection and the mechanisms of evolution (Schluter et al. 2010). In doing so, a major goal has been to identify not only the gene but also the causal nucleotide(s) that contribute to phenotypic variation and evolution [i.e. the quantitative trait nucleotide (QTN) program (Rockman 2012)]. But, is that goal even possible for the phenotypes that matter to evolution?

Rockman (2012) makes the point that it really depends on the distribution of effect sizes. While theory suggests that evolution is largely driven by many loci of small effect (Fisher's infinitesimal model), the majority of QTN identified have large phenotypic effects (Orr 2005; Rockman 2012). In this way, the QTN program likely biases our understanding about the nature of the relevant mutations underlying evolution. If the goal is to understand the entire range of phenotypic effect sizes that mutations have on evolutionary relevant traits with one or a few approaches, the QTN program will fall short. However, if gaining an understanding of how genotypes affect phenotypes through the vetting process of development and environmental conditions in natural populations is still an interesting question - as it is for many of us - then the QTN program might be a reasonable approach. Even though methods are advancing, the QTN program is still quite

difficult to achieve, and researchers should undertake it with full knowledge of the efforts required. It must also still be recognized, though, that successful QTN efforts cannot fully represent the complexity of evolution, but they do provide an important piece of the evolutionary puzzle.

Major Methods for Defining the Genotype-to-Phenotype Map in Evolutionary Genomics

Quantitative trait locus (QTL) mapping studies have been a fruitful approach to link an individual's genotype to a phenotype of interest (G-P map), which allows the genomic regions and in some cases the underlying genetics of phenotypic evolution to be identified (Colosimo et al. 2005; Reed et al. 2011). However, this method suffers in the respect that in most cases, organisms must be brought into the laboratory which, from a practical standpoint, limits the species available to use, and, of biological concern, releases the constraints of selective forces on the G-P map [but see Arnegard et al. (2014)]. As new and cheaper genomic tools have become increasingly available, genome wide association studies (GWAS) have become a dominant method to connect the breadth of natural genetic variation with phenotypic variation among populations in context with their environments and selective forces (Delmore et al. 2016).

As GWAS has become an accessible method in natural populations, researchers have identified some key considerations to ensure the method is successful. Among the major considerations are population structure and linkage disequilibrium (Astle and Balding 2009; Stranger et al. 2011). Successful GWAS often use populations where structure does not contribute to the major axis of phenotypic variation so that any structure that does exist can be easily controlled without removing the genetic signal which contributes to phenotypic variation. Most often, these populations are hybrid zones (Pallares et al. 2014; Delmore et al. 2016). Within these populations, the marker density necessarily is dictated by the patterns of linkage disequilibrium (Malek et al. 2012). With any reduced representation sequencing method, having some linkage disequilibrium within linkage groups is beneficial to ensure that markers will be linked to causal loci. If the populations are in linkage equilibrium, whole genome sequencing will likely be necessary, but this approach is still cost prohibitive for the large sample sizes needed

(Spencer et al. 2009). In addition to these challenges, finding a population which meets these requirements and which display the kinds of phenotypic variation in which one is interested can pose an additional hurdle.

Quantitative Trait Loci Mapping in Stickleback: Findings and Limitations

The threespine stickleback is a preeminent evolutionary model system to interrogate the genetics underlying phenotypic evolution. The analyses completed in this dissertation to connect the G-P map were performed to help usher the threespine stickleback system from a predominantly QTL based system into the genomics era with GWAS. We focused on two well-studied and ecologically relevant traits, lateral plate loss and opercle shape change, which repeatedly undergo stereotypical changes as stickleback adapt to new, freshwater environments. By focusing on traits for which we have expectations about the underlying genetic architectures from QTL studies (Colosimo et al. 2004; Kimmel et al. 2005), we were able to assess the quality of our analyses. Additionally, because we performed the same analyses in two stickleback systems, we were able to learn about and evaluate GWAS performance in populations which experience different selective forces.

Stickleback QTL mapping studies aimed at identifying the genetic basis of diverging traits have been laborious. In some cases, the labor paid off and the causal loci contributing to traits commonly associated with stickleback evolution were identified. First, though, the genomic regions contributing to the now classic examples including lateral plate loss, lateral plate width and height, pelvic structure reduction, and pigmentation changes, were identified using enormous mapping families, and the identified regions regularly spanned large swaths of the linkage group. Then, narrowing down to causal genes, often required even more and different mapping families (Colosimo et al. 2004; Cresko et al. 2004; Shapiro et al. 2004; Colosimo et al. 2005; Miller et al. 2007; Indjeian et al. 2016). While the genetic basis of traits are still being investigated (Kusakabe et al. 2016), often the attention has turned more towards investigating the repeatability of QTL use across many traits and modularity of phenotypic evolution (Miller et al. 2014; Conte et al. 2015; Glazer et al. 2015; Erickson et al. 2016).

Despite this shift in attention among many researchers, there is still much to be learned about evolving traits in stickleback. Because stickleback show such dramatic phenotypic evolution during adaptation from marine and to freshwater environments (Bell and Foster 1994; Bell 2001), still, of primary interest among stickleback researchers is to understand the genetic underpinnings of this particular divergence (Schluter et al. 2010). With improved genomic technologies, it is far easier to address questions regarding the genetic architectures of traits, large effect QTN, and the modularity of evolution within the context of natural populations and evolutionary forces.

Genome Wide Association in Stickleback: Success and Lessons Learned

In Chapter II, we described our efforts to identify a population(s) of freshwater stickleback in the McKenzie River which satisfy the considerations about population structure and linkage disequilibrium, but which also show the range of phenotypes between the marine to freshwater transition. We showed that among four populations along the McKenzie River, lateral plate count covered the desired range of phenotypes between the classic, monomorphic populations of Alaska and British Columbia (Bell 2001). Variation in opercle shape, however, appeared to be confined to freshwater shapes which suggested that the either the action of selection differs between the two phenotypes or that the environment has caused the distribution of opercle shapes to shift. Although the ranges of phenotypic variation were promising, and which were largely similar among populations, we found evidence for population structure most likely due to spatial differentiation. Interestingly, when we evaluated genomic correlation between all pairwise combinations of markers among all populations pooled, we found a genome wide elevation of linkage disequilibrium which suggested that population structure was due to neutral evolutionary processes. A common assumption is that so long as population structure can be modeled and controlled, GWAS linear mixed models (LMM) should be effective (Price et al. 2010; Sul and Eskin 2013). Despite this, we focused on only one population to be sure we were not confounding our results. The Riverbend population reflected the phenotypic variation of all McKenzie River populations, largely lacked structure, and had genomic regions of linkage disequilibrium within, but not among, linkage groups.

During the stickleback marine to freshwater transition, many traits including lateral plates and opercle shape are modified in unison. One hypothesis is that many of these traits which make up the "freshwater syndrome" share, to some degree, a genetic or developmental basis which contributes to a modularity among traits (Barrett et al. 2008; Barrett et al. 2009). Our assessment of the correlations between lateral plate count and opercle shape variation suggested that phenotypic variation present in the Riverbend population have independent genetic architectures. We showed that this expectation was reflected in our GWAS results by identification of non-overlapping genomic regions associated with each of the traits.

Even given the limited sample size of this study, we found that GWAS was effective in identifying the genomic regions which we expected to be associated with each of the traits. Our study also shows the merits of using a GWAS approach to uncover aspects of genetic architectures of simple traits because we were easily able to identify *eda* as a potential candidate gene for lateral plate loss with far less effort than what was needed to identify and fine map the same region with multiple large QTL mapping crosses (Colosimo et al. 2004; Colosimo et al. 2005). In addition, our approach also facilitated the identification of a locus which is potentially epistatic to the locus of major effect at *eda.* We identified β-catenin as a candidate gene which, to our knowledge, has never been previously implicated in lateral plate number variation from QTL studies, and may modify plate number variation in the low plated ecomorph. Our study also showed that by using GWAS we could identify genomic regions associated with traits that are presumed to have more complex genetic architectures such as opercle shape. Although much less of the genetic variation could be explained by our markers, this suggests that opercle shape is polygenic and that each locus has a small to moderate effect on the phenotype. Even though linkage disequilibrium is present within linkage groups, more markers will be necessary to capture a larger percentage of the genetic variation contributing to the shape.

In Chapter II, we showed that GWAS can used be successfully in stickleback populations, and that we can gain insight into the genetic architectures of ecologically relevant traits. However, an aspect that makes the stickleback system fascinating is that, not only do the same traits evolve in similar ways repeatedly and independently during

the marine to freshwater transition, but they can do so very rapidly— on the order of years or decades (Lescak et al. 2015). If we are interested, as a field, in understanding the genetic architectures which contribute to and facilitate very rapid divergence of traits, the freshwater Riverbend population is not quite the appropriate system. Although lateral plate number spans the range of phenotypes between marine and freshwater divergence, opercle shape does not. A better place to look to might be to a stickleback system which had only very recently diverged from marine populations and where we could hopefully capture divergence in action before alleles that contribute to divergence are fixed.

Genome Wide Association in Very Young Stickleback Populations: A Cautionary Tale

In Chapter III we investigated a population of stickleback which recently diverged from the marine ancestors after the Great Alaskan Earthquake of 1964. We used stickleback on Middleton Island from marine habitats and nearby, newly formed freshwater habitats to span phenotypic, genetic, and habitat space common among stickleback populations and in which we are interested. Although we found correlations between phenotypic variation among populations, we did not find correlations within populations. This finding suggested that phenotypic modularity of the "freshwater syndrome" may not be created by a shared genetic or developmental basis but through alternative explanations. The independence of genetic architectures was also reflected in our findings detailed in Chapter II. Despite this result, we identified overlapping and covarying genomic regions associated with lateral plate number and opercle shape variation with our GWAS. One explanation is that although phenotypic variation for the two traits are likely independent, the alleles are genomically co-localized which might act to facilitate rapid divergence through linked selection. While genomic co-localization is an attractive biological hypothesis, an alternative explanation is that the methods by which we controlled for population structure were inadequate.

Further inspection of the structure among the populations analyzed suggested that even though the freshwater populations were only recently formed, by the action of very strong selection, large portions of the genome were in inter- and intra-chromosomal linkage disequilibrium leaving the remaining regions at linkage equilibrium. As we detailed in Chapter III, the current point estimates of relatedness between pairwise

combinations of individuals used to control for structure maybe insufficient to account for the heterogeneity of structure and range of relatedness coefficients seen across these genomes. Whether or not the population structure present on Middleton Island would completely cloud our ability to identify the genomic regions which contribute to variation is an open question which requires further study.

Although we were unable to make conclusive statements about the nature of the genetic architectures of rapidly evolving traits in Chapter III, our analyses have revealed interesting questions about the nature and role of population structure in rapid adaptation. As discussed in Li and Ralph (2016), in using relatedness matrices, GWAS assumes that population structure across the genome is similar, or at least that by assessing many markers to derive a relatedness coefficient, that the coefficient accurately reflects relatedness across the genome. However, in reality, different evolutionary histories of each genomic region can leave a unique signature of relatedness on it and surrounding regions (Li and Ralph 2016). We do not yet understand the subtleties of population structure on Middleton Island, the range of evolutionary histories across genomic regions, or if selection has acted in the same way across all divergent genomic regions, all of which can result in varying patterns of realized relatedness unable to be captured by one point estimate. Generally, divergence has been described largely by summary statistics and broad scale methods to determine structure (Pritchard et al. 2000a; Li and Ralph 2016). On Middleton Island, we have an opportunity to learn about the kinds of structure that may be present which would provide insight into the role of selection in adaptive divergence. Furthermore, by investigating and modeling structure in a way that captures the range of structures across the genome, we may be able to advance GWAS in natural populations where current methods to control population structure fall short.

The work described in this dissertation demonstrates the utility of using GWAS in one stickleback system to address fundamental questions in evolutionary biology and the limitations in another. Population structure can have profound effects on our ability to ascertain the genetic architectures of diverging traits, and a single method to investigate these questions may not be appropriate for every situation. Truly answering questions about the genetic basis of rapidly diverging phenotypes may require a combination of approaches. To understand the genetic architectures of phenotypic variation within a

limited range but within the context of the environment and selective forces, GWAS might be most fruitful, however to identify the genetic architectures of divergent traits between habitats, QTL mapping may be most efficient, and to understand the effect of genes within divergent genomes will require transgenic approaches. However, the ease of access to populations which are amenable to all these approaches is one of the strengths of the stickleback system.

Clearly, lessons were learned about the utility of association mapping approaches in different situations. From an immediate and practical standpoint, a good GWAS study will benefit from upfront, detailed analysis of population structure and linkage disequilibrium to identify a system which will be most lucrative, rather than a polar plunge into what can be harsh GWAS waters. Currently, we simply do not have the tools to deal with localized population structure in a GWAS framework, especially for traits under selection. Though, in instances where we are trying to understand the mechanisms of coordinated rapid evolution in diverging populations, perhaps identifying the genetic mechanisms is not only impractical, but less important. Rather, a focus on the larger evolutionary processes might be most fruitful and interesting. If identifying the QTN is important, we have shown that in populations like Riverbend, the fruit will be plenty.

APPENDIX

SUPPORTING INFORMATION FOR CHAPTER II

Table S2.1 Annotated genes within narrow region around SNP most highly associated with lateral plate count. Bold gene names indicate interesting candidates based on previous studies.

Linkage Group	Start (bp)	Stop (bp)	Name	Ensembl ID
Second most highly associated SNP: snp4028_8 (location: 12,350,223 bp)				
groupIV	12353365	12364750	*kctd12b*	ENSGACG00000018268
groupIV	12395669	12396211	*rhogd*	ENSGACG00000018271
groupIV	12424107	12436050	*ogt.2*	ENSGACG00000018273
groupIV	12438010	12441598	*acrc*	ENSGACG00000018279
groupIV	12442336	12444314	*cetn2*	ENSGACG00000018281
groupIV	12445321	12448373	*nsdhl*	ENSGACG00000018285
groupIV	12451969	12456614	protein_coding	ENSGACG00000018286
groupIV	12459458	12462500	protein_coding	ENSGACG00000018287
groupIV	12463399	12467598	*fut11*	ENSGACG00000018289
groupIV	12468117	12468728	*rab9b*	ENSGACG00000018291
groupIV	12472918	12477723	*plp1a*	ENSGACG00000018292
groupIV	12500111	12585904	*nlgn3a*	ENSGACG00000018296
groupIV	12660845	12838539	*vma21*	ENSGACG00000018298
groupIV	12700707	12768384	*gria3b*	ENSGACG00000018300
Top most highly associated SNP: snp4072_28 (location: 12,797,184 bp)				
groupIV	12800220	12810446	***eda***	ENSGACG00000018311
groupIV	12811602	12817008	protein_coding	ENSGACG00000018312
groupIV	12822782	12824676	protein_coding	ENSGACG00000018313
groupIV	12826542	12827369	*cx31.7*	ENSGACG00000018314
groupIV	12843597	12851169	*mtnr1c*	ENSGACG00000018315

Linkage Group	Start (bp)	Stop (bp)	Name	Ensembl ID
groupIV	12857678	12861775	*neurl1b*	ENSGACG00000018316
groupIV	12886001	12888151	*dusp1*	ENSGACG00000018318
groupIV	12891471	12904168	*ergic1*	ENSGACG00000018319
Third most highly associated SNP: snp4088_51 (location: 12,909,486 bp)				
groupIV	12904952	12925251	*flt4*	ENSGACG00000018320
groupIV	12941555	12943706	protein_coding	ENSGACG00000018322
groupIV	12948567	12950365	*npy7r*	ENSGACG00000018324
groupIV	12951906	12955107	*prelid1a*	ENSGACG00000018325
groupIV	12957378	12959627	*mxd3*	ENSGACG00000018331
groupIV	12962154	12969566	*fam193b*	ENSGACG00000018332
groupIV	12971182	12976506	*DDX41*	ENSGACG00000018334
groupIV	13161092	13215854	*unc5a*	ENSGACG00000018337
groupIV	13220801	13248223	***pdlim7***	ENSGACG00000018344
groupIV	13247849	13251404	*cltb*	ENSGACG00000018348
groupIV	13252044	13253484	*higd2a*	ENSGACG00000018350
groupIV	13258735	13265652	protein_coding	ENSGACG00000018351
groupIV	13282319	13287248	*hnrnph1*	ENSGACG00000018352
groupIV	13287303	13292669	*rufy1*	ENSGACG00000018354
groupIV	13294516	13295502	*hbegfa*	ENSGACG00000018355
groupIV	13331270	13336566	*rmnd5b*	ENSGACG00000018357
groupIV	13339769	13343280	*n4bp3*	ENSGACG00000018359
groupIV	13360790	13361899	protein_coding	ENSGACG00000018361
groupIV	13367495	13372511	protein_coding	ENSGACG00000018362
groupIV	13375789	13385299	***anxa6***	ENSGACG00000018367
groupIV	13389317	13398176	*tnip1*	ENSGACG00000018374
groupIV	13399031	13400196	protein_coding	ENSGACG00000018378
groupIV	13399655	13402595	*gpx3*	ENSGACG00000018379

Linkage Group	Start (bp)	Stop (bp)	Name	Ensembl ID
groupIV	13403603	13410822	*dctn4*	ENSGACG00000018383
groupIV	13445086	13445994	protein_coding	ENSGACG00000018384
groupIV	13448609	13449604	protein_coding	ENSGACG00000018386
groupIV	13452992	13465259	*TSPAN17*	ENSGACG00000018387
groupXX	5267357	5288282	*trak1*	ENSGACG00000006003
groupXX	5304723	5353897	*ulk4*	ENSGACG00000006021
groupXX	5362441	5375095	***ctnnb1***	ENSGACG00000006037
Second most highly associated SNP: snp35149_61 (location 5,422,940bp)				
groupXX	5426871	5428558	*ZG16*	ENSGACG00000006045
groupXX	5442149	5444002	protein_coding	ENSGACG00000006051
groupXX	5451351	5459490	*trmt11*	ENSGACG00000006060
groupXX	5553263	5564403	*rspo3*	ENSGACG00000006080
groupXX	5566021	5567034	*mdh2*	ENSGACG00000006087
groupXX	5568218	5569363	*rnf146*	ENSGACG00000006092
groupXX	5571962	5574407	*ECHDC1*	ENSGACG00000006095
groupXX	5581980	5584362	protein_coding	ENSGACG00000006118
groupXX	5591517	5595182	*soga3a*	ENSGACG00000006121
groupXX	5602022	5606254	*elovl4a*	ENSGACG00000006127
groupXX	5607034	5609358	*prelid3a*	ENSGACG00000006144
groupXX	5611594	5616828	*fbxo32*	ENSGACG00000006161
groupXX	5618666	5622627	*klhl38b*	ENSGACG00000006167
groupXX	5642987	5643790	*zgc:110182*	ENSGACG00000006198
groupXX	5646549	5649676	*nsmce2*	ENSGACG00000006200
groupXX	5649839	5661632	*strumpellin*	ENSGACG00000006206
Top most highly associated SNP: snp35176_18 (location: 5,665,015 bp)				
groupXX	5668131	5691885	*ext1a*	ENSGACG00000006234

Linkage Group	Start (bp)	Stop (bp)	Name	Ensembl ID
groupXX	5696334	5703744	*rad21a*	ENSGACG00000006276
groupXX	5705002	5746913	*eif3ha*	ENSGACG00000006293
groupXX	5803916	5829129	*csmd1a*	ENSGACG00000006303
groupXX	5843406	5955450	*CSMD3 (1 of many)*	ENSGACG00000006307
groupXX	5969700	5976203	*zgc:110410*	ENSGACG00000006328
groupXX	5978144	5999605	*ankib1a*	ENSGACG00000006337
groupXX	6003650	6006502	*eomesb*	ENSGACG00000006345
groupXX	6019972	6025247	*cmc1*	ENSGACG00000006355
groupXX	6027235	6035227	*AZI2*	ENSGACG00000006371
groupXX	6102582	6161999	*rbms3*	ENSGACG00000006377
groupXX	6166089	6172879	*entpd3*	ENSGACG00000006387
groupXX	6176973	6190798	*ddc*	ENSGACG00000006397
groupXX	6202336	6235349	*grb10b*	ENSGACG00000006438
groupXX	6253039	6282798	*cobl*	ENSGACG00000006446

Table S2.2 Annotated genes within narrow region around SNP most highly associated with opercle shape.

Linkage Group	Start (bp)	Stop (bp)	Name	Ensembl ID
groupVIII	10670600	10676404	*zgc:85936*	ENSGACG00000008902
groupVIII	10677035	10682682	*alpi.2*	ENSGACG00000008908
groupVIII	10684744	10692177	*alpi.1*	ENSGACG00000008915
groupVIII	10701650	10702660	*srek1ip1*	ENSGACG00000008958
groupVIII	10768726	10769846	*nppc*	ENSGACG00000008966
groupVIII	10775000	10780521	*ncl*	ENSGACG00000008970
groupVIII	10783233	10785335	*b3gnt7*	ENSGACG00000008999
groupVIII	10794678	10809981	*armc9*	ENSGACG00000009002
groupVIII	10811451	10813116	*polr2h*	ENSGACG00000009019
groupVIII	10815897	10821342	protein_coding	ENSGACG00000009042
groupVIII	11024707	11048659	***EPHB3*** (1 of many)	ENSGACG00000009051
Top most highly associated SNP: snp11139_28 (location: 11213998)				
groupVIII	11265078	11267742	*HYKK* (1 of many)	ENSGACG00000009059
groupVIII	11269682	11272240	*HYKK* (1 of many)	ENSGACG00000009062
groupVIII	11278291	11279836	*nmur1a*	ENSGACG00000009069
groupVIII	11289636	11290485	protein_coding	ENSGACG00000009076
groupVIII	11296839	11300017	protein_coding	ENSGACG00000009077
groupVIII	11301927	11305001	protein_coding	ENSGACG00000009078
groupVIII	11312464	11328558	*rubcn*	ENSGACG00000009086
groupVIII	11336696	11356157	protein_coding	ENSGACG00000009134
groupVIII	11368224	11373962	*pfn2l*	ENSGACG00000009139
groupVIII	11375616	11376881	protein_coding	ENSGACG00000009177
groupVIII	11376567	11401655	*rnf13*	ENSGACG00000009180
groupVIII	11403293	11405044	protein_coding	ENSGACG00000009187
groupVIII	11407029	11415653	*ppp1r2*	ENSGACG00000009192
Second most highly associated SNP: snp11153_57 (location: 11445066)				

Linkage Group	Start (bp)	Stop (bp)	Name	Ensembl ID
groupVIII	11419321	11452012	*acap2*	ENSGACG00000009198
groupVII	7721652	7723223	*arl2*	ENSGACG00000019812
groupVII	7739783	7745404	protein_coding	ENSGACG00000019819
groupVII	7754154	7757339	***b3gat3***	ENSGACG00000019824
groupVII	7760650	7763469	*naa40*	ENSGACG00000019828
groupVII	7771903	7781711	***rcor2***	ENSGACG00000019834
groupVII	7786266	7809439	*mark2b*	ENSGACG00000019840
groupVII	7825878	7829862	*krcp*	ENSGACG00000019844
groupVII	7831193	7837026	*cct7*	ENSGACG00000019847
Top most highly associated SNP: snp15154_46 (location: 7836168)				
groupVII	7838207	7846302	*hspa12b*	ENSGACG00000019861
groupVII	7853665	7861393	*paip2b*	ENSGACG00000019867
groupVII	7869640	7872620	*nagk*	ENSGACG00000019870
groupVII	7873702	7882009	*dok1b*	ENSGACG00000019876
groupVII	7888611	7907687	*m1ap*	ENSGACG00000019877
groupVII	7969174	7974020	protein_coding	ENSGACG00000019881
groupVII	7974727	7975780	protein_coding	ENSGACG00000019883
groupVII	7989463	7995317	*syt4*	ENSGACG00000019884
groupVII	8008457	8018407	*si:dkey-183c6.7*	ENSGACG00000019886
groupVII	8020685	8031725	*si:dkey-183c6.8*	ENSGACG00000019888
groupVII	8044555	8045812	protein_coding	ENSGACG00000019893
groupVII	8067799	8083111	protein_coding	ENSGACG00000019894
groupVII	8092741	8096609	protein_coding	ENSGACG00000019895
groupVII	8099373	8106000	*rpgrip1*	ENSGACG00000019896
groupVII	8107491	8109576	*fam113*	ENSGACG00000019900
groupVII	8116198	8127941	*dctn1a*	ENSGACG00000019902

Linkage Group	Start (bp)	Stop (bp)	Name	Ensembl ID
groupVII	8130248	8142689	*TDRD7* (1 of many)	ENSGACG00000019913
groupVII	8143647	8147227	*CABP4* (1 of many)	ENSGACG00000019917
groupVII	8149984	8153267	*tmem88b*	ENSGACG00000019919
groupVII	8160493	8164391	protein_coding	ENSGACG00000019920
groupVII	8166832	8167860	protein_coding	ENSGACG00000019921

REFERENCES CITED

Abraham, G. and M. Inouye. 2014. Fast Principal Component Analysis of Large-Scale Genome-Wide Data. Plos One 9.

Abzhanov, A., M. Protas, B. R. Grant, P. R. Grant, and C. J. Tabin. 2004. Bmp4 and morphological variation of beaks in Darwin's finches. Science 305:1462-1465.

Ackermann, R. R. and J. M. Cheverud. 2002. Discerning evolutionary processes in patterns of tamarin (genus Saguinus) craniofacial variation. American Journal of Physical Anthropology 117:260-271.

Adams, D. C. and E. Otárola-Castillo. 2013. geomorph: an rpackage for the collection and analysis of geometric morphometric shape data. Pp. 393-399. Methods Ecol Evol.

Aguirre, W. E. and M. A. Bell. 2012. Twenty years of body shape evolution in a threespine stickleback population adapting to a lake environment. Biological Journal of the Linnean Society 105:817-831.

Aguirre, W. E., P. K. Doherty, and M. A. Bell. 2004. Genetics of lateral plate and gillraker phenotypes in a rapidly evolving population of threespine stickleback. Behaviour 141:1465-1483.

Albert, A. Y., S. Sawaya, T. H. Vines, A. K. Knecht, C. T. Miller, B. R. Summers, S. Balabhadra, D. M. Kingsley, and D. Schluter. 2008. The genetics of adaptive shape shift in stickleback: pleiotropy and effect size. Evolution 62:76-85.

Albertson, R. C. 2003. Genetic Basis of Adaptive Shape Differences in the Cichlid Head. Pp. 291-301. Journal of Heredity.

Albertson, R. C., W. Cresko, H. W. Detrich III, and J. H. Postlethwait. 2009. Evolutionary mutant models for human disease. Pp. 74-81. Trends in Genetics.

Albertson, R. C. and T. D. Kocher. 2006. Genetic and developmental basis of cichlid trophic diversity. Pp. 211-221. Heredity.

Albertson, R. C., J. T. Streelman, T. D. Kocher, and P. C. Yelick. 2005. Integration and evolution of the cichlid mandible: the molecular basis of alternate feeding strategies. Pp. 16287-16292. Proc Natl Acad Sci USA.

Amores, A., A. Force, Y. L. Yan, L. Joly, C. Amemiya, A. Fritz, R. K. Ho, J. Langeland, V. Prince, Y. L. Wang, M. Westerfield, M. Ekker, and J. H. Postlethwait. 1998. Zebrafish hox clusters and vertebrate genome evolution. Science 282:1711-1714.

Anderson, J. T., M. R. Wagner, C. A. Rushworth, K. V. S. K. Prasad, and T. Mitchell-Olds. 2014. The evolution of quantitative traits in complex environments. Heredity 112:4-12.

Anker, G. C. 2010. Morphology and kinetics of the head of the stickleback, Gasterosteus aculeatus. Pp. 311-416. The Transactions of the Zoological Society of London.

Arendt, J. and D. Reznick. 2008. Convergence and parallelism reconsidered: what have we learned about the genetics of adaptation? Trends in Ecology & Evolution 23:26-32.

Armbruster, W. S., C. Pelabon, G. H. Bolstad, and T. F. Hansen. 2014. Integrated phenotypes: understanding trait covariation in plants and animals. Pp. 20130245-20130245. Philosophical Transactions of the Royal Society B: Biological Sciences.

Armbruster, W. S. and K. E. Schwaegerle. 1996. Causes of covariation of phenotypic traits among populations. Journal of Evolutionary Biology 9:261-276.

Arnegard, M. E., M. D. McGee, B. Matthews, K. B. Marchinko, G. L. Conte, S. Kabir, N. Bedford, S. Bergek, Y. F. Chan, F. C. Jones, D. M. Kingsley, C. L. Peichel, and D. Schluter. 2014. Genetics of ecological divergence during speciation. Nature 511:307-311.

Arnold, S. J. 1992. Constraints on phenotypic evolution. Pp. S85-107. The American Naturalist.

Arte, S., S. Parmanen, S. Pirinen, S. Alaluusua, and P. Nieminen. 2013. Candidate Gene Analysis of Tooth Agenesis Identifies Novel Mutations in Six Genes and Suggests Significant Role for WNT and EDA Signaling and Allele Combinations. Plos One 8.

Astle, W. and D. J. Balding. 2009. Population Structure and Cryptic Relatedness in Genetic Association Studies. Stat Sci 24:451-471.

Baird, N. A., P. D. Etter, T. S. Atwood, M. C. Currey, A. L. Shiver, Z. A. Lewis, E. U. Selker, W. A. Cresko, and E. A. Johnson. 2008. Rapid SNP discovery and genetic mapping using sequenced RAD markers. PLoS One 3:e3376.

Balding, D. J. 2006. A tutorial on statistical methods for population association studies. Nat Rev Genet 7:781-791.

Banbura, J. 1994. A new model of lateral plate morph inheritance in the threespine stickleback,Gasterosteus aculeatus. Theor Appl Genet 88:871-876.

Banbura, J. and T. C. M. Bakker. 1995. Lateral Plate Morph Genetics Revisited: Evidence for a Fourth Morph in Three-Spined Sticklebacks. Behaviour 132:1153-1171.

Barrett, R. D. 2010. Adaptive evolution of lateral plates in three-spined stickleback Gasterosteus aculeatus: a case study in functional analysis of natural variation. J Fish Biol 77:311-328.

Barrett, R. D. and H. E. Hoekstra. 2011. Molecular spandrels: tests of adaptation at the genetic level. Nat Rev Genet 12:767-780.

Barrett, R. D., A. Paccard, T. M. Healy, S. Bergek, P. M. Schulte, D. Schluter, and S. M. Rogers. 2011. Rapid evolution of cold tolerance in stickleback. Proc Biol Sci 278:233-238.

Barrett, R. D., S. M. Rogers, and D. Schluter. 2008. Natural selection on a major armor gene in threespine stickleback. Science 322:255-257.

Barrett, R. D. and D. Schluter. 2008. Adaptation from standing genetic variation. Trends Ecol Evol 23:38-44.

Barrett, R. D., T. H. Vines, J. S. Bystriansky, and P. M. Schulte. 2009. Should I stay or should I go? The Ectodysplasin locus is associated with behavioural differences in threespine stickleback. Biol Lett 5:788-791.

Barton, N. H. 2017. How does epistasis influence the response to selection? Heredity (Edinb) 118:96-109.

Barton, N. H. and P. D. Keightley. 2002. Understanding quantitative genetic variation. Nat Rev Genet 3:11-21.

Bell, M. A. 2001. Lateral plate evolution in the threespine stickleback: getting nowhere fast. Genetica 112-113:445-461.

Bell, M. A., W. E. Aguirre, and N. J. Buck. 2004. Twelve years of contemporary armor evolution in a threespine stickleback population. Evolution 58:814-824.

Bell, M. A. and S. A. Foster. 1994. The evolutionary biology of the threespine stickleback. Oxford University Press, Oxford ; New York.

Bell, M. A., J. D. Stewart, and P. J. Park. 2009. The World's Oldest Fossil Threespine Stickleback Fish. Copeia:256-265.

Berg, R. L. 1960. The ecological significance of correlation pleiades. Pp. 171. Evolution.

Berner, D., D. Moser, M. Roesti, H. Buescher, and W. Salzburger. 2014. Genetic architecture of skeletal evolution in European lake and stream stickleback. Evolution 68:1792-1805.

Boell, L., L. F. Pallares, C. Brodski, Y. P. Chen, J. L. Christian, Y. A. Kousa, P. Kuss, S. Nelsen, O. Novikov, B. C. Schutte, Y. Wang, and D. Tautz. 2013. Exploring the effects of gene dosage on mandible shape in mice as a model for studying the genetic basis of natural variation. Dev Genes Evol 223:279-287.

Bookstein, F. L. 1997a. Landmark methods for forms without landmarks: morphometrics of group differences in outline shape. Med Image Anal 1:225-243.

Bookstein, F. L. 1997b. Landmark methods for forms without landmarks: morphometrics of group differences in outline shape. Pp. 225-243. Medical Image Analysis.

Bulmer, M. G. 1971. The effect of selection on genetic variability. Am Nat.

Burn, J. E., D. J. Bagnall, J. D. Metzger, E. S. Dennis, and W. J. Peacock. 1993. DNA Methylation, Vernalization, and the Initiation of Flowering. Proceedings of the National Academy of Sciences of the United States of America 90:287-291.

Carroll, S. B. 2008. Evo-devo and an expanding evolutionary synthesis: a genetic theory of morphological evolution. Cell 134:25-36.

Carter, A. J. R., J. Hermisson, and T. F. Hansen. 2005. The role of epistatic gene interactions in the response to selection and the evolution of evolvability. Theoretical Population Biology 68:179-196.

Catchen, J., P. A. Hohenlohe, S. Bassham, A. Amores, and W. A. Cresko. 2013. Stacks: an analysis tool set for population genomics. Mol Ecol 22:3124-3140.

Catchen, J. M., A. Amores, P. Hohenlohe, W. Cresko, and J. H. Postlethwait. 2011. Stacks: building and genotyping Loci de novo from short-read sequences. G3 (Bethesda) 1:171-182.

Chan, Y. F., M. E. Marks, F. C. Jones, G. Villarreal, Jr., M. D. Shapiro, S. D. Brady, A. M. Southwick, D. M. Absher, J. Grimwood, J. Schmutz, R. M. Myers, D. Petrov, B. Jonsson, D. Schluter, M. A. Bell, and D. M. Kingsley. 2010. Adaptive evolution of pelvic reduction in sticklebacks by recurrent deletion of a Pitx1 enhancer. Science 327:302-305.

Charlesworth, D. 2006. Balancing selection and its effects on sequences in nearby genome regions. PLoS Genet 2:e64.

Chen, J. and F. Long. 2013. beta-catenin promotes bone formation and suppresses bone resorption in postnatal growing mice. J Bone Miner Res 28:1160-1169.

Cheverud, J. M. 1988. A comparison of genetic and phenotypic correlations. Evolution.

Cheverud, J. M. 1996. Developmental integration and the evolution of pleiotropy. Am Zool 36:44-50.

Cheverud, J. M., T. H. Ehrich, T. T. Vaughn, S. F. Koreishi, R. B. Linsey, and L. S. Pletscher. 2004. Pleiotropic effects on mandibular morphology II: Differential epistasis and genetic variation in morphological integration. Pp. 424-435. J. Exp. Zool.

Cheverud, J. M., J. J. Rutledge, and W. R. Atchley. 1983. Quantitative Genetics of Development: Genetic Correlations Among Age-Specific Trait Values and the Evolution of Ontogeny. Pp. 895. Evolution.

Clarke, J. H. and C. Dean. 1994. Mapping Fri, a Locus Controlling Flowering Time and Vernalization Response in Arabidopsis-Thaliana. Mol Gen Genet 242:81-89.

Clune, J., J. B. Mouret, and H. Lipson. 2013. The evolutionary origins of modularity. Proc Biol Sci 280:20122863.

Colosimo, P. F. 2005. Widespread Parallel Evolution in Sticklebacks by Repeated Fixation of Ectodysplasin Alleles. Pp. 1928-1933. Science.

Colosimo, P. F., K. E. Hosemann, S. Balabhadra, G. Villarreal, Jr., M. Dickson, J. Grimwood, J. Schmutz, R. M. Myers, D. Schluter, and D. M. Kingsley. 2005. Widespread parallel evolution in sticklebacks by repeated fixation of Ectodysplasin alleles. Science 307:1928-1933.

Colosimo, P. F., C. L. Peichel, K. Nereng, B. K. Blackman, M. D. Shapiro, D. Schluter, and D. M. Kingsley. 2004. The genetic architecture of parallel armor plate reduction in threespine sticklebacks. PLoS Biol 2:E109.

Conner, J. K. 2002. Genetic mechanisms of floral trait correlations in a natural population. Nature 420:407-410.

Conte, G. L., M. E. Arnegard, J. Best, Y. F. Chan, F. C. Jones, D. M. Kingsley, D. Schluter, and C. L. Peichel. 2015. Extent of QTL Reuse During Repeated Phenotypic Divergence of Sympatric Threespine Stickleback. Genetics 201:1189-1200.

Cresko, W. A., A. Amores, C. Wilson, J. Murphy, M. Currey, P. Phillips, M. A. Bell, C. B. Kimmel, and J. H. Postlethwait. 2004. Parallel genetic basis for repeated evolution of armor loss in Alaskan threespine stickleback populations. Proc Natl Acad Sci U S A 101:6050-6055.

Cresko, W. A., K. L. McGuigan, P. C. Phillips, and J. H. Postlethwait. 2007. Studies of threespine stickleback developmental evolution: progress and promise. Genetica 129:105-126.

Cresko, W. A., Y. L. Yan, D. A. Baltrus, A. Amores, A. Singer, A. Rodriguez-Mari, and J. H. Postlethwait. 2003. Genome duplication, subfunction partitioning, and lineage divergence: Sox9 in stickleback and zebrafish. Dev Dynam 228:480-489.

Currey, M. 2014. The Phenotypic and Genetic Distribution of Threespine Stickleback that Inhabit the Willamette Basin, Oregon, USA. University of Oregon, Eugene, Oregon.

DeFaveri, J., T. Shikano, Y. Shimada, A. Goto, and J. Merila. 2011. Global analysis of genes involved in freshwater adaptation in threespine sticklebacks (Gasterosteus aculeatus). Evolution 65:1800-1807.

DeLaurier, A., T. R. Huycke, J. T. Nichols, M. E. Swartz, A. Larsen, C. Walker, J. Dowd, L. Pan, C. B. Moens, and C. B. Kimmel. 2014. Role of mef2ca in developmental buffering of the zebrafish larval hyoid dermal skeleton. Dev Biol 385:189-199.

Delmore, K. E., D. P. L. Toews, R. R. Germain, G. L. Owens, and D. E. Irwin. 2016. The Genetics of Seasonal Migration and Plumage Color. Current Biology 26:2167-2173.

Eames, B. F., A. Amores, Y. L. Yan, and J. H. Postlethwait. 2012. Evolution of the osteoblast: skeletogenesis in gar and zebrafish. BMC Evol Biol 12:27.

Eames, B. F. and J. A. Helms. 2004. Conserved molecular program regulating cranial and appendicular skeletogenesis. Pp. 4-13. Dev. Dyn.

Eberhart, J. K. 2006. Early Hedgehog signaling from neural to oral epithelium organizes anterior craniofacial development. Pp. 1069-1077. Development.

Edwards, C. E. and C. Weinig. 2010. The quantitative-genetic and QTL architecture of trait integration and modularity in Brassica rapa across simulated seasonal settings. Pp. 661-677. Heredity. Nature Publishing Group.

Ellegren, H., L. Smeds, R. Burri, P. I. Olason, N. Backstrom, T. Kawakami, A. Kunstner, H. Makinen, K. Nadachowska-Brzyska, A. Qvarnstrom, S. Uebbing, and J. B. Wolf. 2012. The genomic landscape of species divergence in Ficedula flycatchers. Nature 491:756-760.

Erickson, P. A., A. M. Glazer, E. E. Killingbeck, R. M. Agoglia, J. Baek, S. M. Carsanaro, A. M. Lee, P. A. Cleves, D. Schluter, and C. T. Miller. 2016. Partially repeatable genetic basis of benthic adaptation in threespine sticklebacks. Evolution 70:887-902.

Etter, P. D., S. Bassham, P. A. Hohenlohe, E. A. Johnson, and W. A. Cresko. 2011. SNP discovery and genotyping for evolutionary genetics using RAD sequencing. Methods Mol Biol 772:157-178.

Flint, J. and E. Eskin. 2012. Genome-wide association studies in mice. Nature Reviews Genetics 13:807-817.

Force, A., W. A. Cresko, F. B. Pickett, S. R. Proulx, C. Amemiya, and M. Lynch. 2005. The origin of subfunctions and modular gene regulation. Genetics 170:433-446.

Franchini, P., C. Fruciano, M. L. Spreitzer, J. C. Jones, K. R. Elmer, F. Henning, and A. Meyer. 2013. Genomic architecture of ecologically divergent body shape in a pair of sympatric crater lake cichlid fishes. Pp. 1828-1845. Molecular Ecology.

Gardner, A. 2009. Adaptation as organism design. Biology Letters 5:861-864.

Gehring, W. J. 1996. The master control gene for morphogenesis and evolution of the eye. Genes Cells 1:11-15.

Gelmond, O., F. A. von Hippel, and M. S. Christy. 2009. Rapid ecological speciation in three-spined stickleback Gasterosteus aculeatus from Middleton Island, Alaska: the roles of selection and geographic isolation. Journal of Fish Biology 75:2037-2051.

Gibson, G. 2005. The synthesis and evolution of a supermodel. Science 307:1890-1891.

Glazer, A. M., E. E. Killingbeck, T. Mitros, D. S. Rokhsar, and C. T. Miller. 2015. Genome Assembly Improvement and Mapping Convergently Evolved Skeletal Traits in Sticklebacks with Genotyping-by-Sequencing. G3 (Bethesda) 5:1463-1472.

GRANT, P. R. 2002. Unpredictable Evolution in a 30-Year Study of Darwin's Finches. Pp. 707-711. Science.

Hagen, D. W. 1973. Inheritance of Numbers of Lateral Plates and Gill Rakers in Gasterosteus-Aculeatus. Heredity 30:303-312.

Hagen, D. W. and L. G. Gilbertson. 1972. Geographic Variation and Environmental Selection in Gasterosteus-Aculeatus L in Pacific Northwest, America. Evolution 26:32-+.

Hagen, D. W. and L. G. Gilbertson. 1973. The genetics of plate morphs in freshwater threespine sticklebacks. Heredity 31:75-84.

Hagen, D. W. and L. G. Gilbertson. 1973b. Selective predation and the intensity of selection acting on the lateral plates of threespine sticklebacks. Heredity 30:273-287.

Haggard, J. E., E. B. Johnson, and D. A. St Clair. 2013. Linkage Relationships Among Multiple QTL for Horticultural Traits and Late Blight (P. infestans) Resistance on Chromosome 5 Introgressed from Wild Tomato Solanum habrochaites. G3-Genes Genom Genet 3:2131-2146.

Hansen, T. F. 2006. The Evolution of Genetic Architecture. Pp. 123-157. Annu. Rev. Ecol. Evol. Syst.

He, Z., W. Zhai, H. Wen, T. Tang, Y. Wang, X. Lu, A. J. Greenberg, R. R. Hudson, C. I. Wu, and S. Shi. 2011. Two evolutionary histories in the genome of rice: the roles of domestication genes. PLoS Genet 7:e1002100.

Hendry, A. P. 2000. Rapid Evolution of Reproductive Isolation in the Wild: Evidence from Introduced Salmon. Pp. 516-518. Science.

Hendry, A. P. and M. T. Kinnison. 1999. Perspective: The Pace of Modern Life: Measuring Rates of Contemporary Microevolution. Evolution 53:1637.

Hendry, A. P., P. Nosil, and L. H. Rieseberg. 2007. The speed of ecological speciation. Funct Ecology.

Hermida, M., C. Fernández, R. Amaro, and E. S. Miguel. 2002. Heritability and "evolvability" of meristic characters in a natural population ofGasterosteus aculeatus. Canadian Journal of Zoology 80:532-541.

Hirasawa, T. and S. Kuratani. 2015. Evolution of the vertebrate skeleton: morphology, embryology, and development. Zoological Lett 1:2.

Hoekstra, H. E., R. J. Hirschmann, R. A. Bundey, P. A. Insel, and J. P. Crossland. 2006. A single amino acid mutation contributes to adaptive beach mouse color pattern. Science 313:101-104.

Hohenlohe, P. A., S. Bassham, M. Currey, and W. A. Cresko. 2012a. Extensive linkage disequilibrium and parallel adaptive divergence across threespine stickleback genomes. Philos Trans R Soc Lond B Biol Sci 367:395-408.

Hohenlohe, P. A., S. Bassham, P. D. Etter, N. Stiffler, E. A. Johnson, and W. A. Cresko. 2010. Population genomics of parallel adaptation in threespine stickleback using sequenced RAD tags. PLoS Genet 6:e1000862.

Hohenlohe, P. A., J. Catchen, and W. A. Cresko. 2012b. Population genomic analysis of model and nonmodel organisms using sequenced RAD tags. Methods Mol Biol 888:235-260.

Hsia, C. C., A. C. Pare, M. Hannon, M. Ronshaugen, and W. McGinnis. 2010. Silencing of an abdominal Hox gene during early development is correlated with limb development in a crustacean trunk. Evolution & Development 12:131-143.

Hulsey, C. D., G. J. Fraser, and J. T. Streelman. 2005. Evolution and Development of Complex Biomechanical Systems: 300 Million Years of Fish Jaws. Zebrafish 2:243-257.

Huycke, T. R., B. F. Eames, and C. B. Kimmel. 2012. Hedgehog-dependent proliferation drives modular growth during morphogenesis of a dermal bone. Pp. 2371-2380. Development.

Indjeian, V. B., G. A. Kingman, F. C. Jones, C. A. Guenther, J. Grimwood, J. Schmutz, R. M. Myers, and D. M. Kingsley. 2016. Evolving New Skeletal Traits by cis-Regulatory Changes in Bone Morphogenetic Proteins. Pp. 45-56. Cell.

Jamniczky, H. A., E. E. Harper, R. Garner, W. A. Cresko, P. C. Wainwright, B. Hallgrimsson, and C. B. Kimmel. 2014. Association between integration structure

and functional evolution in the opercular four-bar apparatus of the threespine stickleback, Gasterosteus aculeatus (Pisces: Gasterosteidae). Biological Journal of the Linnean Society 111:375-390.

Johanson, U., J. West, C. Lister, S. Michaels, R. Amasino, and C. Dean. 2000. Molecular Analysis of FRIGIDA, a Major Determinant of Natural Variation in Arabidopsis Flowering Time. Pp. 344-347. Science. American Association for the Advancement of Science.

Jones, F. C., M. G. Grabherr, Y. F. Chan, P. Russell, E. Mauceli, J. Johnson, R. Swofford, M. Pirun, M. C. Zody, S. White, E. Birney, S. Searle, J. Schmutz, J. Grimwood, M. C. Dickson, R. M. Myers, C. T. Miller, B. R. Summers, A. K. Knecht, S. D. Brady, H. Zhang, A. A. Pollen, T. Howes, C. Amemiya, P. Broad Institute Genome Sequencing, T. Whole Genome Assembly, J. Baldwin, T. Bloom, D. B. Jaffe, R. Nicol, J. Wilkinson, E. S. Lander, F. Di Palma, K. Lindblad-Toh, and D. M. Kingsley. 2012. The genomic basis of adaptive evolution in threespine sticklebacks. Nature 484:55-61.

Jones, K. L., U. Schwarze, M. P. Adam, P. H. Byers, and H. C. Mefford. 2015. A homozygous B3GAT3 mutation causes a severe syndrome with multiple fractures, expanding the phenotype of linkeropathy syndromes. Am J Med Genet A 167:2691-2696.

Kamath, R., M. Szczerba, L. Xiang, and M. D. Benson. 2016. Developmental and Injury-Induced EphB3 Expression in Bone, The FASEB Journal.

Kimmel, C., W. Aguirre, B. Ullmann, M. Currey, and W. Cresko. 2008. Allometric change accompanies opercular shape evolution in Alaskan threespine sticklebacks. Behaviour 145:669-691.

Kimmel, C. B. 2003. Endothelin 1-mediated regulation of pharyngeal bone development in zebrafish. Pp. 1339-1351. Development.

Kimmel, C. B., W. A. Cresko, P. C. Phillips, B. Ullmann, M. Currey, F. von Hippel, B. K. Kristjansson, O. Gelmond, and K. McGuigan. 2012a. Independent Axes of Genetic Variation and Parallel Evolutionary Divergence of Opercle Bone Shape in Threespine Stickleback. Evolution 66:419-434.

Kimmel, C. B., A. DeLaurier, B. Ullmann, J. Dowd, and M. McFadden. 2010. Modes of Developmental Outgrowth and Shaping of a Craniofacial Bone in Zebrafish. Plos One 5.

Kimmel, C. B., P. A. Hohenlohe, B. Ullmann, M. Currey, and W. A. Cresko. 2012b. Developmental dissociation in morphological evolution of the stickleback opercle. Evol Dev 14:326-337.

Kimmel, C. B., B. Ullmann, C. Walker, C. Wilson, M. Currey, P. C. Phillips, M. A. Bell, J. H. Postlethwait, and W. A. Cresko. 2005. Evolution and development of facial bone morphology in threespine sticklebacks. Proc Natl Acad Sci U S A 102:5791-5796.

Kingsley, D. M., B. L. Zhu, K. Osoegawa, P. J. De Jong, J. Schein, M. Marra, C. Peichel, C. Amamiya, D. Schluter, S. Balabhadra, B. Friedlander, Y. M. Cha, M. Dickson, J. Grimwood, J. Schmutz, W. S. Talbot, and R. Myers. 2004. New genomic tools for molecular studies of evolutionary change in threespine sticklebacks. Behaviour 141:1331-1344.

Klingenberg, C. P. 2008. Morphological Integration and Developmental Modularity. Pp. 115-132. Annu. Rev. Ecol. Evol. Syst.

Klingenberg, C. P. 2010. Evolution and development of shape: integrating quantitative approaches. Pp. 623-635. Nature Publishing Group. Nature Publishing Group.

Kopp, M. and S. Matuszewski. 2013. Rapid evolution of quantitative traits: theoretical perspectives. Pp. 169-191. Evol Appl.

Korte, A. and A. Farlow. 2013. The advantages and limitations of trait analysis with GWAS: a review. Plant Methods 9.

Kramer, I., C. Halleux, H. Keller, M. Pegurri, J. H. Gooi, P. B. Weber, J. Q. Feng, L. F. Bonewald, and M. Kneissel. 2010. Osteocyte Wnt/beta-catenin signaling is required for normal bone homeostasis. Mol Cell Biol 30:3071-3085.

Kusakabe, M., A. Ishikawa, M. Ravinet, K. Yoshida, T. Makino, A. Toyoda, A. Fujiyama, and J. Kitano. 2016. Genetic basis for variation in salinity tolerance between stickleback ecotypes. Mol Ecol.

Lande, R. 1979a. Quantitative genetic analysis of multivariate evolution, applied to brain: body size allometry. Pp. 402. Evolution.

Lande, R. 1979b. Quantitative Genetic-Analysis of Multivariate Evolution, Applied to Brain - Body Size Allometry. Evolution 33:402-416.

Lande, R. 1980. The Genetic Covariance between Characters Maintained by Pleiotropic Mutations. Genetics 94:203-215.

Lande, R. and S. J. Arnold. 1983. The Measurement of Selection on Correlated Characters. Evolution 37:1210-1226.

Laporte, M., S. M. Rogers, A. M. Dion-Cote, E. Normandeau, P. A. Gagnaire, A. C. Dalziel, J. Chebib, and L. Bernatchez. 2015. RAD-QTL Mapping Reveals Both Genome-Level Parallelism and Different Genetic Architecture Underlying the Evolution of Body Shape in Lake Whitefish (Coregonus clupeaformis) Species Pairs. G3 (Bethesda) 5:1481-1491.

Le Rouzic, A., K. Ostbye, T. O. Klepaker, T. F. Hansen, L. Bernatchez, D. Schluter, and L. A. Vollestad. 2011. Strong and consistent natural selection associated with armour reduction in sticklebacks. Mol Ecol 20:2483-2493.

Lee, Y. W., B. A. Gould, and J. R. Stinchcombe. 2014. Identifying the genes underlying quantitative traits: a rationale for the QTN programme. AoB Plants 6.

Lescak, E. A., S. L. Bassham, J. Catchen, O. Gelmond, M. L. Sherbick, F. A. von Hippel, and W. A. Cresko. 2015. Evolution of stickleback in 50 years on earthquake-uplifted islands. Proc Natl Acad Sci U S A 112:E7204-7212.

Li, H. and P. Ralph. 2016. Local PCA Shows How the Effect of Population Structure Differs Along the Genome. bioRxiv.

Lippert, C., J. Listgarten, Y. Liu, C. M. Kadie, R. I. Davidson, and D. Heckerman. 2011. FaST linear mixed models for genome-wide association studies. Nature Methods 8:833-U894.

Listgarten, J., C. Lippert, C. M. Kadie, R. I. Davidson, E. Eskin, and D. Heckerman. 2012. Improved linear mixed models for genome-wide association studies. Pp. 525-526. Nature Methods.

Liu, J., T. Shikano, T. Leinonen, J. M. Cano, M. H. Li, and J. Merila. 2014. Identification of major and minor QTL for ecologically important morphological traits in three-spined sticklebacks (Gasterosteus aculeatus). G3 (Bethesda) 4:595-604.

Mackay, T. F., E. A. Stone, and J. F. Ayroles. 2009. The genetics of quantitative traits: challenges and prospects. Nat Rev Genet 10:565-577.

Magwene, P. M. 2001. New tools for studying integration and modularity. Pp. 1734-1745. Evolution.

Malek, T. B., J. W. Boughman, I. Dworkin, and C. L. Peichel. 2012. Admixture mapping of male nuptial colour and body shape in a recently formed hybrid population of threespine stickleback. Mol Ecol 21:5265-5279.

Marchini, J., L. R. Cardon, M. S. Phillips, and P. Donnelly. 2004. The effects of human population structure on large genetic association studies. Nature Genetics 36:512-517.

Marchinko, K. B. and D. Schluter. 2007. Parallel evolution by correlated response: lateral plate reduction in threespine stickleback. Evolution 61:1084-1090.

Marroig, G. and J. M. Cheverud. 2001. A comparison of phenotypic variation and covariation patterns and the role of phylogeny, ecology, and ontogeny during cranial evolution of new world monkeys. Pp. 2576-2600. Evolution.

Matsuo, K. and N. Otaki. 2012. Bone cell interactions through Eph/ephrin: bone modeling, remodeling and associated diseases. Cell Adh Migr 6:148-156.

McGee, M. D., D. Schluter, and P. C. Wainwright. 2013. Functional basis of ecological divergence in sympatric stickleback. BMC Evol Biol 13:277.

McGuigan, K., N. Nishimura, M. Currey, D. Hurwit, and W. A. Cresko. 2011. Cryptic genetic variation and body size evolution in threespine stickleback. Evolution 65:1203-1211.

McKinnon, J. S. and H. D. Rundle. 2002. Speciation in nature: the threespine stickleback model systems. Trends in Ecology & Evolution 17:480-488.

Meirmans, P. G. and P. H. Van Tienderen. 2004. GENOTYPE and GENODIVE: two programs for the analysis of genetic diversity of asexual organisms. Mol Ecol Notes 4:792-794.

Melo, D. and G. Marroig. 2015. Directional selection can drive the evolution of modularity in complex traits. Pp. 470-475. Proc Natl Acad Sci USA.

Merrill, A. E., B. F. Eames, S. J. Weston, T. Heath, and R. A. Schneider. 2008. Mesenchyme-dependent BMP signaling directs the timing of mandibular osteogenesis. Pp. 1223-1234. Development.

Mezey, J. G., J. M. Cheverud, and G. P. Wagner. 2000. Is the genotype-phenotype map modular? A statistical approach using mouse quantitative trait loci data. Pp. 305-311. Genetics. Genetics Society of America.

Mezmouk, S., P. Dubreuil, M. Bosio, L. Décousset, A. Charcosset, S. Praud, and B. Mangin. 2011. Effect of population structure corrections on the results of association mapping tests in complex maize diversity panels. Pp. 1149-1160. Theor Appl Genet.

Miller, C. T., S. Beleza, A. A. Pollen, D. Schluter, R. A. Kittles, M. D. Shriver, and D. M. Kingsley. 2007. cis-Regulatory changes in Kit ligand expression and parallel evolution of pigmentation in sticklebacks and humans. Cell 131:1179-1189.

Miller, C. T., A. M. Glazer, B. R. Summers, B. K. Blackman, A. R. Norman, M. D. Shapiro, B. L. Cole, C. L. Peichel, D. Schluter, and D. M. Kingsley. 2014. Modular skeletal evolution in sticklebacks is controlled by additive and clustered quantitative trait loci. Genetics 197:405-420.

Müller, G. B. 2007. Evo–devo: extending the evolutionary synthesis. Pp. 943-949. Nat. Rev. Genet.

Münzing, J. 1963. The evolution of variation and distributional patterns in European populations of the three-spined stickleback, Gasterosteus aculeatus. Pp. 320. Evolution.

O'Brown, N. M., B. R. Summers, F. C. Jones, S. D. Brady, and D. M. Kingsley. 2015. A recurrent regulatory change underlying altered expression and Wnt response of the stickleback armor plates gene EDA. Elife 4:e05290.

O'Steen, S., A. J. Cullum, and A. F. Bennett. 2002. Rapid evolution of escape ability in Trinidadian guppies (Poecilia reticulata). Evolution 56:776-784.

Olsen, B. R., A. M. Reginato, and W. F. Wang. 2000. Bone development. Annu Rev Cell Dev Bi 16:191-220.

Olson, E. C. and R. L. Miller. 1958. Morphological Integration. University of Chicago Press, Chicago.

Ornitz, D. M. and P. J. Marie. 2002. FGF signaling pathways in endochondral and intramembranous bone development and human genetic disease. Genes Dev 16:1446-1465.

Orr, H. A. 2005. The genetic theory of adaptation: a brief history. Nat Rev Genet 6:119-127.

Orr, H. A. 2009. Fitness and its role in evolutionary genetics. Pp. 531-539. Nature Publishing Group.

Paaby, A. B. and M. V. Rockman. 2013. The many faces of pleiotropy. Trends in Genetics 29:66-73.

Pallares, L. F., P. Carbonetto, S. Gopalakrishnan, C. C. Parker, C. L. Ackert-Bicknell, A. A. Palmer, and D. Tautz. 2015. Mapping of Craniofacial Traits in Outbred Mice Identifies Major Developmental Genes Involved in Shape Determination. Pp. e1005607. PLoS Genet.

Pallares, L. F., B. Harr, L. M. Turner, and D. Tautz. 2014. Use of a natural hybrid zone for genomewide association mapping of craniofacial traits in the house mouse. Pp. 5756-5770. Molecular Ecology.

Pasaniuc, B. and A. L. Price. 2016. Dissecting the genetics of complex traits using summary association statistics. Nature Reviews Genetics advance online publication.

Pavlicev, M., J. M. Cheverud, and G. P. Wagner. 2011. Evolution of adaptive phenotypic variation patterns by direct selection for evolvability. P Roy Soc B-Biol Sci 278:1903-1912.

Pavlicev, M., J. P. Kenney-Hunt, E. A. Norgard, and J. M. Cheverud. 2006. Genetic variation in pleiotropy. Integrative and Comparative Biology 46:E236-E236.

Pavlicev, M., J. P. Kenney-Hunt, E. A. Norgard, C. C. Roseman, J. B. Wolf, and J. M. Cheverud. 2008. Genetic variation in pleiotropy: Differential epistasis as a source of variation in the allometric relationship between long bone lengths and body weight. Evolution 62:199-213.

Pearson, J. C., D. Lemons, and W. McGinnis. 2005. Modulating Hox gene functions during animal body patterning. Nature Reviews Genetics 6:893-904.

Peichel, C. L., K. S. Nereng, K. A. Ohgi, B. L. Cole, P. F. Colosimo, C. A. Buerkle, D. Schluter, and D. M. Kingsley. 2001. The genetic architecture of divergence between threespine stickleback species. Nature 414:901-905.

Pepper, J. W. 2003. The evolution of evolvability in genetic linkage patterns. Biosystems 69:115-126.

Phillips, P. C. and S. J. Arnold. 1989. Visualizing multivariate selection. Pp. 1209. Evolution.

Pigliucci, M. 2010. Genotype-phenotype mapping and the end of the 'genes as blueprint' metaphor. Philos T R Soc B 365:557-566.

Pirie, A., A. Wood, M. Lush, J. Tyrer, and P. D. P. Pharoah. 2015. The effect of rare variants on inflation of the test statistics in case-control analyses. Bmc Bioinformatics 16.

Pottin, K., H. Hinaux, and S. Retaux. 2011. Restoring eye size in Astyanax mexicanus blind cavefish embryos through modulation of the Shh and Fgf8 forebrain organising centres. Pp. 2467-2476. Development.

Price, A. L., N. A. Zaitlen, D. Reich, and N. Patterson. 2010. New approaches to population stratification in genome-wide association studies. Pp. 459-463. Nature Publishing Group.

Price, A. L., N. A. Zaitlen, D. Reich, and N. Patterson. 2013. Response to Sul and Eskin. Nat Rev Genet 14:300.

Pritchard, J. K., M. Stephens, and P. Donnelly. 2000a. Inference of population structure using multilocus genotype data. Genetics 155:945-959.

Pritchard, J. K., M. Stephens, N. A. Rosenberg, and P. Donnelly. 2000b. Association mapping in structured populations. American Journal of Human Genetics 67:170-181.

Protas, M., I. Tabansky, M. Conrad, J. B. Gross, O. Vidal, C. J. Tabin, and R. Borowsky. 2008. Multi-trait evolution in a cave fish, Astyanax mexicanus. Pp. 196-209. Evolution & Development.

Prud'homme, B., N. Gompel, and S. B. Carroll. 2007. Emerging principles of regulatory evolution. Proceedings of the National Academy of Sciences of the United States of America 104:8605-8612.

Purcell, S., B. Neale, K. Todd-Brown, L. Thomas, M. A. R. Ferreira, D. Bender, J. Maller, P. Sklar, P. I. W. de Bakker, M. J. Daly, and P. C. Sham. 2007. PLINK: A tool set for whole-genome association and population-based linkage analyses. American Journal of Human Genetics 81:559-575.

Purnell, M. A., M. A. Bell, D. C. Baines, P. J. Hart, and M. P. Travis. 2007. Correlated evolution and dietary change in fossil stickleback. Science 317:1887.

Raeymaekers, J. A., N. Konijnendijk, M. H. Larmuseau, B. Hellemans, L. De Meester, and F. A. Volckaert. 2014. A gene with major phenotypic effects as a target for selection vs. homogenizing gene flow. Mol Ecol 23:162-181.

Raj, A., M. Stephens, and J. K. Pritchard. 2014. fastSTRUCTURE: Variational Inference of Population Structure in Large SNP Data Sets. Genetics 197:573-U207.

Reed, R. D., R. Papa, A. Martin, H. M. Hines, B. A. Counterman, C. Pardo-Diaz, C. D. Jiggins, N. L. Chamberlain, M. R. Kronforst, R. Chen, G. Halder, H. F. Nijhout, and W. O. McMillan. 2011. optix drives the repeated convergent evolution of butterfly wing pattern mimicry. Science 333:1137-1141.

Reimchen, T. E. 1983. Structural Relationships Between Spines and Lateral Plates in Threespine Stickleback (Gasterosteus aculeatus). Evolution 37:931.

Remington, D. L. 2015. Alleles versus mutations: Understanding the evolution of genetic architecture requires a molecular perspective on allelic origins. Pp. 3025-3038. Evolution.

Reznick, D. N. 1997. Evaluation of the Rate of Evolution in Natural Populations of Guppies (Poecilia reticulata). Pp. 1934-1937. Science.

Risley, M., D. Garrod, M. Henkemeyer, and W. McLean. 2009. EphB2 and EphB3 forward signalling are required for palate development. Mech Develop 126:230-239.

Roberts, R. B., Y. Hu, R. C. Albertson, and T. D. Kocher. 2011. Craniofacial divergence and ongoing adaptation via the hedgehog pathway. Pp. 13194-13199. Proc. Natl. Acad. Sci. U.S.A. National Acad Sciences.

Rockman, M. V. 2008. Reverse engineering the genotype–phenotype map with natural genetic variation. Pp. 738-744. Nature.

Rockman, M. V. 2012. The Qtn Program and the Alleles That Matter for Evolution: All That's Gold Does Not Glitter. Evolution 66:1-17.

Roels, S. A. and J. K. Kelly. 2011. Rapid evolution caused by pollinator loss in Mimulus guttatus. Evolution 65:2541-2552.

Roff, D. 2000. The evolution of the G matrix: selection or drift? Heredity 84:135-142.

Rohlf, F. 2006. tpsDig, version 2.10. Department of Ecology and Evolution, State University of New York, Stony Brook.

Ronshaugen, M., N. McGinnis, and W. McGinnis. 2002. Hox protein mutation and macroevolution of the insect body plan. Nature 415:914-917.

Rundle, H. D., L. Nagel, J. Wenrick Boughman, and D. Schluter. 2000. Natural selection and parallel speciation in sympatric sticklebacks. Science 287:306-308.

Sansom, R. and R. N. Brandom. 2007. Integrating Evolution and Development: From Theory to Practice. MIT Press, Cambridge, MA.

Sansom, R. and R. N. Brandon. 2007. Integrating Evolution and Development: From Theory to Practice. MIT Press, Cambridge, MA.

Santagati, F. and F. M. Rijli. 2003. Cranial neural crest and the building of the vertebrate head. Pp. 806-818. Nat Rev Neurosci.

Santiago, E. 1998. Linkage and the maintenance of variation for quantitative traits by mutation–selection balance: An infinitesimal model. Genetical research.

Satokata, I. and R. Maas. 1994. Msx1 Deficient Mice Exhibit Cleft-Palate and Abnormalities of Craniofacial and Tooth Development. Nature Genetics 6:348-356.

Savolainen, O., M. Lascoux, and J. Merila. 2013. Ecological genomics of local adaptation. Nat Rev Genet 14:807-820.

Schluter, D. 1995. Adaptive Radiation In Sticklebacks - Trade-Offs In Feeding Performance and Growth. Ecology 76:82-90.

Schluter, D. 1996. Adaptive Radiation Along Genetic Lines of Least Resistance. Pp. 1766. Evolution.

Schluter, D., E. A. Clifford, M. Nemethy, and J. S. McKinnon. 2004. Parallel evolution and inheritance of quantitative traits. Am Nat 163:809-822.

Schluter, D. and G. L. Conte. 2009. Genetics and ecological speciation. Proc Natl Acad Sci U S A 106 Suppl 1:9955-9962.

Schluter, D., K. B. Marchinko, R. D. Barrett, and S. M. Rogers. 2010. Natural selection and the genetics of adaptation in threespine stickleback. Philos Trans R Soc Lond B Biol Sci 365:2479-2486.

Schluter, D. and J. D. McPhail. 1992. Ecological character displacement and speciation in sticklebacks. Am Nat 140:85-108.

Schoenebeck, J. J., S. A. Hutchinson, A. Byers, H. C. Beale, B. Carrington, D. L. Faden, M. Rimbault, B. Decker, J. M. Kidd, R. Sood, A. R. Boyko, J. W. Fondon, R. K.

Wayne, C. D. Bustamante, B. Ciruna, and E. A. Ostrander. 2012. Variation of BMP3 Contributes to Dog Breed Skull Diversity. Pp. e1002849. PLoS Genet.

Scoville, A. G., Y. W. Lee, J. H. Willis, and J. K. Kelly. 2011. Explaining the heritability of an ecologically significant trait in terms of individual quantitative trait loci. Biology Letters 7:896-898.

Shapiro, M. D., M. E. Marks, C. L. Peichel, B. K. Blackman, K. S. Nereng, B. Jonsson, D. Schluter, and D. M. Kingsley. 2004. Genetic and developmental basis of evolutionary pelvic reduction in threespine sticklebacks. Nature 428:717-723.

Shimeld, S. M. H., P W H. 2000. Vertebrate Innovations. PNAS 97:4449-4452.

Shubin, N., C. Tabin, and S. Carroll. 1997. Fossils, genes and the evolution of animal limbs. Pp. 639-648. Nature.

Shubin, N., C. Tabin, and S. Carroll. 2009. Deep homology and the origins of evolutionary novelty. Pp. 818-823. Nature.

Sicard, A. and M. Lenhard. 2011. The selfing syndrome: a model for studying the genetic and evolutionary basis of morphological adaptation in plants. Ann Bot-London 107:1433-1443.

Sinervo, B. and E. Svensson. 2002. Correlational selection and the evolution of genomic architecture. Heredity (Edinb) 89:329-338.

Slate, J. 2005. Quantitative trait locus mapping in natural populations: progress, caveats and future directions. Molecular Ecology 14:363-379.

Slate, J. 2013. From Beavis to Beak Color: A Simulation Study to Examine How Much Qtl Mapping Can Reveal About the Genetic Architecture of Quantitative Traits. Evolution 67:1251-1262.

Slatkin, M. 2008. Linkage disequilibrium — understanding the evolutionary past and mapping the medical future. Pp. 477-485. Nature Publishing Group.

Small, C. M., S. Bassham, J. Catchen, A. Amores, A. M. Fuiten, R. S. Brown, A. G. Jones, and W. A. Cresko. 2016. The genome of the Gulf pipefish enables understanding of evolutionary innovations. Genome Biol 17:258.

Smith, M. W. and S. J. O'Brien. 2005. Mapping by admixture linkage disequilibrium: Advances, limitations and guidelines. Nature Reviews Genetics 6:623-U626.

Spencer, C. C. A., Z. Su, P. Donnelly, and J. Marchini. 2009. Designing Genome-Wide Association Studies: Sample Size, Power, Imputation, and the Choice of Genotyping Chip. Plos Genetics 5.

Steiner, C. C., J. N. Weber, and H. E. Hoekstra. 2007. Adaptive variation in beach mice produced by two interacting pigmentation genes. Plos Biology 5:1880-1889.

Stockwell, C. A., A. P. Hendry, and M. T. Kinnison. 2003. Contemporary evolution meets conservation biology. Trends in Ecology & Evolution 18:94-101.

Stranger, B. E., E. A. Stahl, and T. Raj. 2011. Progress and Promise of Genome-Wide Association Studies for Human Complex Trait Genetics. Pp. 367-383. Genetics.

Sul, J. H. and E. Eskin. 2013. Mixed models can correct for population structure for genomic regions under selection. Pp. 300-300. Nature Publishing Group. Nature Publishing Group.

Talbot, J. C., S. L. Johnson, and C. B. Kimmel. 2010. hand2 and Dlx genes specify dorsal, intermediate and ventral domains within zebrafish pharyngeal arches. Pp. 2507-2517. Development.

Tarkkonen, K., R. A. Majidi, C. Valensisi, L. Saastamoinen, D. Hawkins, and R. Kiviranta. 2016. RCOR2 is a novel regulator of osteoblast differentiation. Bone Abstracts 5:162.

Terekhanova, N. V., M. D. Logacheva, A. A. Penin, T. V. Neretina, A. E. Barmintseva, G. A. Bazykin, A. S. Kondrashov, and N. S. Mugue. 2014. Fast evolution from precast bricks: genomics of young freshwater populations of threespine stickleback Gasterosteus aculeatus. PLoS Genet 10:e1004696.

Visscher, P. M., M. A. Brown, M. I. McCarthy, and J. Yang. 2012. Five Years of GWAS Discovery. American Journal of Human Genetics 90:7-24.

von Hippel, F. 2010. Tinbergen's Legacy in Behaviour: Sixty Years of Landmark Stickleback Papers. Koninklijke Brill NV, Leiden, The Netherlands.

Wagner, G. P. and L. Altenberg. 1996. Perspective: complex adaptations and the evolution of evolvability. Evolution.

Wagner, G. P., M. Pavlicev, and J. M. Cheverud. 2007. The road to modularity. Nat Rev Genet 8:921-931.

Wagner, G. P. and J. Zhang. 2011. The pleiotropic structure of the genotype–phenotype map: the evolvability of complex organisms. Pp. 204-213. Nature Publishing Group. Nature Publishing Group.

Westendorf, J. J., R. A. Kahler, and T. M. Schroeder. 2004. Wnt signaling in osteoblasts and bone diseases. Pp. 19-39. Gene.

Winkler, C. A., G. W. Nelson, and M. W. Smith. 2010. Admixture Mapping Comes of Age. Annu Rev Genom Hum G 11:65-89.

Wood, A. R., T. Esko, J. Yang, S. Vedantam, T. H. Pers, S. Gustafsson, A. Y. Chun, K. Estrada, J. Luan, Z. Kutalik, N. Amin, M. L. Buchkovich, D. C. Croteau-Chonka, F. R. Day, Y. Duan, T. Fall, R. Fehrmann, T. Ferreira, A. U. Jackson, J. Karjalainen, K. S. Lo, A. E. Locke, R. Magi, E. Mihailov, E. Porcu, J. C. Randall, A. Scherag, A. A. E. Vinkhuyzen, H. J. Westra, T. W. Winkler, T. Workalemahu, J. H. Zhao, D. Absher, E. Albrecht, D. Anderson, J. Baron, M. Beekman, A. Demirkan, G. B. Ehret, B. Feenstra, M. F. Feitosa, K. Fischer, R. M. Fraser, A. Goel, J. Gong, A. E. Justice, S. Kanoni, M. E. Kleber, K. Kristiansson, U. Lim, V. Lotay, J. C. Lui, M. Mangino, I. M. Leach, C. Medina-Gomez, M. A. Nalls, D. R. Nyholt, C. D. Palmer, D. Pasko, S. Pechlivanis, I. Prokopenko, J. S. Ried, S. Ripke, D. Shungin, A. Stancakova, R. J. Strawbridge, Y. J. Sung, T. Tanaka, A. Teumer, S. Trompet, S. W. van der Laan, J. van Setten, J. V. Van Vliet-Ostaptchouk, Z. M. Wang, L. Yengo, W. H. Zhang, U. Afzal, J. Arnlov, G. M. Arscott, S. Bandinelli, A. Barrett, C. Bellis, A. J. Bennett, C.

Berne, M. Bluher, J. L. Bolton, Y. Bottcher, H. A. Boyd, M. Bruinenberg, B. M. Buckley, S. Buyske, I. H. Caspersen, P. S. Chines, R. Clarke, S. Claudi-Boehm, M. Cooper, E. W. Daw, P. A. De Jong, J. Deelen, G. Delgado, J. C. Denny, R. Dhonukshe-Rutten, M. Dimitriou, A. S. F. Doney, M. Dorr, N. Eklund, E. Eury, L. Folkersen, M. E. Garcia, F. Geller, V. Giedraitis, A. S. Go, H. Grallert, T. B. Grammer, J. Grassler, H. Gronberg, L. C. P. G. M. de Groot, C. J. Groves, J. Haessler, P. Hall, T. Haller, G. Hallmans, A. Hannemann, C. A. Hartman, M. Hassinen, C. Hayward, N. L. Heard-Costa, Q. Helmer, G. Hemani, A. K. Henders, H. L. Hillege, M. A. Hlatky, W. Hoffmann, P. Hoffmann, O. Holmen, J. J. Houwing-Duistermaat, T. Illig, A. Isaacs, A. L. James, J. Jeff, B. Johansen, A. Johansson, J. Jolley, T. Juliusdottir, J. Junttila, A. N. Kho, L. Kinnunen, N. Klopp, T. Kocher, W. Kratzer, P. Lichtner, L. Lind, J. Lindstrom, S. Lobbens, M. Lorentzon, Y. C. Lu, V. Lyssenko, P. K. E. Magnusson, A. Mahajan, M. Maillard, W. L. McArdle, C. A. McKenzie, S. McLachlan, P. J. McLaren, C. Menni, S. Merger, L. Milani, A. Moayyeri, K. L. Monda, M. A. Morken, G. Muller, M. Muller-Nurasyid, A. W. Musk, N. Narisu, M. Nauck, I. M. Nolte, M. M. Nothen, L. Oozageer, S. Pilz, N. W. Rayner, F. Renstrom, N. R. Robertson, L. M. Rose, R. Roussel, S. Sanna, H. Scharnagl, S. Scholtens, F. R. Schumacher, H. Schunkert, R. A. Scott, J. Sehmi, T. Seufferlein, J. X. Shin, K. Silventoinen, J. H. Smit, A. V. Smith, J. Smolonska, A. V. Stanton, K. Stirrups, D. J. Stott, H. M. Stringham, J. Sundstrom, M. A. Swertz, A. C. Syvanen, B. O. Tayo, G. Thorleifsson, J. P. Tyrer, S. van Dijk, N. M. van Schoor, N. van der Velde, D. van Heemst, F. V. A. van Oort, S. H. Vermeulen, N. Verweij, J. M. Vonk, L. L. Waite, M. Waldenberger, R. Wennauer, L. R. Wilkens, C. Willenborg, T. Wilsgaard, M. K. Wojczynski, A. Wong, A. F. Wright, Q. Y. Zhang, D. Arveiler, S. J. L. Bakker, J. Beilby, R. N. Bergman, S. Bergmann, R. Biffar, J. Blangero, D. I. Boomsma, S. R. Bornstein, P. Bovet, P. Brambilla, M. J. Brown, H. Campbell, M. J. Caulfield, A. Chakravarti, R. Collins, F. S. Collins, D. C. Crawford, L. A. Cupples, J. Danesh, U. de Faire, H. M. den Ruijter, R. Erbel, J. Erdmann, J. G. Eriksson, M. Farrall, E. Ferrannini, J. Ferrieres, I. Ford, N. G. Forouhi, T. Forrester, R. T. Gansevoort, P. V. Gejman, C. Gieger, A. Golay, O. Gottesman, V. Gudnason, U. Gyllensten, D. W. Haas, A. S. Hall, T. B. Harris, A. T. Hattersley, A. C. Heath, C. Hengstenberg, A. A. Hicks, L. A. Hindorff, A. D. Hingorani, A. Hofman, G. K. Hovingh, S. E. Humphries, S. C. Hunt, E. Hypponen, K. B. Jacobs, M. R. Jarvelin, P. Jousilahti, A. M. Jula, J. Kaprio, J. J. P. Kastelein, M. Kayser, F. Kee, S. M. Keinanen-Kiukaanniemi, L. A. Kiemeney, J. S. Kooner, C. Kooperberg, S. Koskinen, P. Kovacs, A. T. Kraja, M. Kumari, J. Kuusisto, T. A. Lakka, C. Langenberg, L. Le Marchand, T. Lehtimaki, S. Lupoli, P. A. F. Madden, S. Mannisto, P. Manunta, A. Marette, T. C. Matise, B. McKnight, T. Meitinger, F. L. Moll, G. W. Montgomery, A. D. Morris, A. P. Morris, J. C. Murray, M. Nelis, C. Ohlsson, A. J. Oldehinkel, K. K. Ong, W. H. Ouwehand, G. Pasterkamp, A. Peters, P. P. Pramstaller, J. F. Price, L. Qi, O. T. Raitakari, T. Rankinen, D. C. Rao, T. K. Rice, M. Ritchie, I. Rudan, V. Salomaa, N. J. Samani, J. Saramies, M. A. Sarzynski, P. E. H. Schwarz, S. Sebert, P. Sever, A. R. Shuldiner, J. Sinisalo, V. Steinthorsdottir, R. P. Stolk, J. C. Tardif, A. Tonjes, A. Tremblay, E. Tremoli, J. Virtamo, M. C. Vohl, P. Amouyel, F. W. Asselbergs, T. L. Assimes, M. Bochud, B. O. Boehm, E. Boerwinkle, E. P. Bottinger, C. Bouchard, S. Cauchi, J. C. Chambers, S. J. Chanock, R. S. Cooper, P. I. W. de

Bakker, G. Dedoussis, L. Ferrucci, P. W. Franks, P. Froguel, L. C. Groop, C. A. Haiman, A. Hamsten, M. G. Hayes, J. Hui, D. J. Hunter, K. Hveem, J. W. Jukema, R. C. Kaplan, M. Kivimaki, D. Kuh, M. Laakso, Y. M. Liu, N. G. Martin, W. Marz, M. Melbye, S. Moebus, P. B. Munroe, I. Njolstad, B. A. Oostra, C. N. A. Palmer, N. L. Pedersen, M. Perola, L. Perusse, U. Peters, J. E. Powell, C. Power, T. Quertermous, R. Rauramaa, E. Reinmaa, P. M. Ridker, F. Rivadeneira, J. I. Rotter, T. E. Saaristo, D. Saleheen, D. Schlessinger, P. E. Slagboom, H. Snieder, T. D. Spector, K. Strauch, M. Stumvoll, J. Tuomilehto, M. Uusitupa, P. van der Harst, H. Volzke, M. Walker, N. J. Wareham, H. Watkins, H. E. Wichmann, J. F. Wilson, P. Zanen, P. Deloukas, I. M. Heid, C. M. Lindgren, K. L. Mohlke, E. K. Speliotes, U. Thorsteinsdottir, I. Barroso, C. S. Fox, K. E. North, D. P. Strachan, J. S. Beckmann, S. I. Berndt, M. Boehnke, I. B. Borecki, M. I. McCarthy, A. Metspalu, K. Stefansson, A. G. Uitterlinden, C. M. van Duijn, L. Franke, C. J. Willer, A. L. Price, G. Lettre, R. J. F. Loos, M. N. Weedon, E. Ingelsson, J. R. O'Connell, G. R. Abecasis, D. I. Chasman, M. E. Goddard, P. M. Visscher, J. N. Hirschhorn, T. M. Frayling, E. M. R. G. e. C, M. Consortium, P. Consortium and L. C. Study. 2014. Defining the role of common variation in the genomic and biological architecture of adult human height. Nature Genetics 46:1173-1186.

Wu, T. D. and C. K. Watanabe. 2005. GMAP: a genomic mapping and alignment program for mRNA and EST sequences. Bioinformatics 21:1859-1875.

Yamamoto, Y., M. S. Byerly, W. R. Jackman, and W. R. Jeffery. 2009. Pleiotropic functions of embryonic sonic hedgehog expression link jaw and taste bud amplification with eye loss during cavefish evolution. Pp. 200-211. Developmental Biology. Elsevier Inc.

Yang, J., N. A. Zaitlen, M. E. Goddard, P. M. Visscher, and A. L. Price. 2014. Advantages and pitfalls in the application of mixed-model association methods. Pp. 100-106. Nature Publishing Group. Nature Publishing Group.

Yuan, Y. W., J. M. Sagawa, R. C. Young, B. J. Christensen, and H. D. Bradshaw. 2013. Genetic Dissection of a Major Anthocyanin QTL Contributing to Pollinator-Mediated Reproductive Isolation Between Sister Species of Mimulus. Genetics 194:255-+.

Zhou, X. and M. Stephens. 2012. Genome-wide efficient mixed-model analysis for association studies. Nature Genetics 44:821-U136.

Zhou, X. and M. Stephens. 2014. Efficient multivariate linear mixed model algorithms for genome-wide association studies. Nature Methods 11:407-+.